



**PRO GRADU**

**ANIONIC BIOPOLYMER DERIVATIVES AND THEIR PERFORMANCE IN FLOCCULATION**

Brita Peltokoski

Department of Chemistry

University of Helsinki

October 2018

Faculty Faculty of science		Degree programme Master of science	
Author Brita Peltokoski			
Title Anionic biopolymer derivatives and their performance in flocculation			
Level Master of science	Month and year October 2018	Number of pages 76	
<p>Abstract</p> <p>The aim of the thesis is to identify and test anionic biopolymer derivatives in flocculation application. Several potential polysaccharides are listed in literature, but chemical modification is often needed to improve their performance in the selected application. Totally 28 polysaccharide derivatives were received from varying suppliers and screened by rheology and charge. The most potential biobased products in addition to synthetic polyacrylamide references were purified by dialysis and characterized by charge density, apparent viscosity in water and brine and intrinsic viscosity in brine. Xanthan gum, carboxymethyl cellulose and guar gum appeared to have the best combination of high viscosity and charge density. Xanthan gum revealed exceptional behavior in brine as its viscosity increases upon salt addition due to helix formation. This phenomenon opens numerous possibilities in brine applications.</p> <p>In the application testing 9 biopolymer derivatives representing 6 different types of polysaccharides in addition to two reference polyacrylamides were studied by flocculating bentonite. The evolution of flocs was monitored online with focused beam reflectance measurement. Xanthan gum, carboxymethyl cellulose and guar gum have the best performance in flocculation as expected based on the characterization results supporting the statement that size and charge are key parameters in flocculation performance. The biobased products fall behind in flocculation efficiency compared to polyacrylamides, but their performance can be improved by chemical modification. A quick thermal stability screening was also performed, and xanthan gum appeared to be even more thermally stable compared to the polyacrylamide reference in the selected environment.</p> <p>As a conclusion it is justified to claim that in the future the biobased products have a great potential to offer alternative solutions in the applications where synthetic fossil-based polymers are currently used. The recommended path forward is to find suitable modification mechanisms to increase the flocculation performance of xanthan gum, carboxymethyl cellulose and guar gum. Nucleophilic reaction of the saccharide oxygen is a typical example of chain modification for polysaccharide chemistry. Based on the results presented in this thesis, the future of biobased products from renewable resources looks promising.</p>			
<p>Keywords</p> <p>Biobased, renewable, polysaccharide, polymer, polyelectrolyte, flocculation, FBRM</p>			
<p>Where deposited</p> <p>Kumpula Campus Library and Digital Repository of the University of Helsinki / E-thesis</p>			
<p>Supervisors</p> <p>Heikki Tenhu, Ph.D., Professor, Department of Chemistry, University of Helsinki Jonni Ahlgren, M.Sc., Sr Principal Scientist, R&amp;D and Technology, Kemira Oyj</p>			

## Preface

The thesis was performed together with the Polymer chemistry laboratory at the University of Helsinki and Espoo Research and development center at Kemira. The need for biobased materials is increasing around the world. Kemira is actively developing alternatives to meet the customer needs regarding biobased portfolio to sustain good position in the value chain. Kemira has strong competence in manufacturing anionic polyacrylamide flocculants and their use in varying industries. Flocculation was selected as the target application of this thesis to increase the knowledge regarding currently available biobased opportunities.

It was a pleasure to perform the thesis in collaboration between the University and Kemira and I look forward to continue the good liaison between the institutes in the future as well. I would like to take this opportunity to thank both of my supervisors, Heikki Tenhu and Jonni Ahlgren, for guiding me through the process of creating this thesis. I am very grateful of all the support and trust I got during the work. Studying biobased polymers has been very interesting and I am glad that Jonni offered me this topic for my thesis.

I would also like to acknowledge the whole project team for contribution and good discussions in the weekly meetings. Thank you, Jaakko, Chunlin and Michael. Taking academic leave to get a higher degree after working for several years in chemical industry as a lab technician was exciting and I am very grateful of all the support I got from colleagues from the beginning of my educational journey. Thank you Sussu for encouraging me to take the step of applying to the University although having a permanent job in your team and for giving me interesting topics for many essays written during the lectures. Thank you Vesa for teaching me to think theoretically and predict by calculating to make life in lab much easier. Thank you Lasse for helping me to choose such an interesting major as polymer chemistry is, and thank you Mikko for sparring me during the thesis work. I would also like to thank my friends and family for being there and listening whenever I needed that.

The biggest acknowledgement goes to my best friend and soulmate Tomppa. Words are not enough to describe how much I appreciate your support along the way, so I'll get you a big box of chocolate. Continuing studies was one of the best decisions I've made. I have really enjoyed all the new information and adventures that decision brought to my life, especially the student exchange in Australia. Cannot wait to see what kind of doors the new degree opens in my career.

## Contents

INTRODUCTION .....	1
THEORY .....	2
1 Polyelectrolytes.....	2
1.1 Properties and applications .....	2
1.2 Thermodynamics and physical parameters of polyelectrolyte solutions .....	4
1.3 Rheology of polyelectrolyte solutions.....	7
2 Colloids.....	10
2.1 Electrostatic properties .....	11
2.2 Charge density measurement .....	12
3 Flocculation and particle size measurement .....	13
3.1 Mechanism of flocculation.....	14
3.2 Coagulation-flocculation .....	17
3.3 Focused beam reflectance measurement.....	18
4 Biobased flocculants .....	19
4.1 Polysaccharides .....	19
4.2 Chemical modification of polysaccharides.....	29
EXPERIMENTAL.....	31
5 Screening and purification .....	31
5.1 Screening.....	32
5.2 Purification .....	35
6 Characterization of selected polymers .....	37
6.1 Charge density.....	37
6.2 Apparent viscosity .....	39
6.3 Intrinsic viscosity .....	42

7 Setting up the FBRM parameters.....	49
7.1 Flocculation matrix.....	49
7.2 pH of the bentonite sample .....	50
7.3 Coagulant dosage.....	51
7.4 Result interpretation.....	51
8 Performance of the biobased products in bentonite flocculation.....	54
8.1 Optimal dosage .....	55
8.2 Floc stability and re-flocculation ability .....	58
9 Additional performance testing.....	60
9.1 Flocculation of oil sands tailings.....	60
9.2 Thermal stability.....	62
SUMMARY .....	64
References.....	67
Appendix 1. Intrinsic viscosity graphs .....	70
Appendix 2. Bentonite flocculation graphs.....	72
Appendix 3. Viscosity profiles of thermal stability test.....	75

## Symbols and abbreviations

$R$	average end-to-end distance
$l_B$	Bjerrum length
$k_B$	Boltzmann constant
CMC	carboxymethyl cellulose
cP	centipoise
$c^*$	critical overlap concentration
Da	dalton
$N_p$	degree of polymerization
DLVO	Derjaquin, Landau, Verwey and Overbeek
DADMAC	diallyldimethylammonium chloride
$\epsilon$	dielectric constant
$D$	diffusion coefficient
$e$	elementary charge
FBRM	focused beam reflectance measurement
$k_H$	Huggins constant
$R_H$	hydrodynamic radius
$\eta_{inh}$	inherent viscosity
$\chi$	interaction parameter
$[\eta]$	intrinsic viscosity
IPA	isopropanol
$\nu$	kinematic viscosity
$k_K$	Kraemer constant
meq/g	milliequivalent/gram
mPas	millipascal second
ppm	parts per million
PAM	polyacrylamide
PAC	polyaluminium chloride
$\vec{r}$	position vector
$R_g$	radius of gyration
$\eta_{red}$	reduced viscosity
$\eta_{rel}$	relative viscosity
rpm	revolutions per minute
$\dot{\gamma}$	shear rate
$\sigma$	shear stress
$\eta_{sp}$	specific viscosity
$\eta$	viscosity

## INTRODUCTION

The aim of this thesis is to study biobased anionic high molecular weight polymers and their performance in flocculation application. Due to depleting oil reserves and global consciousness of sustainable way of living, the renewable raw-materials are gaining more and more attention in the industrial production of materials. Green image and tightening regulations are also drivers for companies to develop alternative product lines. The major benefits of biobased products are safety and biodegradability which prevents harmful substances of accumulating in the soil and ground water. The biobased polymers are rather easily available from wood industry and agricultural resources, and their production does not induce secondary pollution. The research question is whether biobased products from renewable resources could replace synthetic oil-based polymers in flocculation application in the future.

Flocculation refers to a process where suspended particles are aggregated by adsorption of long polymer chains. Colloidal particles in aqueous solutions carry typically negative surface charge, and the polymer adsorption occurs by electrostatic interactions. Therefore, the polymers used in flocculation are polyelectrolytes. As the particle surface charge is commonly negative, polycations typically perform in flocculation solely. However, the scope of this thesis is to study the performance of polyanions which are used together with cationic coagulants delivering cationic charge on the surface. Based on their chemical structure, many biobased products do not have high enough inherent charge density to perform well in flocculation, and therefore biopolymer derivatives with increased charge density are studied. Although the synthetic polyacrylamides are currently expected to demonstrate superior performance in flocculation compared to the biobased derivatives, the idea is to find the most potential renewable chemistries to keep up with the global progress of biochemistry.

The literature part of the thesis explains the theory of the selected application by describing the theories of polyelectrolytes and colloids in addition to different flocculation mechanisms. Eventually, different anionic biopolymer derivatives having potential in flocculation are introduced. In the experimental section, all gathered samples are screened, and selected products are purified by dialysis. Next, the purified products are characterized by charge density and rheological properties in water and brine. Based on the results, the most potential products are selected and tested in bentonite flocculation comparing to synthetic polyacrylamide references. At the end, thermal stability of some samples is measured. Based on the results, xanthan gum, carboxymethylcellulose and guar gum derivatives appear to be the most potential products for flocculation application.

# THEORY

## 1 Polyelectrolytes

Polyelectrolytes are polymers containing functional groups that can dissociate into charged macroions and small counterions when the polymer is dissolved in a polar solvent. Polyelectrolytes can be classified as strong or weak depending on the relative number of charged groups along the chain. This can be characterized by measuring the specific charge quantity, commonly expressed as milliequivalents per grams of polymer (meq/g).<sup>1</sup> Experimentally analyzed specific charge quantity, also called as charge density, is a measure of effective charge. It is the charge the polyelectrolyte has freely in use in the specific environment. Some of the counterions are trapped by the electric field around the polyion and this so-called ion binding reduces the effective charge of a polyelectrolyte. The magnitude of ion binding depends on several factors such as pH, temperature and ionic strength of the surrounding medium.

Conformation of the polymer chain in a solvent is highly affected by electrostatic interactions. The shape of a strong polyelectrolyte is controlled by electrostatic coupling as the charged groups dissociate completely independent of the surrounding pH. In case of a weak polyelectrolyte, the conformation of the chain is correlated by pH and solvent quality, for example ionic strength and temperature. When the charge density is low, the dominating inter- and intramolecular interactions are hydrophobic forces and hydrogen bonding. Due to hydrogen bonding, especially natural weak polyelectrolytes may adopt special structures like helices. The entropy of the chain can be decreased by changing the monovalent counter ions to multivalent species which have higher interaction energy.<sup>1</sup>

### 1.1 Properties and applications

Polyelectrolytes have been studied for a long time but understanding their behavior has not been clear until recent decades. The research has been challenging due to simultaneous interplay of several interactions such as repulsion and attraction of charged groups, hydrophobic forces and hydrogen bonding. The complex set of interactions in polyelectrolyte solution reveal unique properties. Opposite to neutral polymers, reduced viscosity of polyelectrolyte solution often increases while decreasing the polymer concentration in water.<sup>1</sup> This is called a polyelectrolyte effect and it is caused by conformational changes of the polymer chains. When the polymer concentration is high, the amount of intermolecular interactions is increased, and chain conformation is forced to compact coil leading to decreased viscosity of the solution. In more diluted solution there are less intermolecular interactions and more ionized functional groups.



This leads to intramolecular repulsion between the like-charges and the coil opens to an extended rod-like conformation increasing the solution viscosity.<sup>2</sup>

When small amounts of electrolytes are added to the solution, the polyelectrolyte effect is eliminated by charge screening and the coil contracts to random coil conformation. In case of high salt concentration, the affinity of polyelectrolyte to the solution decreases and eventually the polymer precipitates out of the solution. Especially multivalent ions coordinate themselves with the ionized functional groups and above certain level of concentration they incur polymer precipitation. Due to the release of counterions, osmotic pressure of the polyelectrolyte solution is higher compared to a solution of neutral polymer.

Polymer solutions exist in three different concentration regimes: dilute, semi-dilute and concentrated. In dilute solution, the intermolecular interactions between individual polymer chains are minor and can be neglected. In semi-dilute solutions overlapping of the chains becomes important, and in concentrated solutions chain entanglements have a major influence on the properties of the polymer solution. Due to electrostatic repulsion between the functional groups, polyelectrolyte chains are relatively stiff. The stiffness leads to an extended coil conformation and thus the critical concentration describing the cross-over between dilute and semi-dilute regions is lower compared to neutral polymers. When the coils entangle, viscosity of the solution increases and therefore polyelectrolytes serve as good viscosifiers even at low concentrations.<sup>3</sup> In addition, polyelectrolytes are able to form special structures like blobs and necklaces depending on the charge and solvent quality.

High molecular weight, HMW, polyelectrolytes find use in many applications for example in paper, oil, mining, food and pharmaceutical industries in addition to wastewater treatment. In papermaking, polyelectrolytes are commonly used for example as retention aids and flocculating agents in solid-liquid separation. In oilfield applications their typical function is to increase viscosity for example in drilling and enhanced oil recovery fluids. Sludge dewatering and drinking water treatment are examples of water treatment applications. The research of biological polyelectrolytes for human health care is constantly increasing. Owing to their biodegradability and nontoxicity they have a great potential for example in medical applications such as drug delivery and targeted release. Polyelectrolytes are also used in corrosion control, optics, lubrication and biofouling control. Oppositely charged polymer chains can form electrical double layer complexes opening new opportunities for polyelectrolyte applications.<sup>1</sup>

## 1.2 Thermodynamics and physical parameters of polyelectrolyte solutions

Dissolution capability of an amorphous polymer into a solvent depends on the thermodynamic potential known as the Gibbs free energy. When the change in Gibbs free energy of mixing is negative, mixing is spontaneous and polymer dissolves into the solution. If the value is positive, dissolution does not occur as the polymer and the solvent separates into two phases. When high molecular weight macromolecules are dissolved in a solution, the entropy always increases at least to some extent and therefore the governing factor in mixing is the enthalpy term. The Gibbs free energy of mixing ( $\Delta G_m$ ) can be calculated by Equation 1 where  $\Delta H_m$  is the change in mixing enthalpy,  $\Delta S_m$  is the change in mixing entropy and T is an absolute temperature in kelvins.<sup>4</sup>

$$\Delta G_m = \Delta H_m - T\Delta S_m \quad \text{Equation 1}$$

Due to the complex set of simultaneous interactions, aqueous solutions of polyelectrolytes are thermodynamically extremely non-ideal. To describe thermodynamics of polyelectrolyte solutions, some mathematical models have been developed. The two most commonly used theories are Debye-Hückel and Flory-Huggins. The main perception of the Debye-Hückel theory is that similar charges along the polyelectrolyte chain cause intramolecular self-repulsion influencing the chain conformation. This is observed especially in dilute polyelectrolyte solutions as the chain adopts extended rod-like conformation.<sup>1,5</sup>

The Flory-Huggins theory, also called as the mean field approach, assumes that all monomer-monomer and solvent-solvent interactions have the same energy and chain locations cannot overlap. The theory is typically visualized by a lattice model shown in Figure 1<sup>5</sup>. The solvent molecules and polymer segments are assumed to be of the same size and fluctuations of the segment positions are neglected. By averaging over all monomer sites along the polymer chain, the quality of the solution and general interactions can be forecasted. The entropy of mixing is estimated based on the number of possible configurations of the polymer on the lattice and the enthalpy depends on the interactions between the components. The model can be used to indirectly predict blobs and coiling of the chain.<sup>1,5</sup> Blob is a term used for a larger repeating unit along the chain that behaves as an ideal Gaussian chain. Each chain can be divided into a sequence of blobs consisting of a certain number of constitutional repeating units and each blob looks like an isolated chain.

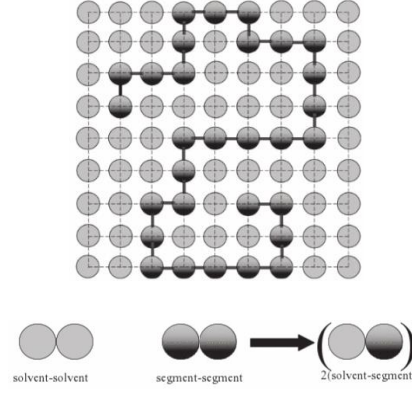


Figure 1. Lattice model of Flory-Huggins theory.

Polymer chain adopts many different conformations in solution and therefore it can be characterized only by average properties. The commonly measured parameters are radius of gyration and end-to-end distance. The radius of gyration is the average distance of the polymer segments from the center of mass of the polymer coil and it can be measured by light scattering techniques. The radius is affected by local interactions along the chain induced for example by configuration, excluded volume effects caused by monomer repulsion and a balance between the solvent-monomer and monomer-monomer interactions measured by Flory-Huggins interaction parameter. Radius of gyration ( $R_g$ ) is calculated by Equation 2, and the average end-to-end distance ( $R$ ) by Equation 3. In the equations,  $\vec{r}$  is the position vector with subscripts referring to  $i^{\text{th}}$  position ( $i$ ), center of mass ( $cm$ ) or degree of polymerization ( $N_p$ ).<sup>3,5</sup>

$$R_g^2 = \frac{\sum_{i=1}^p |\vec{r}_i - \vec{r}_{cm}|^2}{N_p} \quad \text{Equation 2}$$

$$R^2 = \langle |\vec{r}_{N_p} - \vec{r}_1|^2 \rangle \quad \text{Equation 3}$$

The Flory-Huggins interaction parameter ( $\chi$ ) is defined as the internal energy change ( $\Delta U_{sp}$ ) multiplied by a coordination number for the lattice contacts ( $z$ ) relative to thermal energy ( $k_B T$ ). It can be calculated for example by Equation 4.

$$\chi = \frac{\Delta U_{sp} z}{k_B T} \quad \text{Equation 4}$$

Based on the solubility parameter, polymer-solvent systems can be divided into three solvent regimes: good, bad and theta solvents. When  $\chi$  is less than 0,5 the solvent is good and conformational entropy leads to an open polymer chain. In this case polymer and solvent are miscible. If the solvent is poor  $\chi$  is greater than 0,5 and the monomer-monomer interactions are much stronger compared to the monomer-solvent interactions. This causes the polymer coil to adopt a dense coil conformation. As the value of the solubility parameter increases, polymer solubility decreases. However, the polymer might still be swollen by the solvent.

In theta solvent  $\chi$  equals 0,5 and the coil is as close to a random coil conformation as is obtainable. This is a transition phase between good and poor solvents wherein the steric repulsion and solvent interactions are balanced. Also, a molar volume of solvent affects miscibility and phase equilibrium between polymer and solvent.<sup>4,5</sup>

Stiffness of a polymer chain is described by a parameter called persistence length. Any chain segment shorter than the persistence length is considered to be a rigid rod. This means that the end-to-end distance of a segment is the same as its contour length. In case of polyelectrolytes, the persistence length is highly affected by intra- and intermolecular electrostatic interactions. Due to the complexity of interactions it is recommended to use the persistence length of a polyelectrolyte only as a qualitative guideline rather than a quantitative relation.<sup>3</sup> Contour length describes the length of a polymer chain at its maximum physical extension while the chain length takes into account the bond angles. Therefore, the chain length is shorter than the contour length. Segments having the size of a persistence length behave nearly independently and they are called effective segments or Kuhn segments. When diluted into a solvent, the center of mass of the polymer is in diffusive motion and the shape of the chain follows a Brownian trajectory. The conformation and diffusion by Brownian motion can be described by a mathematical model called Random walk. In the model, Kuhn segments are freely jointed to each other pointing to random directions.<sup>3,6</sup>

Intensity of electrostatic interactions of a polyelectrolyte in aqueous solvent is characterized by a quantity called Bjerrum length. By definition it is the distance at which electrostatic interaction between two elementary charges is the same as thermal energy ( $k_B T$ ). Bjerrum length ( $l_B$ ) is calculated by Equation 5, where  $e$  is elementary charge,  $\epsilon$  is dielectric constant of the solvent,  $k_B$  is Boltzmann constant and  $T$  is temperature.<sup>1</sup>

$$l_B = \frac{e^2}{\epsilon k_B T} \quad \text{Equation 5}$$

When the charge density of a polyelectrolyte exceeds the critical value of one elementary charge per Bjerrum length, the electrostatic attraction of counterions to polymer becomes strong causing some of the counterions to condense on the polyelectrolyte chain. This phenomenon is called Manning's condensation and it reduces the effective charge density of a polymer back to the critical value.<sup>7</sup> When polyelectrolyte is dissolved into an electrolyte solution, charges are screened by counterions having the opposite sign, and the strength of interactions decreases along with the Debye length. The distance over which the interaction between the charges becomes insignificant is called Debye length.

When dissolved into a solution, particles are in continuous movement. The movement is caused for example by concentration gradient, electrical field, stirring, flow or Brownian motion arising from thermal energy. The diffusion coefficient ( $D$ ) of a spherical particle in a solution is determined by Equation 6 where  $k_B$  is the Boltzmann constant,  $T$  is temperature,  $r$  is radius of the particle and  $\eta$  is the solution viscosity.<sup>1</sup>

$$D = \frac{k_B T}{6\pi r \eta} \quad \text{Equation 6}$$

The diffusion coefficient can be used to calculate the size of a polymer as the hydrodynamic radius. The hydrodynamic radius is a radius of a hypothetical hard sphere without any interactions that diffuses with the same speed as the particle under examination. Commonly used analytical methods to measure the hydrodynamic radius are for example light scattering and nuclear magnetic resonance spectroscopy. Hydrodynamic radius ( $R_H$ ) is calculated by Equation 7<sup>1</sup>.

$$R_H = \frac{k_B T}{6\pi \eta D} \quad \text{Equation 7}$$

### 1.3 Rheology of polyelectrolyte solutions

Rheology is a study of flow and deformation of materials. When studying polyelectrolyte solutions, special emphasis is usually placed on the flow characteristics which are measured by viscosity. Viscosity is the internal friction of liquid caused by molecular attraction, and it represents a resistance of matter to flow. According to Newton's law for viscous fluids the internal friction that exists between the layers in a matter creates resistance to move against the applied force. Each layer in the sample moves at slightly different rate depending on the internal friction. For samples exhibiting Newtonian behavior the resultant velocity is directly proportional to the applied force and the flow continues as long as the force is applied. The relationship between shear stress and shear rate is linear and viscosity is independent of the share rate. Viscosity ( $\eta$ ) is calculated by Equation 8, where  $\sigma$  is shear stress and  $\dot{\gamma}$  is shear rate.<sup>8</sup> Fundamental unit of viscosity is poise. When a shear stress of  $10^{-5}$  Newtons per square centimeter is needed to produce a shear rate of one reciprocal second, the material has a viscosity of one poise. The SI unit for viscosity is millipascal-second (mPas) which equals one centipoise (cP).

$$\eta = \frac{\sigma}{\dot{\gamma}} \quad \text{Equation 8}$$

Polyelectrolytes, like other polymers, behave in non-Newtonian manner. They exhibit non-linear relationship between shear stress and shear rate implying that the viscosity is shear-dependent. Non-Newtonian flow can be described as a mixture of molecules with varying sizes and shapes.

These parameters and their cohesiveness determine how much force is needed to move the molecules. The alignment of the molecules is different at varying shear rates and therefore the force needed to sustain the motion also alters. Materials possessing decrease in viscosity as the shear rate increases are called pseudoplastic and most polymers belong to this category. Shear-thickening materials are called dilatant. In addition to shear rate, also time is a significant factor for some fluids under conditions of constant shear. When viscosity decreases as a function of time, the fluid is called thixotropic and in case it increases the material is called rheopectic. When viscosity is measured using a viscometer, the result is apparent viscosity of the fluid and it is accurate only with the explicit experimental parameter information.<sup>9</sup>

Rheology is a sensitive method for polymer characterization since the flow properties highly depend on the molecular weight and its distribution. Molecular weight of polymers with complex set of interactions in solution may be difficult to quantify by analytical tools, but rheology enables comparing relative differences between the polyelectrolytes. It is a useful tool to study for example the effect of mechanical, chemical or thermal treatments and the effect of additives. Also performance in the final application in addition to material behaviour can be predicted by rheological properties.<sup>9</sup> Compared to neutral polymers the rheological properties of polyelectrolyte solutions are complex and peculiar due to the multiple simultaneous intra- and intermolecular interactions. Rheological parameters depend on the molecular structure, entanglements and interactions of a polymer, but also on the surrounding medium. Viscosity of the solvent and polymer-solvent interactions affect the movement of polymer chains as the macromolecule drags along some of the solvent molecules. The polymer-solvent interactions are affected by several external factors such as temperature, pH and ionic strength of the medium.

### **1.3.1 Dynamic and kinematic viscosity**

There are many techniques available to study viscosity of polymer solutions. One of the most conventional methods is capillary viscometry by Ubbelohde viscometer. According to Poiseuille's law, dynamic viscosity of solution ( $\eta$ ) is related to the flow time in capillary and can be calculated by Equation 9 where  $r$  is capillary radius,  $g$  is gravitational acceleration,  $h$  is fluid height,  $\rho$  is fluid density,  $t$  is the time it takes for the fluid to flow through the capillary,  $V$  is fluid volume and  $l$  is capillary length.<sup>10</sup>

$$\eta = \frac{\pi r^4 g h \rho t}{8 V l} \quad \text{Equation 9}$$

Dynamic viscosity ( $\eta$ ) divided by density of the material ( $\rho$ ) is called kinematic viscosity ( $\nu$ ). It is calculated by Equation 10 and its SI unit is  $\text{m}^2/\text{s}$ . In practice, the unit  $\text{mm}^2/\text{s}$  is more often used as  $1 \text{ mm}^2/\text{s}$  equals  $1 \text{ mPas}$ . The kinematic viscosity of water in  $20^\circ\text{C}$  is  $1 \text{ mPas}$ .

$$\nu = \frac{\eta}{\rho} \quad \text{Equation 10}$$

### 1.3.2 Intrinsic viscosity

Intrinsic viscosity ( $[\eta]$ ), also called as the limiting viscosity number, describes the intrinsic ability of a polymer coil to increase viscosity of fluid. It defines the hydrodynamic volume occupied by a single macromolecule. The parameter depends on size and conformation of the chain but is independent of polymer concentration. The intrinsic viscosity is measured with capillary viscometer by extrapolating reduced viscosity to infinitely dilute solution as shown by the definition in Equation 11 where  $\eta_{\text{red}}$  is the reduced viscosity. To measure the intrinsic viscosity of a polyelectrolyte, the charges are screened to eliminate the polyelectrolyte effect.

$$[\eta] = \lim_{c \rightarrow 0} \eta_{\text{red}} \quad \text{Equation 11}$$

The reduced viscosity ( $\eta_{\text{red}}$ ) is calculated by specific viscosity ( $\eta_{\text{sp}}$ ) which is calculated by the relative viscosity ( $\eta_{\text{rel}}$ ). The calculations are shown in Equations 12, 13 and 14 where  $c$  is concentration,  $\eta$  is sample viscosity,  $\eta_0$  is solvent viscosity,  $t$  is time for the sample to flow through and  $t_0$  is time for the solvent to flow through. Polymer concentration is typically expressed as grams of solute per one deciliter of solution leading to a unit of deciliters per gram,  $\text{dl/g}$ , for the intrinsic viscosity.

$$\eta_{\text{red}} = \frac{\eta_{\text{sp}}}{c} \quad \text{Equation 12}$$

$$\eta_{\text{sp}} = \eta_{\text{rel}} - 1 \quad \text{Equation 13}$$

$$\eta_{\text{rel}} = \frac{\eta}{\eta_0} = \frac{t}{t_0} \quad \text{Equation 14}$$

Alternatively, the intrinsic viscosity can be determined by linear extrapolation of so-called inherent viscosity ( $\eta_{\text{inh}}$ ) to zero concentration. The inherent viscosity is calculated by Equation 15.

$$\eta_{\text{inh}} = \frac{\ln \eta_{\text{rel}}}{c} \quad \text{Equation 15}$$

The experimental values for intrinsic viscosity are obtained either by Huggins Equation 16 or by Kraemer Equation 17 where  $k_H$  and  $k_K$  are Huggins and Kraemer coefficients respectively. According to both equations, the intrinsic viscosity is an intercept of the linear curve. Theoretically it has been proven that  $K_H - K_K = 0.5$  as long as the measurements are performed in the linear region.<sup>1</sup>

$$\eta_{reduced} = [\eta] + k_H[\eta]^2 c \quad \text{Equation 16}$$

$$\eta_{inherent} = [\eta] + k_K[\eta]^2 c \quad \text{Equation 17}$$

Intrinsic viscosity depends on the molecular weight of the polymer. The intrinsic viscosity can be used to calculate viscosity average molecular weight ( $M_v$ ) by Mark-Kuhn-Houwink-Sakurada Equation 18 where K and a are molecule specific constants depending on the sample matrix and other external parameters.<sup>1,11</sup>

$$[\eta] = KM_v^a \quad \text{Equation 18}$$

When polymer is dissolved into thermodynamically good solvent, the coils expand up to a volume where the solvent occupies most of the space within the polymer sphere. As the swelling continues, the polymer chains eventually start to pervade each other's space and the coils become entangled. The entanglements occur only after certain threshold amount of the polymer which is called the critical entanglement concentration. In dilute solutions, the chains are isolated, but as the polymer concentration in the solution is increased, a point where the molecules just touch each other will be reached. This threshold concentration is called the critical overlap concentration. The intrinsic viscosity essentially describes the volume occupied by the swollen polymer coil. Consequently, the critical overlap concentration ( $c^*$ ) equals the reciprocal of the intrinsic viscosity and it can be calculated by Equation 19.

$$c^* = \frac{1}{[\eta]} \quad \text{Equation 19}$$

## 2 Colloids

Colloids are systems consisting of at least two phases where one is dispersed into the other. The size of the dispersed particle can be anything within the range of 1 nm to 10  $\mu\text{m}$ . Key factors in understanding the behavior of colloids are particle size, which is similar in magnitude to the forces existing between the particles, and diffusive movement which is driven by Brownian motion. All molecules in the system are in random thermal motion and the local concentrations at any given instant fluctuate randomly. The direction and velocity of the colloidal particles is governed by a hydrodynamic drag towards region of lower concentration. When suspended in water, most solid particles exhibit a surface charge caused for example by ionization of functional groups, adsorption of ions, uneven distribution of constituent ions or dipole orientation. In aqueous systems the overall charge is usually negative and due to electrostatic repulsion, the colloidal suspension is stable. The function of flocculants and coagulants is to disturb this stability.<sup>5</sup>



## 2.1 Electrostatic properties

Surface charge of particles in aqueous liquid affects the distribution of nearby ions causing the counterions to accumulate onto the particles. For that reason, there are more ions close to the colloidal particles compared to the liquid bulk. Concentration of counterions decreases as the distance from the particle surface increases. The charged surface and neutralizing excess of counterions form an electrical double layer which instantiates an electric potential called Nernst potential. The dense layer of counterions fixed to the surface of a particle is called Stern layer and it moves along with the particle. The next layer of ions is called diffuse layer and there is a shear plane between the bound and diffuse layers. The potential difference between the shear plane and the bulk solution is known as zeta potential and it describes the potential at the surface of a particle. Increase in the value of zeta potential indicates that the repulsion between particles of the same charge increases and therefore the colloid becomes more stable. Formation of the electrical double layer is demonstrated in Figure 2.<sup>12</sup>

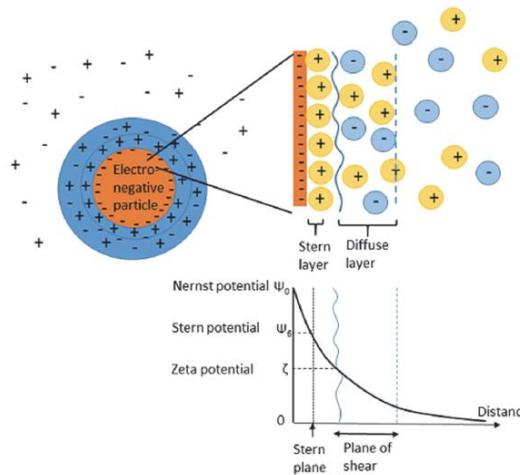


Figure 2. Demonstration of the electrical double layer.

Colloids are stable when particles in the suspension do not aggregate. The stability is described by a phenomenon called DLVO theory named after its creators Derjaquin, Landau, Verwey and Overbeek. The model combines the effects of attractive dispersion forces and electrostatic repulsion between the particles. The total potential energy ( $V_{tot}$ ) is calculated as a sum of these two forces as shown in Equation 20 and example of the potential curves are shown in Figure 3.<sup>5</sup>

$$V_{tot} = V_{attraction} + V_{repulsion} \quad \text{Equation 20}$$

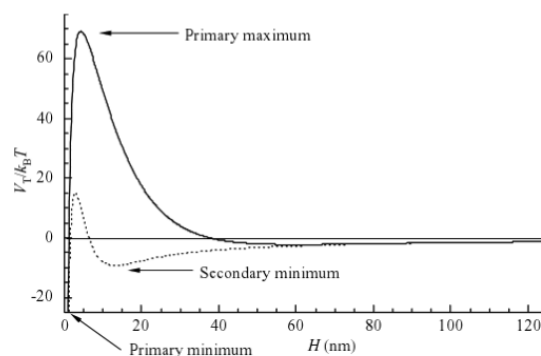


Figure 3. Potential curves demonstrating DLVO theory.

At the primary minimum in Figure 3, van der Waals attraction is much larger than the electrostatic repulsion. At this point, energy reaches the minimum and particles aggregate. When the distance between the particles increase, the electrostatic repulsion increases and eventually reaches the maximum potential value as shown in the figure. This maximum potential in the curve is called the primary maximum, and it quantifies the activation energy needed for aggregation to occur. As the separation increases, the interaction decreases again and at the secondary minimum the attractive forces become slightly larger than the repulsion.<sup>5</sup> The motion of particles depends on thermal energy which can be described by Boltzmann distribution. When the total potential energy exceeds the thermal energy ( $k_B T$ ), particles are in colloidally stable state. In the secondary minimum in Figure 3, the net attractive energy is only slightly larger compared to the average thermal energy and aggregation occurring at this point is reversible.<sup>5</sup> The balance between attractive and repulsive forces can be controlled by changing the type and concentration of electrolytes in the solution. Charged particles form the most stable colloidal system in a medium with low electrolyte concentration.<sup>1</sup>

## 2.2 Charge density measurement

As the surface charge of colloidal particles determines their reaction mechanism in aqueous solution, knowing the charge density enables predicting colloidal behaviour. Particle charge detector is used to continuously monitor the total charge of polyelectrolyte solution. The detector gives response to all dissolved and undissolved substances in the sample. In static solution, the oppositely charged counterions concentrate on the colloid surface. However, when the counterions are separated from or sheared off the macromolecule, a streaming current can be measured. When the streaming current result is zero millivolts, all charges in the sample are neutralized. Otherwise, the sign of the potential indicates whether the colloidal charge is anionic or cationic.

The potential is a relative measure depending on several external factors such as conductivity and viscosity of the sample, molecular weight and particle size of the macromolecule in addition to temperature and measuring cell dimensions. In the measuring cell, the colloiddally dissolved macromolecules adsorb by van der Waal forces onto the plastic surface of cell and piston. The piston is oscillated to create a flow which separates the free counterions from the adsorbed molecules. The measuring cell contains electrodes to measure the current induced by the counterions. To quantify the charge density of a polymer, the sample is titrated with an oppositely charged polyelectrolyte having a known charge density. The volume of the titrant needed to neutralize the charge of the macromolecule analyte is quantified. The specific charge quantity of the polyelectrolyte is calculated by Equation 21 where  $q$  is specific charge quantity,  $c$  and  $V$  are concentration and volume of the titrant respectively, and  $m$  is the mass of the studied polyelectrolyte. The specific charge quantity is typically recorded as milliequivalents per gram (meq/g). The total charge quantity can be obtained by multiplying the specific charge quantity by Faraday constant.<sup>13</sup>

$$q = \frac{cV}{m} \quad \text{Equation 21}$$

In the experimental part of this thesis, the anionic polyelectrolytes are titrated with cationic polydiallyldimethylammonium chloride, polyDADMAC, shown in Scheme 1.



Scheme 1. PolyDADMAC (1)

### 3 Flocculation and particle size measurement

Flocculation is aggregation of suspended fine particles by adsorption of long polymer chains onto the particle surface.<sup>5</sup> The clustered particles form large flocs which typically either settle to the bottom or float on top of the liquid. Compared to the fine particles, flocs are easier to be separated from the liquid phase for example by filtration. Flocculation process is typically used in solid-liquid separation in varying aqueous applications. The molecular weight of flocculating polymers is typically up to several millions.

### 3.1 Mechanism of flocculation

Flocculation of particles can be described by different mechanisms. The most typical mechanisms are bridging and patch, but also charge neutralization and sweep flocculation occurs. In bridging, patch and charge neutralization, the polymeric flocculant adsorbs onto the surface of solid particles. When bridging occurs, the adsorption takes place either by electrostatic attraction, hydrogen bonding or salt linkage. Electrostatic attraction occurs when the polymeric flocculant carries functional groups with a charge opposite to the surface charge of the particle. For non-ionic polymers, hydrogen bonding is a typical phenomenon. In that case, the positive partial charge of hydrogen is attracted by the negative surface charge of colloidal particle. Although individual hydrogen bonding is relatively weak, the polymer adsorption is strong due to a large number of hydrogen bonds. When minerals are flocculated, the mechanism may be formation of salt linkages. The overall surface charge of mineral particle is negative, but the charges are unevenly distributed and therefore the mineral particle contains also cationic metal ions on the surface. Anionic flocculants adsorb onto these positive groups by salt linkage forming a bridge between the mineral particles.<sup>8</sup>

When polymeric flocculant is added to aqueous suspension, some segments of the chain adsorb immediately to one or more particles. These segments are called trains while the rest of the polymer chain extends into the solution as tails and loops. When stirring of the suspension proceeds, tails and loops continue attracting more particles and eventually flocs are formed. The floc size depends on particle and polymer characteristics such as size, dose and type. The length of the polymer should be sufficient to extend from one particle to another and therefore the higher the molecular weight, the more efficient flocculation performance. It also follows that linear polymers would be more efficient than branched ones. In fact, the most important feature is the hydrodynamic volume of the polymer in the solution.<sup>14</sup>

For efficient flocculation, the colloidal particles should contain sufficiently unoccupied surface to be able to adsorb the polymer. Therefore, the polymer concentration should not be excessive or otherwise one chain could block all sites preventing bridging between the particles. On the other hand, too low amount of polymer leads to ineffective bridging between multiple particles and large flocs are not formed. Consequently, the concentration of polymeric flocculant should be optimized for each varying sample. Flocculation is a dynamic process and continuous mechanical shear causes a floc breakdown. In case of bridging mechanism, the floc breakdown is typically permanent, but the flocs are more shear resistant compared to the flocs formed by other mechanisms.<sup>8,15</sup>

Patch mechanism is a typical phenomenon when organic or inorganic coagulants are used together with high molecular weight flocculants. Polymeric coagulants have significantly lower molecular weight and higher charge density compared to flocculants, and for that reason they tend to adsorb onto the surface of a singular particle. When abundantly charged positive coagulant adsorbs onto negatively charged particle, localized charge reversal takes place. When negative flocculant is added, it interacts with the positive coagulant patches binding particles together as described for the bridging mechanism. Flocculation by patch mechanism is also shear sensitive, but re-flocculation occurs easily in low shear conditions. Flocs formed by patch mechanism are weaker than those formed by bridging, but stronger compared to flocs grown by charge neutralization process. Relatively high charge density is needed for polyelectrolytes to perform well in patch flocculation.<sup>8,15</sup>

In charge neutralization, the flocculation occurs simply as a result of reduced surface charge caused by adsorption of an oppositely charged flocculant onto a particle surface. The adsorption leads to a reduction of zeta potential and therefore the electrostatic repulsion between colloidal particles also reduces. Eventually the van der Waals forces of attraction encourage initial aggregation and micro-flocs form. The optimum flocculation is achieved with polyelectrolyte concentration decreasing zeta potential close to zero. This is called an isoelectric point where the colloidal suspension becomes destabilized. If polymer concentration is an overdose, charge reversal from negative into positive occurs and due to electrostatic repulsion, particles become dispersed again. The flocs formed by charge neutralization might be more fragile compared to the flocs formed by bridging or patch mechanisms.<sup>15</sup>

In sweep flocculation, a metal salt is added to an aqueous solution in sufficiently high concentration to cause precipitation of amorphous metal hydroxides. The colloid particles are then swept by these metal hydroxide precipitates. The mechanism is a combination of destabilization and transport, and it is mostly used in the systems having very low solids concentration.<sup>14</sup> Although different flocculation mechanisms can be distinguished, it is possible that several mechanisms operate simultaneously. Figure 4 represents the mechanisms of charge neutralization, sweep coagulation, bridging and patch flocculation.<sup>12</sup>

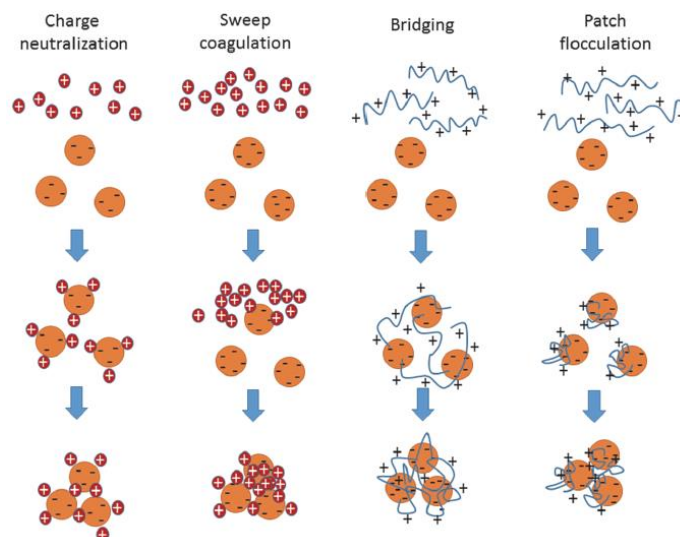


Figure 4. Mechanisms of charge neutralization, sweep coagulation, bridging and patch flocculation.

Flocculation occurs when particles and polymer chains collide as the solution is stirred. The stirring energy enables collisions, but it also causes the weak absorption linkages to break simultaneously. The maximum flocculation efficiency is achieved by extended period of low shear mixing.<sup>8</sup> Flocculation is a dynamic process and the floc structure changes continuously during stirring. Shear forces cause internal bonds to break, but they can be re-established when more favourable conditions prevail. The rate of floc formation can be regarded as a balance between aggregation and breakage, and at the chosen shear rate a steady state is eventually reached.

The floc strength is affected by the floc structure, bond strength and number of individual bonds between the particles as well as the size and shape of the constituent particles. Dense aggregates have high fractal dimension while highly branched and loosely bound large flocs have low fractal properties. The floc breakdown occurs either by fragmentation into smaller particles or by erosion. The ability of the particles to re-flocculate depends on the mechanism of flocculation. When the chemical bonds are broken during the disruption of flocs, the breakage is irreversible. In case of physical interactions between the particles, for example Van der Waals or electrostatic attraction, the aggregates are able to form again. In patch mechanism and charge neutralization, re-growth of flocs is typically detected. In sweep flocculation the collision efficiency is reduced as the broken flocs are covered by positively charged metal hydroxides, and therefore the ability to re-flocculate is poor. When high molecular weight polymeric flocculants are used, the polymer chains are susceptible to scission under high shear forces. This may lead to adsorption of chains into flattened configuration during the floc breakage preventing re-aggregation of particles by bridging mechanism.<sup>12</sup>

### 3.2 Coagulation-flocculation

Since most of the colloidal particles in aqueous solutions carry negative surface charge, coagulation-flocculation is typically performed using positive coagulants and non-ionic or anionic long chain flocculants. Coagulants are generally multivalent metal salts or low molecular weight polymers. Polyaluminium and ferric salts are currently the most widely used coagulants as they perform over a wide range of pH, temperature and colloid concentration.<sup>12</sup> When coagulant is added to the medium it hydrolyses rapidly, and the cationic species adsorb onto particles. The formation of cationic patches leads to the growth of micro-flocs. The flocs formed upon coagulation are often fragile, and they break when exposed to physical forces. To increase the efficiency of solid-liquid separation, polymeric flocculants are used after coagulation. Flocculants agglomerate the slowly settling micro-flocs forming larger and denser flocs which separate more efficiently. Unlike direct flocculation, the coagulation-flocculation is highly dependent on pH of the medium as the metal hydroxide precipitates are obtained only at certain pH. Compared to conventional flocculation, the advantage is better performance in inorganic-based waters. The direct flocculation is mostly limited to organic-based waters with high concentration of suspended solids.<sup>15</sup>

Typical coagulants are salts of multivalent metals, for example alum, aluminium chloride, ferric chloride, ferrous sulphate, calcium chloride and magnesium chloride. The disadvantages of using the metal-containing coagulants are environmental impacts since the metal hydroxide sludge is toxic, and metal residues in the treated water cause health implications to humans and animals. Aluminium salt coagulants are also claimed to induce Alzheimer's disease. Other drawbacks of coagulants include high sensitivity to pH and inefficiency towards very fine particles. In addition, the efficiency of some coagulants, such as polyaluminium chloride, is dependent on water temperature.<sup>15,16</sup>

Synthetic high molecular weight polymers have been used as flocculants in coagulation-flocculation for very many years. They are typically water soluble linear organic polymers consisting of various monomers, such as acrylamide and acrylic acid. The raw materials are often derived from oil-based non-renewable resources. Polymers vary in structure, composition, molecular weight, charge density and charge type. Compared to coagulants, the price of synthetic flocculants can be more than ten times higher slowing down the development of flocculants. Like coagulants, also synthetic flocculants reveal some environmental and health concerns. Their contaminants are generally unreacted monomer and chemicals used in the monomer production in addition to the reaction by-products. For example acrylamide is extremely toxic with a risk of severe neurotoxic and carcinogenic effects.<sup>15</sup>

### 3.3 Focused beam reflectance measurement

In this study, the flocculation process and floc properties are monitored by non-imaging scanning laser microscope technique called focused beam reflectance measurement, FBRM. The method is used to study the optimal dosage of polymers in flocculation based on particle size measurement. FBRM is a dynamic technique allowing to follow also the floc stability and resistance to shear forces. In addition, re-flocculation tendency can be analyzed, and interpretations of the flocculation mechanism can be made.<sup>17</sup>

The method is based on light scattering. A probe with the FBRM technology is inserted into a flowing medium of any concentration or viscosity. A laser beam is projected through a sapphire window and focused just outside the window surface. The highly focused beam rotates at high speed rate to eliminate the effect of a particle movement. As particles pass the window, the focused laser beam intersects the edge of a particle and backscatters the light until the laser reaches the opposite side of the particle. The FBRM probe contains optics to collect the backscattered light which is converted into an electronic signal. A unique discrimination circuit is used to isolate the duration of light reflection from each particle and a distance is calculated by multiplying the time period by the known scanning speed. The distance is a straight line between any two points of the particle structure and it is called a chord length. Tens of thousands of chords are measured every second to create a histogram in which the number of observed counts is divided into several chord length bins over the size range of 1-1000  $\mu\text{m}$ . The widths of the bins can be determined individually in the program. The number of particles as a function of size is reported as a result and varying statistical parameters can be calculated. The statistical parameters possible to be calculated automatically are for example mean, median, squared or cubic mean chord sizes and the number of counted chords between any size intervals.<sup>18</sup>

FBRM is used to analyze the evolution of statistical parameters during a dynamic test. The method allows to study the flocculation process of suspended particles in real time. In a conventional measurement, it is assumed that the average shape of particles is constant over millions of particles. The change in chord length distribution is considered as a function of change in particle dimension and number. In case the shape of the particle changes, the information can be filtered out or enhanced in the program depending on the application studied. Materials that produce only spectral reflection, such as glass beads, optically clear polystyrene and pure oil in water, do not backscatter and therefore cannot be analyzed by the FBRM technique.<sup>18</sup>



## 4 Biobased flocculants

Polymeric flocculants can be divided into synthetic polymers and biopolymer derivatives. Most of the polymers used worldwide are synthetic products based on fossil resources but due to increasing oil price, sustainability issues and environmental consciousness, renewable biobased materials are gaining more and more interest around the world. Biobased alternatives are currently important topics in many industrial research and development functions.

Biopolymer derivatives are chemically modified macromolecules originating from living organisms such as wood and other plants, animals, bacteria and fungi. After harvest and extraction, chemical structure of the biopolymers is often modified to change their chemical, physical and biological characteristics and thereby enhance their performance in selected applications. Typical examples of tailored functional properties are water-solubility, stability, polyelectrolyte nature and rheology.<sup>19</sup> Charge density is a key parameter required to be changed for the biopolymer derivatives to perform well in flocculation applications since majority of the naturally occurring macromolecules carry relatively low charge. By adding charged functional groups along the chain, performance of the polysaccharides in flocculation of colloidal particles may be improved. The major benefits of biobased derivatives are safety and biodegradability. In addition, they are relatively shear stable, easily available from renewable agricultural resources and do not produce secondary pollution as their sludge can be efficiently degraded with micro-organisms.<sup>8</sup>

Although biodegradability is a key advantage, it also reveals some disadvantages when biopolymer derivatives are used as flocculants. The polymer itself has a shorter self-life compared to synthetic products and the flocs lose stability and strength over time due to biodegradation. Biobased products also tend to be more susceptible to hydrolysis.<sup>15</sup> As the biopolymer derivatives typically have lower molecular weight and charge density compared to synthetic flocculants their performance is often less efficient. To enhance the functionality of natural polymers, hybrids of natural and synthetic polymers have been synthesized. For example, acrylamide functional group has been grafted onto amylose, amylopectin, alginate, cellulose ethers, chitosan, dextran, glycogen, guar gum, starch and xanthan gum<sup>14,20</sup>.

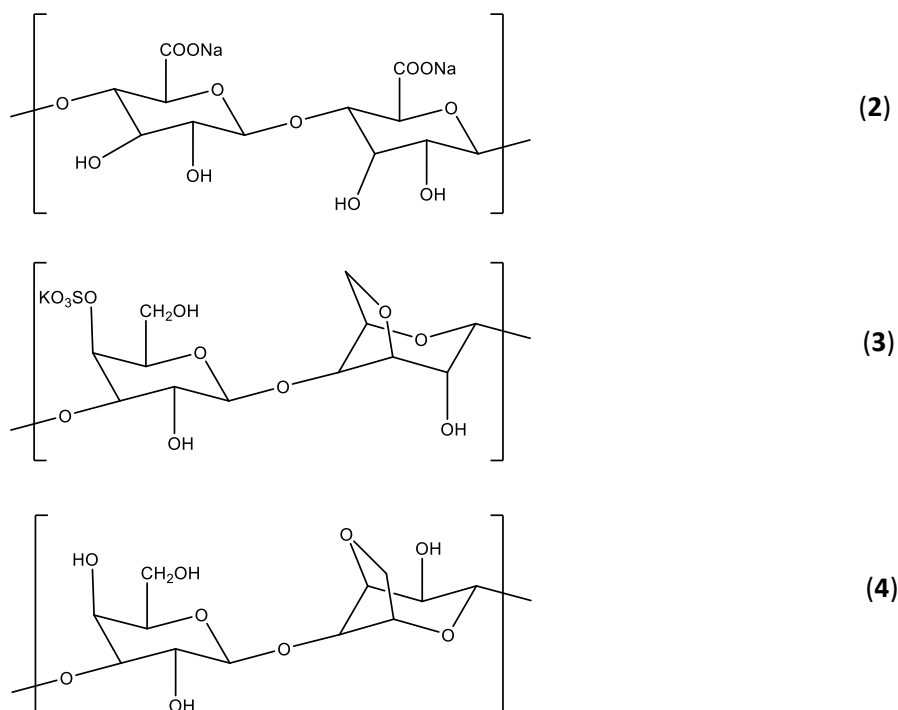
### 4.1 Polysaccharides

There are several different ways to categorize biobased polymers. One example is to divide them into three different groups being polyesters, polypeptides and polysaccharides. Polysaccharides are natural polymers produced by photosynthesis followed by further biosynthetic modifications. They are extracted from plants, trees, roots, arthropods or seaweed, and some products can be produced by microbial fermentation.

Monomer units are held together by glycosidic bonds and the polymer structure may be linear or branched. Key feature of polysaccharides is an ability to form stiff expanded structures by intramolecular hydrogen bonding, and certain structures form gel even at low concentrations. Polysaccharides are abundant, and their production can be even cheaper compared to synthetic oil-based products. They are typically used as viscosifying agents in varying applications such as water treatment, textile, oil, mining, cosmetology, pharmacology, food and fermentation industries.<sup>1,5,16</sup> There are several different polysaccharides having potential to be used in flocculation applications especially as chemically modified derivatives. These are for example agar, agarose, alginate, carrageenan, cellulose, chitosan, dextran, glucan, glycogen, guar gum, lignin, pullulan, starch, tannin and xanthan gum<sup>3,5,15,16,20</sup>. Although not being a polysaccharide, also gelatin protein extracted from animals has potential as a flocculant.<sup>5</sup>

#### 4.1.1 Seaweed polysaccharides

Three main polysaccharides from seaweed are agar, alginate (carboxylic polysaccharide) and carrageenan (sulphated polysaccharide). Agar and carrageenan are typically obtained from red seaweeds. Alginate is an intracellular structural component in brown seaweed, but it can also be produced extracellularly in bacteria.<sup>16,21</sup> The structures of alginate<sup>16</sup>,  $\kappa$ -carrageenan<sup>22</sup> and agar<sup>21</sup> are shown in Scheme 2.



Scheme 2. Structures of alginate (2), carrageenan (3) and agar (4).

Alginates exist in the kelp cell wall as insoluble salts of alginic acid with a counterion of calcium, magnesium, sodium or potassium. They are linear block copolymers consisting of  $\beta$ -D-(1 $\rightarrow$ 4)-mannuronic acid and  $\alpha$ -L-guluronic acid. There are over 200 different alginates with varying lengths and copolymer compositions. The distribution of the blocks highly affects the rigidity of the chain and thus the physical properties of the polymer. The molecular weight of commercially available sodium alginate varies between 32 and 400 kDa.<sup>21</sup>

Chemical and physical properties of alginates can be adjusted by derivatization. They can be modified for example by adding amine, carboxymethyl, acetate or sulphate ester groups to the backbone. Propylene glycol ester of alginic acid is commercially available and it has proved to have better acid stability compared to the natural product. It is also able to resist precipitation caused by multivalent metal ions such as calcium. Multivalent ions form crosslinks between the alginate chains. As their concentration increase the viscosity increases until gel is formed and eventually the polymer precipitates. Calcium is typically used to alter the rheological properties and gel characteristics of alginate solutions. Rheological behavior can be modified also by mixing the polymer with other polysaccharide such as xanthan gum.<sup>23</sup>

Alginates are used as thickening agents having also good ion exchange ability due to the free hydroxyl and carboxyl groups distributed along the chain. With monovalent counterions (except  $\text{Ag}^+$ ) alginates form soluble salts, but in the presence of multivalent cations (except  $\text{Mg}^{2+}$ ) they form gels or precipitate out of solution. Viscosity of aqueous alginate solution depends on the concentration, molecular weight and external salt concentration. At moderate concentrations, viscosity of alginate solution is quite constant between pH 6-8 but increases remarkably when pH is dropped below 4,5 reaching its maximum at around 3-3,5. At very low pH alginic acid forms a gel. This behavior is explained by hydrogen bonding which dominates over electrostatic repulsion. In dilute solutions, the viscosity of alginates decreases when pH is lowered from pH 6 as the electrostatic repulsion is screened and the chain conformation changes. In the range of pH 1-4 the alginic acid is hydrolyzed and thus the dilute solutions of alginates are considered to be stable approximately in the range of pH 5-10.<sup>21</sup> Commercially available water-soluble alginates are typically sodium, potassium, ammonium or calcium salts of alginic acid, propylene glycol alginate and alginic acid as such.<sup>23</sup>

The most important polymers extracted from red algae are agar and carrageenan<sup>21</sup>. Agar is a complex water-soluble polysaccharide consisting typically of alternating  $\beta$ -D-(1 $\rightarrow$ 4) and  $\alpha$ -L-(1 $\rightarrow$ 4) linked galactose residues. Agar has a rigid rod-shaped structure due to a high charge density.

It is relatively insoluble in cold water, but soluble in boiling water. Upon cooling it forms a gel even at as low concentration as 0,04 %. The gelation is primarily determined by the methoxy concentration in the chemical structure and therefore agars from different species have remarkably varying gelation temperatures. Common modifications for agar are substitutions of sulphate, pyruvate or methoxy groups.<sup>1,23</sup>

Carrageenan is a generic term used for a diverse group of sulphated polysaccharides extracted from cell walls of seaweed. There are three main types of carrageenan: iota, kappa and lambda. They are all linear copolymers comprising of repeating disaccharide sequence of  $\alpha$ -D-(1 $\rightarrow$ 3) and  $\beta$ -D-(1 $\rightarrow$ 4)-galactopyranose units. Some carrageenans are able to form gels when conformation changes from coil to helix upon cooling and cations are present to aggregate helices. Gelling depends on the level of sulphonation: the less sulphate ester groups in the structure, the higher the gel strength. Kappa carrageenan is able to form strong but brittle gels with a high gel strength while iota gels are typically elastic and cohesive. Lambda carrageenan is not able to form gels due to higher degree of substitution which leads to a configuration that prevents the formation of a helix. Carrageenans are susceptible to acid-catalyzed hydrolysis causing depolymerization. Typical molecular weight for commercial product is 400-600 kDa and the polydispersity is high. The product might contain up to 5 % of low molecular weight species (<100 kDa).<sup>22</sup>

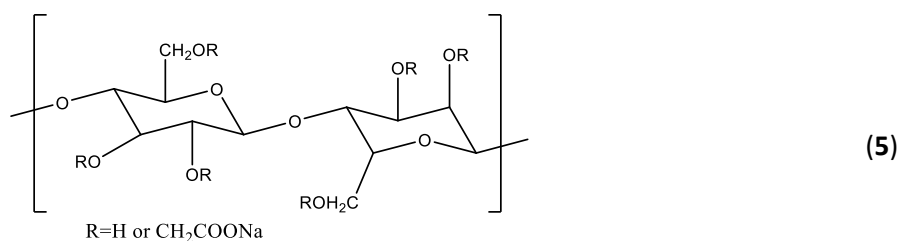
#### **4.1.2 Cellulose derivatives**

Cellulose is the most abundant renewable biopolymer consisting of  $\beta$ -D-(1 $\rightarrow$ 4)-glucose units. It is a linear homopolymer forming strong fibers that maintain the structure of plant cell walls, and it can be extracted from various plants, wood and micro-organisms. Cellulose has four different allomorphic forms (I-IV) depending on the location of hydrogen bonds between and within the strands. Natural cellulose, also called as cellulose I, has two slightly different crystalline forms known as cellulose I $_{\alpha}$  and I $_{\beta}$ . The properties of cellulose fibers vary greatly between plant species and even between different parts of the same plant. Cellulose derived from plants is typically a mixture of hemicellulose, lignin, pectin and other substances while bacterial-based cellulose is completely pure. The latter has much higher water content and tensile strength. Hemicelluloses are heteropolymers consisting of various monomers such as xylan, glucuronoxylan, arabinoxylan, mannan, glucomannan and galactoglucomannan. They have irregular structure, and chain branching is possible. Natural cellulose is insoluble in water and in most organic solvents. It also has relatively low reactivity towards adsorption or flocculation and therefore introducing new functional groups on the surface increases its polarity and hydrophilicity.<sup>12,16,21</sup>

Natural cellulose can be modified by derivatizing the polymer. There are three hydroxyl groups available for nucleophilic substitution reaction in each glucopyranosyl ring. Physical and chemical properties of the final product are affected by the type, distribution and uniformity of the substituents. Examples of cellulose derivatives are cellulose ethers, such as alkyl and hydroxyalkyl celluloses.<sup>23</sup> Cellulose xanthate can be produced as an intermediate of the viscose process. It has been used for selective flocculation of minerals but has a decreasing interest due to high cost and questionable environmental impact. Phosphorylated cellulose derivatives are formed for example by reaction of pulp or linters with phosphoric acid or via transesterification with alkyl phosphites. Their specialty is an ability to exchange ions and they also have fire-retarding properties. In addition, cellulose sulphates and borates can be produced, but their industrial applications are minor.<sup>21</sup>

Carboxymethyl cellulose, CMC, is one of the most important and most widely used water soluble cellulose derivative. It is a linear macromolecule obtained by substituting hydroxyl groups with ether groups by reaction of alkali-cellulose with sodium chloroacetate or chloroacetic acid. After etherification, the reaction slurry may be neutralized with hydrochloric or acetic acid leading to a relatively high salt content up to 40 %. To purify the product, salts may be extracted with water-alcohol mixtures.<sup>21</sup> Alkali metals and ammonium ions form water-soluble salts with CMC, but multivalent ions such as calcium prevents CMC from gaining high viscosity. At high polyvalent cation concentrations CMC precipitates out of solution.<sup>23</sup>

CMC becomes water soluble when the degree of substitution (average number of carboxymethyl groups per glucose unit) is larger than approximately 0,5. Typical raw materials for cellulose ethers are wood pulp and cotton linters. Compared to other cellulose ethers, the advantage of CMC is that it can be produced in atmospheric pressure. Commercially available CMC sodium salts are white hygroscopic and non-toxic solids with a degree of substitution typically between 0,3 and 1,2. Degree of substitution up to 3 has been achieved in a laboratory scale. Solutions of CMC are pseudoplastic revealing also thixotropic behavior especially in case of non-uniform distribution of substituents. Thixotropic behavior is explained by the presence of aggregates in aqueous dispersions. Viscosity of aqueous solution depends on pH and the maximum value is gained in neutral environment. Viscosity is also highly influenced by salt concentration due to the polyelectrolyte effect.<sup>21</sup> Cellulose derivatives are biodegradable and therefore also susceptible to microbiological attack depending on external factors such as temperature, pH, oxygen, moisture, concentration and contaminants present in the sample matrix. Biodegradation can be detected by decreased viscosity which indicates chain scission.<sup>23</sup> The structure of CMC is shown in Scheme 3.<sup>24</sup>



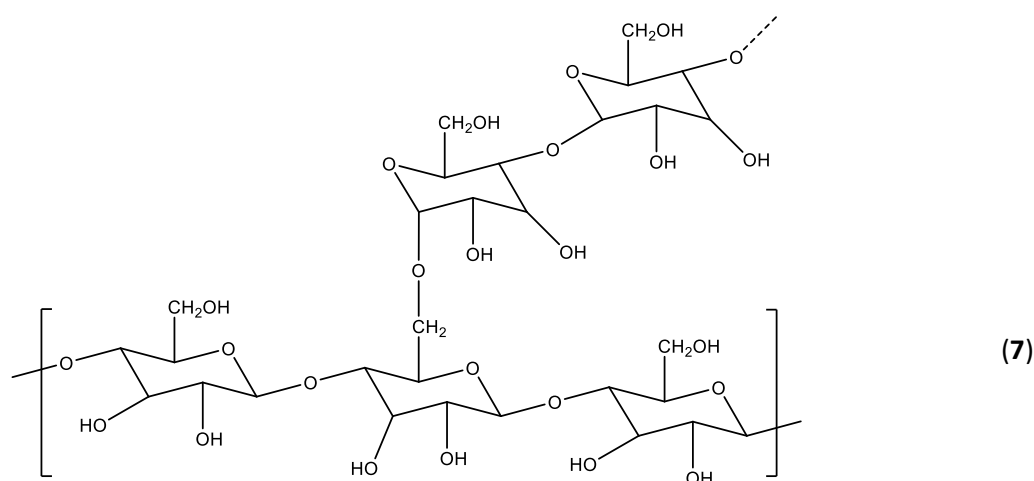
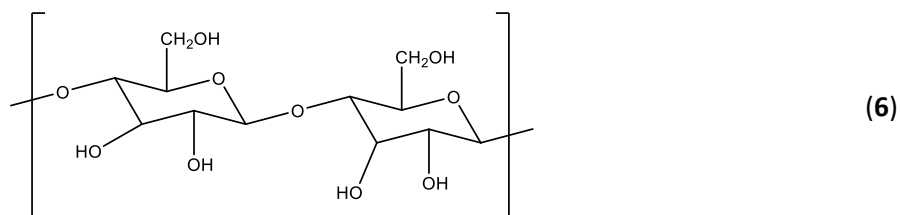
*Scheme 3. Structure of carboxymethyl cellulose (5).*

#### 4.1.3 Starch

Starch is the major carbohydrate found in various parts of different plants and it is one of the main energy resources required to sustain life. It is produced industrially from many different plants such as corn, rice, wheat, potato and tapioca. Native starch generally consists of amylose and amylopectin. Amylose is a linear water-soluble macromolecule containing mostly  $\alpha$ -D-(1 $\rightarrow$ 4)-glucopyranose units while amylopectin is a highly branched compound insoluble in water consisting of  $\alpha$ -D-(1 $\rightarrow$ 4)-glucopyranose units with  $\alpha$ -(1 $\rightarrow$ 6)-linkages. Amylopectin does not have a single definite structure and owing to the very high degree of branching it is one of the largest naturally occurring polymers. The amount of amylose and amylopectin present in starch varies depending on the plant it is extracted from. The amylose content varies up to 25 % while amylopectin content may be as high as 95 %. Typical molecular weight of starch varies between 0,01-10 million Da. Native starch is soluble in hot water, but insoluble in cold water, alcohol and other solvents.<sup>16,21</sup>

When amylose is dispersed in water the linear chains align side by side and intermolecular hydrogen bonds are formed by the hydroxyl groups. As the amount of hydrogen bonding is sufficient, the polymer aggregates and hydration capability lowers decreasing the product solubility. In dilute solution, with concentration less than 1 %, amylose precipitates and in more concentrated dispersion it forms a gel. The process of alignment, association and precipitation is known as retrogradation. The rate of retrogradation depends on temperature and pH as well as the size and concentration of amylose. The phenomenon occurs already at room temperature and is faster in lower temperatures. The process can be reverted or prevented by any process or additive that interferes the molecular alignment and hydrogen bonding, for example by addition of monovalent ions.<sup>23</sup>

Starch is one of the most studied biopolymers and one of the most versatile materials used in polymer technology. It is easily available from renewable resources and the price is low even in large quantities. In addition to polymer production, starch can be used as a raw material to produce ethanol, acetone and organic acids. It can also be used to produce biopolymers by fermentative processes or it can be hydrolyzed to employ as a monomer or an oligomer. Diversity of starch is increased by chemical modification which enables tailor-making products for varying applications. Chemical structures of amylose and amylopectin are shown in Scheme 4.<sup>21</sup>



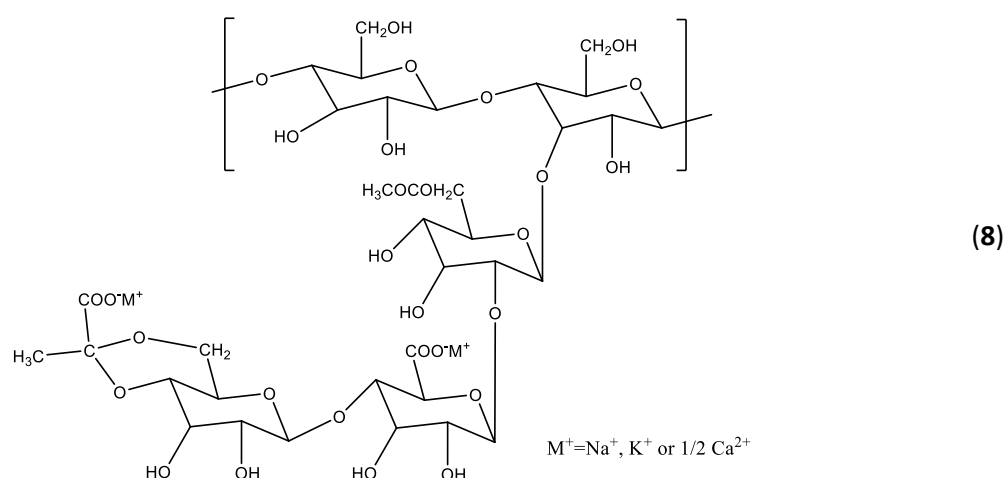
Scheme 4. Structures of amylose (6) and amylopectin (7).

#### 4.1.4 Xanthan gum

Xanthan gum is a microbial extracellular polysaccharide produced by *Xanthomonas* bacterium. It is a heteropolysaccharide with each repeating block containing five sugar units. The backbone of xanthan gum is the same as in cellulose consisting of D-glucose units linked by  $\beta$ -(1 $\rightarrow$ 4)-glycosidic bonds. However, xanthan gum has side chains that are trisaccharides of  $\alpha$ -mannose,  $\alpha$ -glucuronic acid and  $\beta$ -mannose attached to every other glucose unit at the position C<sub>3</sub>. The trisaccharide composition may vary as the terminal mannose may contain ketal-linked pyruvate group, and inner mannose may be acetylated at position O<sub>6</sub>. Pyruvate and acetate groups may attach to the pentasaccharide repeat units by different patterns, and their relative abundance affects the stability of the ordered structure.<sup>25,26</sup>

The amount of side chains including the pyruvate group varies between 0 and 100 % depending on the fermentation conditions and bacterial strain.<sup>27</sup> Xanthan gum has an extraordinary resistance to enzymes which may be explained by large side chains shielding the backbone.<sup>23</sup> Typical molecular weight for xanthan gum is 0,9-1,6 million Da<sup>21</sup> but it has been reported to be found in as high size as 13-50 million Da<sup>23</sup>.

Side chains of xanthan gum consist of charged functional groups which play a vital role in its aqueous solubility and structural conformation. Conformation of the xanthan gum chain undergoes a reversible transition between helix and random coil depending on the environment, for example ionic strength, nature of added electrolytes and temperature of the medium. In solid state, xanthan chains form antiparallel right-handed double helix which is stabilized by four intramolecular and one intermolecular hydrogen bonds. In solution of low ionic strength or at high temperature xanthan gum adopts a disordered random coil conformation as the anionic side chains repel each other. When electrolytes are added to the solution, electrostatic repulsion between the side chains is screened causing them to fold down compactly against the backbone. 5-fold ordered structure is formed and maintained by hydrogen bonding. This causes the polymer chain to straighten into a relatively rigid helical rod which has a persistence length greater than 100 nm. As the polymer chains are in extended conformation viscosity of the solution increases. Xanthan gum is one of the stiffest biopolymers. If the solution is diluted or heated, the random coil is reverted, but increasing electrolyte concentration maintains the rod shape also at higher temperatures and greater dilutions. Xanthan gum is able to form gels when cross-linked with certain metal ions or interacted with other polysaccharides. In highly concentrated solution xanthan gum may present liquid crystalline phases.<sup>21,25,26</sup> The structure of xanthan gum is shown in Scheme 5.<sup>23</sup>



*Scheme 5. Structure of xanthan gum (8).*

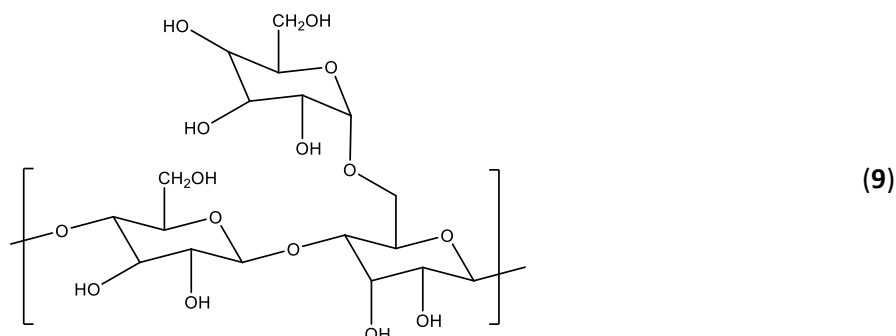


#### 4.1.5 Guar gum

Guar gum is a polysaccharide present in the seed endosperm of annual leguminous plants *Cyamopsis tetragonalobus* and *Psoraleoides*. The polymer is galactomannan consisting of galactose and mannose building blocks with slightly varying ratios depending on the origin of the seed. The average is typically 1,5-2 mannose residues for every galactose units with only a few or none non-substituted regions. The backbone is linear  $\beta$ -D-(1 $\rightarrow$ 4)-mannopyranose with random branches of  $\alpha$ -(1 $\rightarrow$ 6)-D-galactose units. A typical molecular weight of commercial guar gum product is 0,1-1 million Da. Guar gum is generally dissolved in water, but it tolerates also limited concentrations of water-miscible solvents such as alcohols. Solutions of commercial guar gum products are often turbid due to the presence of insoluble residues from the seed endosperm. Solubility and clarity of the guar gum polymer can be highly adjusted by derivatization, for example by hydroxyalkylation or carboxymethylation. Also biodegradability of the polymer can be changed by suitable substitution. Derivatization is typically performed by etherification but also some esterification reactions are possible.<sup>20,23</sup>

Each sugar residue in the guar gum backbone carries two hydroxyl groups in cis-form. This configuration leads to a characteristic reaction with dissociated borate ions. In alkaline aqueous solution guar gum forms gel in the presence of borate. The reaction is fully reversible depending on the pH, and guar gum dissolves again when the pH is dropped below 7. The critical pH where guar gum forms gel can be adjusted by varying concentration of dissolved salts. Guar gum derivatives are less susceptible to gelation with borate compared to the natural product because the substituents change the configuration. They might also prevent adjacent chains from approaching each other and decrease the number of unsubstituted positions available for the reaction to occur.

In addition to the borate reactions, gels with varying strengths may be formed by other reactions, for example by complexation with transition metals via cis-hydroxyl positions. Guar gum reacts strongly also with certain inorganic polyvalent cations. For example high concentration of calcium salt in alkaline medium leads to the guar gum gelation. Compared to gelation by the borate reaction, gels formed by multivalent cations often lead to precipitation or unstable gel formation. The structure of guar gum is shown in Scheme 6.<sup>23</sup>

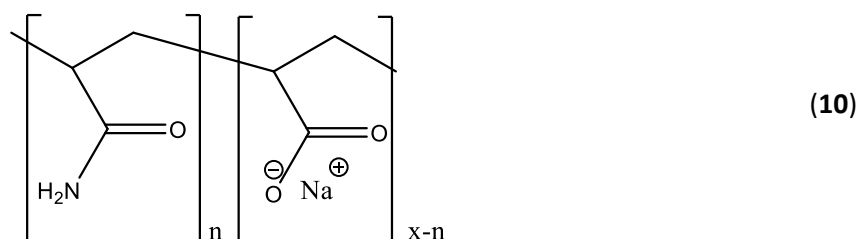


Scheme 6. Structure of guar gum (9).

#### 4.1.6 Polyacrylamide reference

Most commonly used anionic polymers in coagulation-flocculation treatment are synthetic oil-based polymers such as polyacrylamide, polyacrylic acids, polystyrene sulphonic acids and their derivatives<sup>12</sup>. In this study two polyacrylamide samples with varying molecular weights are used as references when comparing flocculation performance of the biobased products. Anionic polyacrylamide, PAM, is a synthetic linear copolymer consisting of acrylamide and acrylate repeating units. It is produced either by chain polymerization of acrylamide and sodium acrylate monomers or by hydrolyzing polyacrylamide polymer. During the hydrolysis some of the amide groups hydrolyze into carboxylic acids dissociating into negative carboxylate ions that attract positive counterions such as sodium and potassium. A degree of hydrolysis is a measure used to describe the mole fraction of hydrolyzed amide groups. For commercially available PAMs the degree of hydrolysis typically varies between 15 and 35 %.

PAMs are used as flocculants in a large variety of industries due to low manufacturing cost even in large quantities. The properties of PAMs can be easily modified by tailoring the structure, and they are available in varying molecular weight, ionic charge type and charge density. PAMs are widely used as flocculants as they have a very high molecular weight, typically between 5 and 20 million Da<sup>8</sup>. Chemical structure of partially hydrolyzed polyacrylamide with sodium as the counterion is shown in Scheme 7.



Scheme 7. Partially hydrolyzed PAM with sodium counterion (10).

## 4.2 Chemical modification of polysaccharides

The importance of renewable raw materials and sustainable processes continue increasing in the future, and to meet the efficient performance criteria, modified biobased products are needed. The feasibility of polysaccharides in varying industries can be broadened by introducing functional groups to their structures to change their chemical, physical and biological properties. One of the most typical modification reactions of polysaccharides is nucleophilic reaction of the saccharide oxygen to form ether or ester. Other reactions are for example introduction of heteroatomic nucleophiles into the polymer chain with saccharide carbon as the electrophile, oxidation, reactions of carboxylic acid or nitrogen and formation of unsaturated polysaccharide derivatives. The oxidative reactions are for example chemical oxidation of alcohols into aldehydes or carboxylic acids and oxidative glycol cleavage. The extent of derivatization reaction is typically described by the degree of substitution which defines the number of substitutions per monomer unit.<sup>28</sup>

In etherification the saccharide alcohol reacts with alkylating agent in the presence of base. Strong base is used to deprotonate alcohol to form negatively charged alkoxide which reacts with the alkylating agent, such as alkyl halide or sulphonate. Esterification is a reaction of saccharide alcohol with acylating agent. Carboxylate esters may be formed for example by acid catalyzed Fischer esterification of carboxylic acid and alcohol or by using activated derivatives such as acid chloride or anhydride as the acylating agent. In the latter case the reaction proceeds either by acid or base catalyzed. The primary alcohol in the saccharide unit is more nucleophilic compared to the secondary alcohols and therefore typically more susceptible for reaction.

Complete regioselectivity of reacting alcohols is often not achieved because there might be differences in the reactivities between primary and secondary alcohols. As the reaction proceeds, the concentration of primary alcohol decreases faster affecting the rate of reaction, and therefore regioselectivity is decreased. Derivatization of polysaccharides is typically performed in solvent rather than in solid phase. In solvent, the network of hydrogen bonds is disturbed, and therefore reactions may be carried out in milder conditions. Water is poor solvent for alkylation reactions since it might hydrolyze the alkylating agent.

In the reaction of saccharide carbon as an electrophile, the saccharide oxygen is replaced by nucleophilic substitution. The hydroxyl group is first transformed into a good leaving group making the attached carbon susceptible for the nucleophilic attack. In the second phase the electrophilic carbon reacts with the nucleophile while the leaving group is displaced. Compared to their hydrocarbon-derived counterparts saccharide electrophiles are less reactive and the reaction proceeds almost inevitably by  $S_N2$  mechanism. This is explained by the electron withdrawing hydroxyl groups which would strongly destabilize the intermediate carbocation in case of  $S_N1$  mechanism.

Oxidation of polysaccharides may be carried out in several different ways depending on the target end product. One of the simplest reactions is oxidizing the free primary alcohol to give aldehyde or carboxylic acid. When oxidized all the way to carboxylic acid functionality, polysaccharide based uronic acid is formed resembling the structure of natural polyuronic acids such as alginate or pectin. The oxidation may be performed by chemical or enzymatic mechanisms. In the oxidative cleavage dicarbonyl compound may be attained by ring-opening reaction, but selective cleavage is a challenge.

Reactions of carboxylic acids are based on uronic acid residues. Several polysaccharides, for example alginate and pectin, carry uronic acid residues already in their native structure. The carboxylic acid in C<sub>6</sub> position may undergo varying electrophilic and nucleophilic reactions such as esterification, amide formation and multicomponent reactions. The nitrogen reactions concern polysaccharide amines. The saccharide nitrogen acts as a nucleophile reacting with electrophiles to give amides, higher order of amines, ammonium salts or imines. The difference between nitrogen and oxygen reactivities allows nitrogen derivatizations to be performed in aqueous solutions without the need to protect the free hydroxyl groups. The unsaturated derivatives with carbon-carbon double bond can also be synthesized, but they represent unusual types of functional groups in modified polysaccharides.

## EXPERIMENTAL

The aim of this thesis is to study the potential of biobased polymers to be used in the applications where synthetic polyacrylamides are currently widely used. There are several drivers for the research of which the most prominent are the importance of sustainability and safety. Depleting oil reserves and awareness of environmental risks of oil-based polymers lead to constantly tightening regulations all around the world. Biobased polymers offer a safe alternative to replace the synthetic materials to meet the constraints.

The selected application for the thesis is flocculation. Based on chemical structures of the biobased polymers it is assumed that their performance in flocculation is not as efficient compared to the synthetic polyacrylamides. Natural polymers typically have lower charge density and molecular weight which are the key characteristics affecting flocculation performance. For that reason, the aim is to study chemically modified biopolymer derivatives in the application testing. To limit the subject for the assigned time period, the scope of this thesis is to study only anionically modified derivatives.

The first task was to find out what types of anionically modified biopolymers exist and how they have been tested in flocculation application. Commercially available products of varying chemistries were gathered and screened by viscosity and charge density. Based on the results, the most potential products were selected and purified. The purification was an essential step to be able to compare the biopolymers as such eliminating the effect of salts and other impurities formed during the manufacturing process. Next, the purified products were characterized by intrinsic and apparent viscosities in brine and water and by charge density in two different pH environments. Finally, the samples were tested in flocculation application monitoring the flocculation performance by focused beam reflectance measurement.

### 5 Screening and purification

Totally 28 samples representing 10 different types of biobased polymers were received from different suppliers. The samples are chemically modified derivatives of the biobased products, and some contain additional anionic functional groups attached to increase their charge densities. Two anionic synthetic polyacrylamides with varying molecular weights were selected for reference. This thesis is done for academic purposes only, and the scope is to compare different types of biobased derivatives. To avoid making conclusions of specific trademarks, the tradenames are not published. The studied biobased polymer derivatives and their coding are listed in Table 1.

Table 1. Biobased polymer derivatives and sample coding.

Biobased polymer derivative	Amount	Codes
Carboxymethyl cellulose	5	CMC S1, S2, C2, C2, W1
Xanthan gum	7	Xanthan gum S1, S2, S3, S4, X1, X2, G1
Starch	7	Starch W1, W2, H1, H2, G1, G2, V1
Alginate	2	Alginate 1, 2
Guar gum	1	Guar gum
Carrageenan	1	Carrageenan
Polyacrylamide	2	PAM 1, 2
Methyl cellulose	1	Methyl cellulose
Hydroxyethyl cellulose	2	HEC 1, 2
Hydroxypropyl methylcellulose	1	Hydroxypropyl methylcellulose
Agar	1	Agar

### 5.1 Screening

In flocculation application molecular weight and charge of the polymer play an important role in determining how efficient the chemical treatment is. As described previously, colloidal particles in aqueous solution carry surface charge and therefore polyelectrolytes are used to floc the particles. Molecular weight affects the hydrodynamic radius of the polymer coil in the solution and that determines the distance over which the polymer is able to gather particles together. All 30 samples were decided to be screened based on charge and size to select the most potential products for further testing.

Due to complex set of interactions and lack of accurate reference material for the selected biobased products, the molecular weight of the samples appeared to be difficult to determine reliably by absolute or relative quantification methods. Therefore, it was decided to study rheology, namely viscosity, of the samples to indicate the difference between molecular weights. All 30 samples were dissolved as 1 % or 0,5 % solution into deionized water. The smaller concentration was used for two CMC samples and the two reference PAMS to get their viscosities low enough to be able to be measured with the selected apparatus. Viscosities were measured by Brookfield LVT viscometer in 25 °C using small sample adapter and spindle number SC4-31. Viscosities were recorded at several rotation speeds, but the comparison is made at the highest speed and maximum torque value.

Charge densities of most of the samples were analyzed by polyelectrolyte titration. Polydiallyldimethylammonium chloride, polyDADMAC, with a specific charge quantity of 1 meq/l was used as the cationic titrant. The anionic biobased polymers in addition to the two polyacrylamide references were dissolved as 1000 ppm stock solution in deionized water.

The stock solutions were diluted down to 100 ppm or 500 ppm, and the diluted samples were titrated. pH of the samples was not adjusted, but it was measured. All samples were titrated in approximately neutral environment. Based on the chemical structure of carboxymethyl cellulose it is known to have comparatively high charge density, and for that reason the best CMC samples were selected based on viscosity only. Example of the charge density calculation by Equation 21 is shown below for the sample Xanthan gum S1. In the titration, 1,61 ml of polyDADMAC with a specific charge density of 1 meq/l was required to titrate 1,0014 mg of the Xanthan gum S1 anionic polymer leading to a charge density result 1,6 meq/g.

$$q = \frac{cV(\text{polyDADMAC})}{m(\text{Xanthan gum S1})} = \frac{1 \frac{\text{meq}}{\text{l}} * 1,61 * 10^{-3} \text{l}}{1,0014 * 10^{-3} \text{g}} = 1,6 \text{ meq/g}$$

The apparent viscosities and charge densities of the screened samples are listed in Table 2. Based on the results, the most potential samples were selected for purification and further testing. The selection includes four CMCs, three xanthan gums, two starches, one alginate, the guar gum, and the carrageenan in addition to the two reference PAMs. Although the viscosities of the starch and carrageenan samples are very low, they were picked due to their moderate charge densities to get a varying selection of biobased products. The 14 bolded samples in Table 2 were purified and tested further.

Table 2. Apparent viscosity and charge density results for screening the samples.

	Apparent viscosity, 1 % in H <sub>2</sub> O			Anionic charge density	pH
	Speed, rpm	Viscosity, mPas	Torque, %		
CMC S2	100	40	13		
<b>CMC C1</b>	1	23 900	80		
<b>CMC C2</b>	4	7 350	98		
<b>Xanthan gum S1</b>	5	5 410	88	1,6 meq/g	6,2
Xanthan gum S2	5	5 470	91	1,6 meq/g	6,0
Xanthan gum S3	5	5 440	89	1,6 meq/g	5,9
Xanthan gum S4	10	2 550	85	1,8 meq/g	5,8
<b>Xanthan gum X1</b>	2	11 600	97	1,4 meq/g	6,4
Xanthan gum X2	20	1 170	78	1,6 meq/g	6,3
<b>Xanthan gum G1</b>	1	29 400	98	1,7 meq/g	6,7
<b>Starch W1</b>	100	32	10	2,0 meq/g	7,9
Starch W2	100	35	11	0,1 meq/g	6,7
<b>Starch H1</b>	100	30	10	2,0 meq/g	7,5
Starch H2	100	34	11	1,4 meq/g	6,9
Starch G1	100	8	3	0,3 meq/g	5,9
Starch G2	100	7	2	0,5 meq/g	6,1
Starch V1	100	48	16	0,1 meq/g	6,0
<b>Alginate S1</b>	20	670	46	4,8 meq/g	7,6
Alginate S2	50	450	75		
<b>Guar gum</b>	50	390	65	0,6 meq/g	7,3
<b>Carrageenan</b>	100	40	13	2,3 meq/g	5,7
Methyl cellulose	50	361	60	0,1 meq/g	5,9
Hydroxypropyl methyl cellulose	50	244	57	0,2 meq/g	7,9
HEC 1	2	10 800	72	0,2 meq/g	6,8
HEC 2	20	1 330	88	0,2 meq/g	6,8
Agar		gel		0,4 meq/g	7,3

	Apparent viscosity, 0,5 % in H <sub>2</sub> O		
	Speed, rpm	Viscosity, mPas	Torque, %
<b>CMC S1</b>	10	2 440	80
<b>CMC W1</b>	20	1 500	99
<b>PAM 1</b>	20	1 300	87
<b>PAM 2</b>	10	2 750	91



## 5.2 Purification

The samples analyzed in this thesis are commercially available products that may include plenty of impurities formed during the industrial production. For example, neutralization of the CMC slurry with hydrochloride acid induces formation of sodium chloride salt in the sample, and the concentration may raise up to several dozens of percentages. When the sample is dissolved in aqueous medium, the additional ions affect the polyelectrolyte effect changing rheological behavior and effective charge of the product. Multivalent cations cause even more drastic effect on the ion binding phenomena compared to monovalent ions. To be able to compare the polymers of interest without seeing the effect of impurities formed in the production, the samples need to be purified. Three different purification procedures were tested with a selected carboxymethyl cellulose sample called CMC C1.

In the first test impurities, being mostly salts, were tried to be removed based on the density difference between the salts and the polymer. The product was dispersed in chloroform where neither sodium chloride nor the polymer is soluble. In the ideal case, the polymer should float at the surface while salts drop to the bottom. However, in this case also the CMC polymer sank, and therefore this purification method was decided to be discarded.

The next purification test was extraction with water-isopropanol mixture. Isopropanol (IPA) forms a homogeneous azeotropic mixture with pure water, but when salt is added the two liquids are separated.<sup>29</sup> The suitable water-isopropanol ratio was first solved by studying how much water can be added to isopropanol to be able to dissolve sodium chloride without dissolving the polymer. The water concentration of 20 % appeared to be the most suitable. Consequently, the CMC C1 polymer was extracted with 20 % H<sub>2</sub>O in IPA -solvent. After extraction, the polymer was filtered in Büchner funnel and dried in 105 °C for two hours.

The third purification method was dialysis. The sample was dialyzed against deionized water in a tube having a cutoff 6-8 kDa. The cutoff describes the size of the smallest solute which is retained inside the membrane. The sample is dissolved in water and placed in a dialysis membrane tubing. The tubing is sealed, immersed in the dialysis buffer and incubated in magnetic stirring changing the buffer occasionally. Due to the concentration difference across the membrane, the molecules able to pass the membrane strive for balancing the concentrations in both sides. By changing the outer buffer solution and increasing its volume in comparison to the sample, the dialysis efficiency is enhanced. The dialysis requires dissolved and dilute solution for the purification to be efficient. After dialysis, the polymer was freeze-dried in vacuum to get solid polymer for further testing. To quantify the effect of dialysis, conductivity of the deionized water and the sample was measured.

However, the change in conductivity was minor so either the sample didn't contain much electrolytes to begin with or the resolution of the conductivity measurement was not sufficient for this purpose.

To compare the purification efficiency between the H<sub>2</sub>O-IPA extraction and dialysis, charge densities of the samples were measured by polyDADMAC titration. The results are shown in Table 3 as a comparison to the unpurified sample. The charge density of the dialyzed sample is the highest indicating that the sample contains least counterions that screen the effective charge. As described in the screening tests, also these samples were dissolved as 1000 ppm solution in deionized water and diluted down to 100 ppm for the measurement. By visual inspection it was noticed, that the dialyzed sample dissolved better compared to the extracted one. For the reasons explained above, the purification method for all samples was decided to be dialysis. The dialysis was performed over at least two days by changing the deionized water buffer five times.

*Table 3. Comparison of purification methods for the sample CMC C1.*

<b>Sample</b>	<b>Anionic charge density, meq/g</b>
As such	3,4
Dialyzed	4,5
H <sub>2</sub> O-IPA extracted	3,9

For the dialysis, samples were dissolved as 1 % concentration in deionized water in 500 ml volume. The biobased polymer particles are very fine compared to the synthetic PAMs and could not be dispersed homogeneously in water in that large volume and concentration without additives. Therefore, the polymers were first suspended into isopropanol. The suspension was then poured into the water vortex to get a proper dissolution of the sample as 1 % concentration. The added isopropanol was removed in the dialysis. After the dialysis, samples were freeze-dried in vacuum to get solid polymer for further testing. The physical composition of freeze-dried polymer is very fluffy, and the polymer chains are in loose physical form making the dialyzed polymer easily dissolvable also at high concentration.

Purifying the samples appeared to be an essential step to be able to compare the polymers without the effect of the impurities and additives. An extreme example of the effect of purification is the guar gum sample. In Figure 5, the Brookfield apparent viscosities of dialyzed and unpurified samples are plotted as a function of rotational speed in 25 °C by spindle SC4-31. The viscosity of purified sample is much higher compared to the original sample due to removal of charge screening electrolytes.

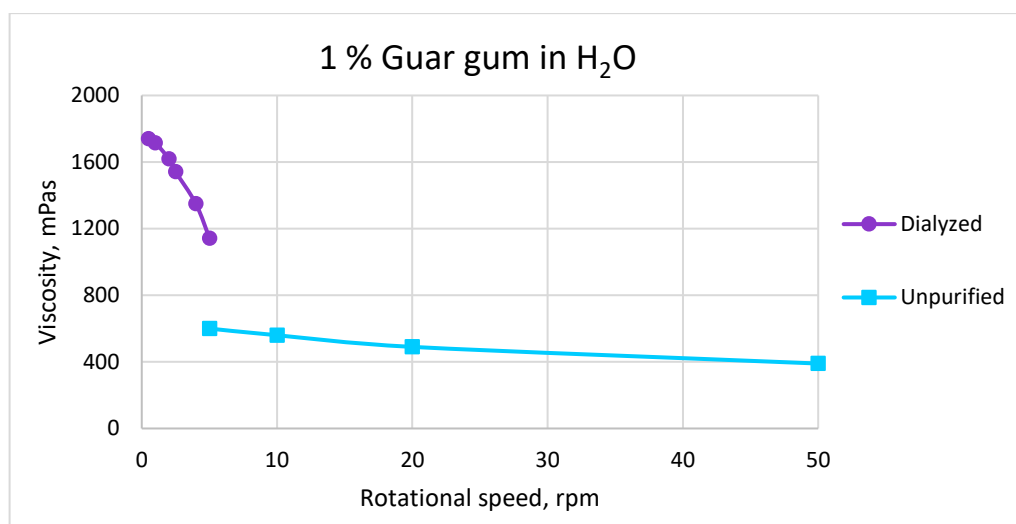


Figure 5. The effect of purification on Guar gum viscosity.

## 6 Characterization of selected polymers

The 12 purified biobased anionic polymers in addition to the two synthetic references were characterized by charge density titration in two different pH environments, by apparent Brookfield viscosity in water and in sodium chloride solution, and by intrinsic viscosity in sodium chloride solution. After dialyzing and freeze-drying the samples, they were stored in room temperature in normal atmosphere. The equilibrium moisture content was assumed to be equivalent in all samples.

Molecular weights of the polymers were tried to be quantified by size exclusion chromatography and dynamic light scattering methods. However, due to the intra- and intermolecular electrostatic interactions determining the sizes of biobased polyelectrolytes accurately appeared to be extremely challenging and the measured chromatograms revealed poor resolution. The analytical method development is out of scope of this thesis due to time restrictions, and therefore the comparison between the samples was decided to be made only by rheology and charge.

### 6.1 Charge density

Charge density of the samples was measured by titrating with 1 meq/l polyDADMAC using Charge analyzing system from AFG Analytical GMBH. Polymers were dissolved as 1000 ppm concentration and diluted down to 100 ppm in deionized water. Two samples of each polymer were transferred to separate beakers for pH adjustment. One sample was adjusted to pH 7,5 with sodium hydroxide solution and the other to pH 4 with acetic acid. The consumptions of acid and base were recorded and taken into account when calculating the results.

Charge densities were measured in acidic and neutral environments to get an indication about the strength of the anionic groups in the polymers. Strong acids dissociate totally also in low pH minimizing the difference between charge densities measured in low and high pH. In case of weak acid, such as carboxylic acid, the anionic charge is larger in high pH since the functional group protonates only partially in acidic environment. Charge densities are calculated by Equation 21 as demonstrated previously in the screening chapter 5.1. The results are shown in Table 4.

*Table 4. Charge density results of purified samples in pH 7,5 and 4.*

Sample	pH	Anionic charge density, meq/g
CMC C1	7,5	4,2
	4	3,4
CMC C2	7,5	4,2
	4	3,4
CMC S1	7,5	4,7
	4	2,6
CMC W1	7,5	4,3
	4	3,5
Xanthan gum X1	7,5	0,4
	7,5	0,4
	4	1,5
	4	1,6
Xanthan gum S1	7,5	1,9
	4	1,7
Xanthan gum G1	7,5	2,2
	4	2,2

Sample	pH	Anionic charge density, meq/g
Alginate 1	7,5	5,5
	4	5,0
Guar gum	7,5	0,8
	4	0,7
Carrageenan	7,5	2,8
	4	2,8
Starch W1	7,5	2,0
	4	1,3
Starch H1	7,5	2,1
	4	1,5
PAM 1	7,5	4,0
	4	1,6
PAM 2	7,5	3,1
	4	1,7

When the anionic functional group in the polymer is a weak acid the charge density in pH 7,5 is notably higher than the charge density in pH 4. This phenomenon is most clearly seen for the two synthetic polyacrylamide samples known to contain carboxylic acid groups. The effect of pH is also clearly observed for the CMC and starch samples and slightly for the alginate. Carrageenans are sulphated polysaccharides already by nature and thus contain strong acid groups which dissociate also in low pH. Charge density of carrageenan is independent of pH as expected by the natural structure. Based on the results, charge density of the guar gum derivative seems to be almost independent of pH. However, the charge value is relatively low to begin with compared to the other samples.

Xanthan gum has a peculiar behavior in aqueous solution. For the sample Xanthan gum G1, the charge density appears to be independent of pH and nearly independent for the sample S1. The behavior of Xanthan gum X1 having lower anionic charge at higher pH is unrealistic. The sample was measure twice to confirm the result. According to Table 2 the charge density of unpurified Xanthan gum X1 in pH 6,4 is 1,4 meq/g being very close to the result of 1,5-1,6 meq/g in pH 4. The anionic charge density of the sample decreases remarkably when pH of the sample is raised with sodium hydroxide although the charge of anionic polyelectrolyte should behave oppositely.

It is suggested that the peculiar phenomenon could be explained by the exceptional capability of xanthan gum to form helices. It has been discussed before that when electrolytes are added to aqueous solution of xanthan gum, they screen the anionic repulsion between the side chains allowing them to wrap around and form hydrogen bonds to the backbone. Based on the unrealistic charge density result at high pH, it is suggested that increasing the pH by sodium hydroxide promotes hydrogen bonding and helix formation leading to biased charge density result at high pH. This is most clearly seen for the sample Xanthan gum X1, but it is assumed to affect also the results of Xanthan gum S1 and G1.

## 6.2 Apparent viscosity

The apparent viscosity was analyzed by Brookfield viscometer in deionized water where the polyelectrolyte effect dominates and in salt solution where the charges are screened. To decide a suitable salt-polymer concentration, previous test was referred. In that test, six different synthetic polyacrylamides were dissolved in deionized water, and sodium chloride was added calculating the amount as mass ratio of NaCl per dry polymer. Sodium chloride was added in the ratios of 1:1, 2:1, 5:1 and 10:1 NaCl per dry polymer, and viscosity of the samples was measured with Brookfield viscometer with spindle SC4-18 at rotational speed of 30 rpm. The results are shown in Figure 6. Based on the results the sodium chloride ratio needed to screen the charges and eliminate the polyelectrolyte effect at a sufficient level is 5:1. Therefore, the apparent viscosities of the anionic biobased polymer derivatives were decided to be measured using the NaCl ratio 5:1 per dry polymer.

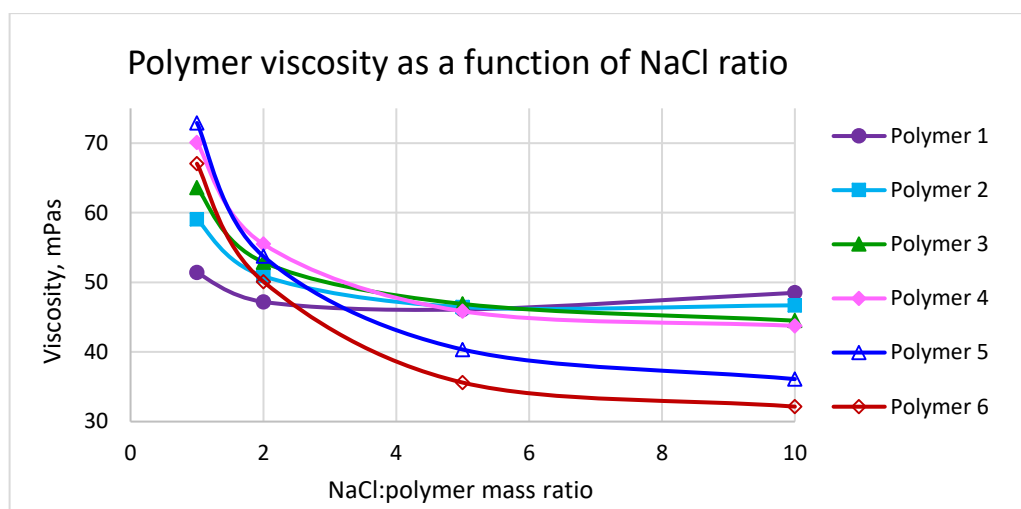


Figure 6. Polymer viscosity as a function of NaCl-ratio.

The dialyzed carboxymethyl cellulose, xanthan gum and polyacrylamide samples were dissolved in deionized water as 0,5 % concentration and the rest of the samples were dissolved as 1 % concentration. Half of the dissolved samples was then transferred to another beaker and sodium chloride was added calculating the 5:1 ratio as mass of NaCl per dry polymer. Apparent viscosities of the samples in water and salt solution were measured with Brookfield viscometer using small sample adapter and spindle SC4-31 in 25 °C temperature. The results were recorded at several rotational speeds but for comparison they are listed at one selected speed. The numerical results are listed in Table 5 and graphical presentation is shown in Figure 7.

Table 5. Apparent viscosity results in water and NaCl solution.

Sample	Speed, rpm	Viscosity in H <sub>2</sub> O, mPas	Torque, %	Viscosity in 1:5 NaCl, mPas	Torque, %
0,5 % CMC C1	10	1 300	43 %	470	16 %
0,5 % CMC S1	10	2 270	75 %	580	19 %
0,5 % CMC W1	10	1 250	42 %	400	13 %
0,5 % CMC C2	10	740	25 %	300	10 %
0,5 % Xanthan gum G1	10	1 480	49 %	2 440	81 %
0,5 % Xanthan gum X1	10	830	28 %	1 050	35 %
0,5 % Xanthan gum S1	10	630	21 %	1 660	55 %
0,5 % PAM 1	10	2 840	95 %	230	8 %
0,5 % PAM 2	10	2 470	82 %	250	8 %
1 % Carrageenan	5	4 020	67 %	2 090	35 %
1 % Guar gum	5	1 540	26 %	1 230	41 %
1 % Alginate 1	5	670	11 %	720	12 %
1 % Starch W1	5	2 750	46 %	-	-
1 % Starch W1	50	-	-	30	4 %
1 % Starch H1	5	3 220	54 %	-	-
1 % Starch H1	50 rpm	-	-	30	4 %

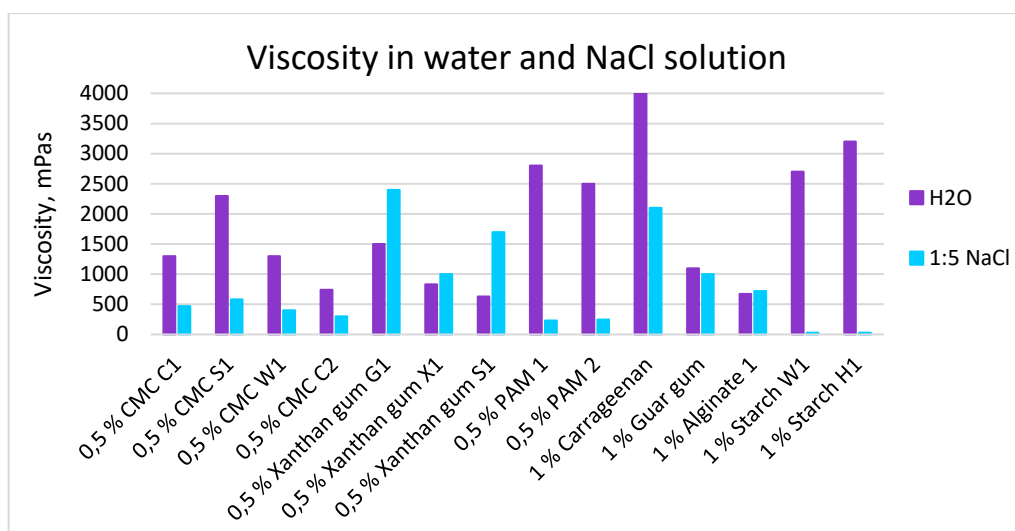


Figure 7. Viscosity in water and NaCl solution.

The remaining viscosity after sodium chloride addition is calculated as a percentage of viscosity in salt solution compared to the viscosity in water to visualize the effect of salt to the polymer rheology. The results are shown in Figure 8.

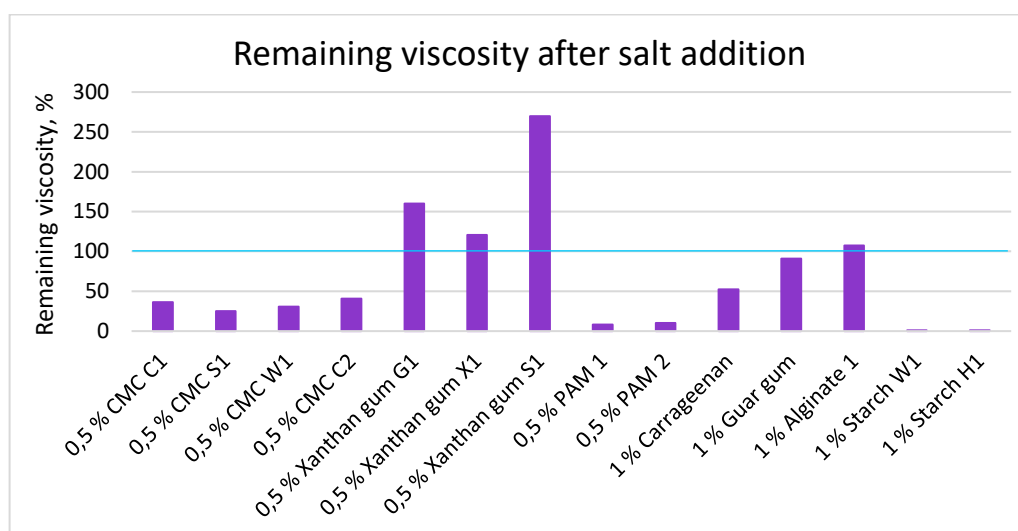


Figure 8. Remaining viscosity after salt addition.

When polyelectrolytes are measured in water, the charged groups repel each other, and therefore the polymer conformation is extended increasing the viscosity. Upon electrolyte addition, the charges are screened and the conformation changes into a random coil. The radius of gyration is smaller in the random coil conformation compared to the extended rod-like conformation, and therefore the viscosity of polyelectrolytes is smaller in salt solution.

The viscosity reduction in sodium chloride solution is most dramatic for the starch and polyacrylamide samples and clearly observed also for the carboxymethyl cellulose and carrageenan samples. The results are expected as they all have relatively high anionic charge. The viscosity reduction for Guar gum in salt solution is only minor, but this behavior is explained by the fact that the guar gum sample has relatively low charge density, and therefore the polyelectrolyte effect in water is not as remarkable as for the other samples.

Viscosity of the alginate and all three xanthan gum samples increase when salt is added to the sample. Alginate has the highest anionic charge compared to the other biobased polymers and the two synthetic PAM references. For that reason, it was expected that the polyelectrolyte effect would be the most dominant for this sample, but the result is the opposite. The viscosity increase is explained by hydrogen bonding that dominates over the electrostatic interactions when the charges are screened by salt addition. The chain conformation changes when the repelling charges are screened leading to formation of inter- or intramolecular junctions which cause increase in viscosity. Alginates are block copolymers of mannuronic and guluronic acids, and the distribution of the blocks highly affect the rigidity of the chain and therefore also the viscosity. In case multivalent ions are added to the aqueous solution of alginate, they induce crosslinking between the polymer chains increasing viscosity of the solution<sup>30</sup>.

The viscosity increase in salt solution is significant for the xanthan gum samples and most evident for the sample Xanthan gum S1. In electrolyte solution, the intramolecular electrostatic interactions between the side chains are shielded, and therefore the side chains fold down compactly to the backbone by hydrogen bonding. This phenomenon promotes helix formation. The helical structure is much stiffer compared to the coiled structure which xanthan gum adopts in water. The electrostatic interactions between the charged groups and the screening counterions determine the xanthan gum conformation in the solution.<sup>26</sup> Owing to their exceptional capability of preserving viscosity in salt solution, alginate and xanthan gum have a great potential as viscosifiers in the applications where the polymer is dissolved into brine, for example in the offshore oilfields.

### 6.3 Intrinsic viscosity

Intrinsic viscosity is an inherent property of a single macromolecule chain in the selected solvent in specific external parameters such as pH, temperature and electrolyte concentration. It is a measure of hydrodynamic volume occupied by one polymer chain. Based on the previous results, four dialyzed biopolymer derivatives were selected for the intrinsic viscosity measurement.



The measured samples are CMC C1, Xanthan gum G1, Guar gum and Starch W1 in addition to both reference PAMs 1 and 2. Intrinsic viscosity was measured in NaCl solution to screen the charges in the polyelectrolytes. The salt concentration was chosen to be 1 mol/l NaCl based on the Mark-Kuhn-Houwink constants listed in Polymer Handbook for polyacrylamide in 25 °C<sup>4</sup>.

Intrinsic viscosity is determined by preparing several dilutions of the polymer and measuring the samples by Ubbelohde capillary viscometer. The initial plan was to dissolve a stock solution of 1000 ppm polymer straight into 1 M NaCl. However, only the PAMs dissolved well while the biopolymers revealed lots of insolubles even after mixing overnight. It has been noticed before that the salt compatibility of CMC is much higher if the salt is dissolved into the CMC solution rather than dissolving the CMC into a salt solution. The salt is explained to prevent separation of the polymer chains due to electrostatic interactions and therefore the chains remain aggregated<sup>23</sup>. The same behavior was observed also for xanthan gum, guar gum and starch samples. By visual inspection, CMC seemed to be the most dissolvable in salt solution out of these four products. That is explained by the structure of CMC with the smallest side groups and therefore least entanglements compared to the other polymers. The simplicity of the chemical structure also explains why the polyacrylamides dissolved straight into the salt solution.

Consequently, the stock solutions were prepared by dissolving the polymers as 5000 ppm concentration into deionized water followed by an intermediate dilution of 1000 ppm into NaCl solution leading to a final concentration of 1 M NaCl. When samples were prepared this way, they dissolved well and remained dissolved when the stock solutions were diluted into the salt solution. Several samples of varying concentrations were diluted into 1 M NaCl.

The samples were measured in 23 °C with automated Ubbelohde capillary viscometer (Schott Nr 1, EVG 718 Mikro-KPG Ubbelohde auto, capillary constant  $K=0,01$ ). The program was set to perform one premeasurement and three main measurements with a maximum standard deviation of 0,75 seconds. From the practical point of view, it is recommended that the thickness of the capillary is chosen so that the flow time of pure solvent exceeds 100 seconds. Based on common practice the polymer concentrations in the measured samples are suggested to be selected to reach sample/solvent flow time ratio of 1,2-1,8. If the ratio is too low the difference between the polymer sample and solvent is difficult to be observed, and if the ratio is too high the curve starts to bend. It is important to be sure that the intrinsic viscosity is calculated based on the results in the linear region.

For the intrinsic viscosity determination, reduced viscosities of the diluted samples are calculated. The reduced viscosities are plotted as a function of concentration and based on the Huggins Equation 16 the intrinsic viscosity equals the intercept of the linear curve. The reduced viscosities are calculated by Equation 12 as demonstrated below for 150 mg/l Xanthan gum G1 sample. The flow through times are 100,67 seconds for the 1 M NaCl solvent and 156,51 seconds for the sample.

$$\eta_{red} = \frac{\eta_{sp}}{c} = \frac{\left(\frac{t}{t_0}\right) - 1}{c} = \frac{\left(\frac{156,51 \text{ s}}{100,67 \text{ s}}\right) - 1}{0,015 \text{ g/dl}} = 37,0 \text{ dl/g}$$

The intrinsic viscosity can also be determined by Kraemer Equation 17 by plotting inherent viscosity as a function of concentration. The inherent viscosity is calculated by Equation 15 as demonstrated below for the same Xanthan gum G1 sample.

$$\eta_{inh} = \frac{\ln \eta_{rel}}{c} = \frac{\ln \left(\frac{t}{t_0}\right)}{c} = \frac{\ln \left(\frac{156,51 \text{ s}}{100,67 \text{ s}}\right)}{0,015 \text{ g/dl}} = 29,4 \text{ dl/g}$$

Figure 9 demonstrates an example of plotting the data both ways including the linear equations of the Huggins and Kraemer curves for the sample Xanthan gum G1. The intrinsic viscosity for Xanthan gum G1 sample by Huggins equation is 24,3 dl/g and by Kraemer equation it is 25,5 dl/g. The squared coefficient of correlation between the dots in the Huggins curve is close to 1 and higher compared to the value of Kraemer curve. Therefore, it is statistically proven that the intrinsic viscosity value by Huggins equation is more accurate.

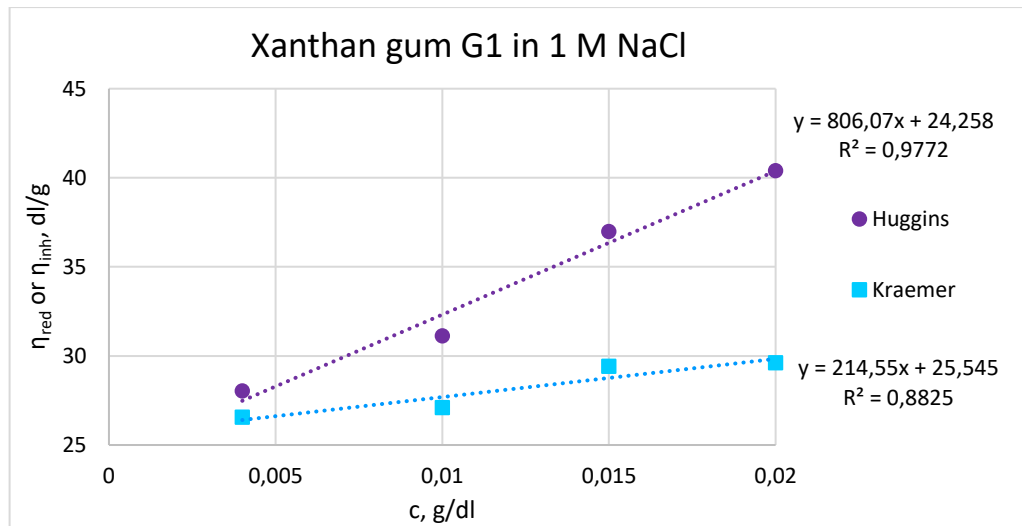


Figure 9. Intrinsic viscosity determination of Xanthan gum G1 in 1 M NaCl-solution.

Since the apparent Brookfield viscosity of xanthan gum is higher in electrolyte solution compared to water, it was decided to quantify the intrinsic viscosity of the sample Xanthan gum G1 also in deionized water. The Huggins and Kraemer curves are shown in Figure 10.

It is observed in the figure that the reduced viscosity does not increase as a function of concentration as it should, and also the squared coefficient of correlation for the Huggins curve is very low. The same behavior was observed for the synthetic polyacrylamides when measuring them in deionized water.

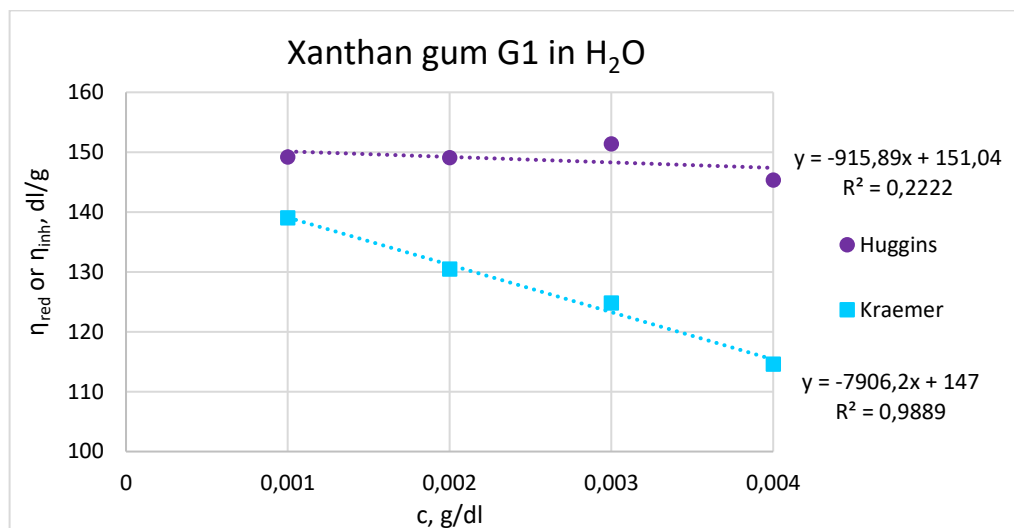


Figure 10. Intrinsic viscosity determination of Xanthan gum G1 in water.

It is suggested that the concentration dependence of reduced viscosity is not observed for the polyelectrolytes in deionized water due to the polyelectrolyte effect, and therefore the results are biased. As the concentration is increased, the viscosity of uncharged polymers would also increase because the sample contains more chains to entangle with each other. However, increasing polyelectrolyte concentration often decreases the viscosity because the electrostatic interchain repulsion drives the change in polymer conformation from extended rod-like shape to a more compact coil. The occurrence and magnitude of the polyelectrolyte effect depends on the charge density and distribution along the polymer chain. When the intrinsic viscosity of the xanthan gum was measured in deionized water, the two phenomena of increased polymer concentration and polyelectrolyte effect compete, and therefore the concentration dependence of the reduced viscosity is lost. For that reason, the intrinsic viscosity value measured in water (147 dl/g) is not accurate.

When comparing the Figures 9 and 10 it can be observed that the intrinsic viscosity of Xanthan gum G1 is higher in water than in sodium chloride solution. This result is opposite to the apparent viscosity result obtained by Brookfield rotational viscometer. It is claimed that the effect of salt on the viscosity of xanthan gum solution is concentration dependent<sup>31</sup>.

When the concentration of xanthan gum is low, moderate addition of monovalent cations decreases the solution viscosity opposite to the behavior in more concentrated solution. It is suggested that in a dilute solution the chains are further apart and therefore intermolecular interactions enhancing the helix formation are minimized. The increase in viscosity upon salt addition is observed only after certain threshold concentration. The apparent viscosity is measured at very high concentration where the helix formation due to salt screening is dominating whereas the intrinsic viscosity is measured at very low concentration to extrapolate the curve to infinite dilution, and therefore the viscosity increase upon salt addition is not observed.

The intrinsic viscosities of Xanthan gum G1, CMC C1, Guar gum and the two reference PAMs measured in 1 M NaCl are listed in Table 6. Based on the results, xanthan gum has the highest molecular weight. The graphs showing the Huggins and Kraemer curves for the CMC, guar gum and PAM samples are shown in Appendix 1. Intrinsic viscosity of the sample Starch W1 was also tried to be measured, but the molecular weight of the sample seems to be very small. To get a numerical value out of the data, much more concentrated samples should have been prepared. For a comparison to the other samples listed in Table 6 it is sufficient to mention, that the molecular weight of Starch W1 is very low.

*Table 6. Intrinsic viscosities.*

<b>Sample</b>	<b>Intrinsic viscosity, dl/g</b>
Xanthan gum G1	24,3
PAM 2	17,6
PAM 1	15,9
CMC C1	11,4
Guar gum	5,5

Out of the two synthetic PAM references, the sample PAM 2 has higher intrinsic viscosity although the apparent viscosity result in Table 5 is the opposite. According to product specification, the standard viscosity of PAM 2 is 6,2 mPas and for PAM 1 it is 5,2 mPas. The standard viscosity is measured as 1000 ppm concentration in 5,5 % sodium chloride with Brookfield rotational viscometer using UL spindle at 60 rpm in 25 °C. Determining the apparent viscosity is suitable only for screening purposes since it is not academically defined and validated method. Instead, the intrinsic and standard viscosity measurements are quantitative methods and therefore it can be concluded that the molecular weight of PAM 2 is higher compared to the PAM 1.

### 6.3.1 Relative viscosity

Relative viscosity demonstrates the flow time of the polymer compared to the flow time of pure solvent. It is calculated by Equation 14 as demonstrated below for the sample 150 mg/l Xanthan gum G1 with flow times 165,51 s for the samples and 100,67 s for the solvent.

$$\eta_{\text{rel}} = \frac{t}{t_0} = \frac{156,51 \text{ s}}{100,67 \text{ s}} = 1,55$$

Relative viscosities of Xanthan Gum G1, CMC C1, Guar Gum and reference PAMs 1 and 2 in 1 M NaCl are drawn as a function of concentration and results are shown in Figure 11. The graphical presentation visualizes the viscosities of the biobased products compared to the synthetic polyacrylamides. The xanthan gum sample has higher viscosity while CMC and guar gum samples have lower viscosity compared to the reference PAMs.

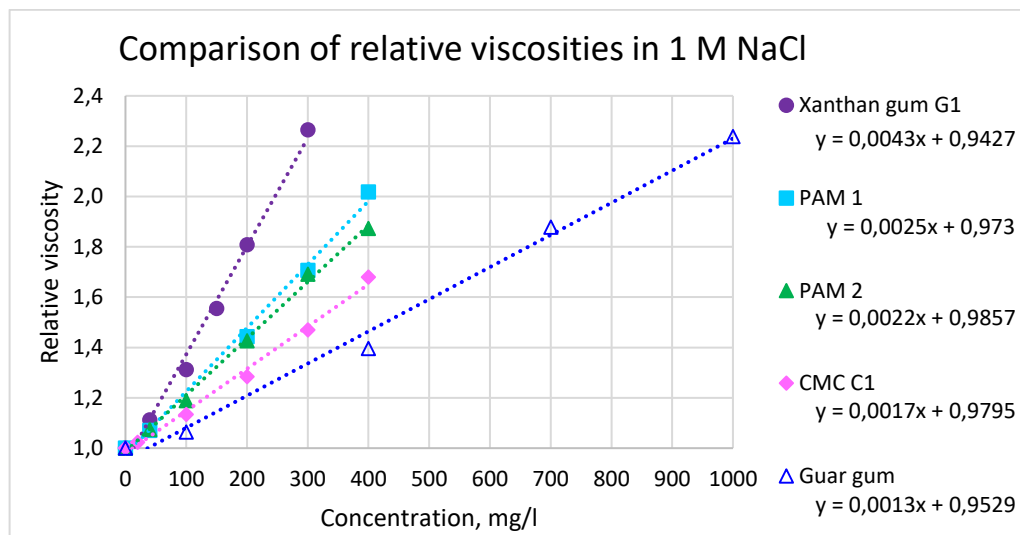


Figure 11. Comparison of relative viscosities in 1 M NaCl.

Using the linear equations of the curves it is possible to calculate the polymer concentration needed to achieve the same viscosity. Table 7 shows a comparison of the polymers. The concentration in the table demonstrates how much polymer is needed to achieve relative viscosity of 1,6.

Table 7. Concentrations required to achieve relative viscosity of 1,6.

Sample	c, mg/l
Xanthan gum G1	153
PAM 1	251
PAM 2	279
CMC C1	365
Guar gum	498

### 6.3.2 Molecular weight

Molecular weight of a polymer can be calculated by Mark-Kuhn-Houwink-Sakurada Equation 18 when the constants K and a are known. The constant values could not be found in the literature for all the selected biobased polymers in the specified conditions, but they are listed for polyacrylamide in 1 M sodium chloride solution in 25 °C. According to Polymer Handbook the constant values for PAM are 0,0191 ml/g for K and 0,71 for a<sup>4</sup>. To get an indication about the size of the polymers, the viscosity average molecular weights were calculated using the constant values found for PAM. However, it is important to understand that the results are only indicative due to the lack of specified K and a values for the biobased products, and therefore the viscosity averaged molecular weight in this case is called apparent molecular weight. An example of the calculation is demonstrated below for the sample Xanthan gum G1 having intrinsic viscosity of 2430 ml/g. The apparent molecular weight results for the samples are listed in Table 8.

$$M_v = \left( \frac{[\eta]}{K} \right)^{\frac{1}{a}} = \left( \frac{2430 \text{ ml/g}}{0,0191 \text{ ml/g}} \right)^{\frac{1}{0,71}} = 9,8 * 10^6$$

Table 8. Molecular weight results.

Sample	Apparent molecular weight, 10 <sup>6</sup> Da
Xanthan gum G1	16
PAM 2	9,8
PAM 1	8,5
CMC C1	5,3
Guar gum	1,9

It is important to emphasize that for example molecular weight distribution has a major effect in the values of K and a constant, and to get accurate results they should be determined separately for each product of interest. However, the results calculated here give an indication of the magnitude of the size when comparing different types of polymers in the flocculation application.

### 6.3.3 Critical overlap concentration

The critical overlap concentration (c\*) describes the concentration of the polymer at which the polymer coils start to overlap. After this point, the rheological behavior of the polymer is not caused by the individual chains, but the interchain interactions become significant due to entanglements. In the measurement of intrinsic viscosity this is observed by bending of the Huggins and Kraemer curves. The critical overlap concentration is calculated by Equation 19 as demonstrated below for the sample Xanthan gum G1 having intrinsic viscosity 24,3 dl/g. The critical overlap concentration results for all samples are listed in Table 9.

$$c^* = \frac{1}{[\eta]} = \frac{1}{24,3 \frac{dl}{g}} * 10^4 = 412 \text{ mg/l}$$

Table 9. Critical overlap concentrations.

Sample	c*, mg/l
Xanthan gum G1	412
PAM 2	568
PAM 1	629
CMC C1	877
Guar gum	1818

## 7 Setting up the FBRM parameters

The performance of the biobased polymers was decided to be tested in flocculation application comparing the efficiency to synthetic polyacrylamides. The flocculation efficiency was monitored by focused beam reflectance measurement, FBRM, using and equipment provided by Lasentec. As the surface charge of the bentonite is negative, all the bentonite flocculation tests in this thesis are performed by coagulation flocculation using commercially available polyaluminium chloride, PAC, as the coagulant. A schematic presentation of the FBRM equipment is shown in Figure 12 <sup>17</sup>.

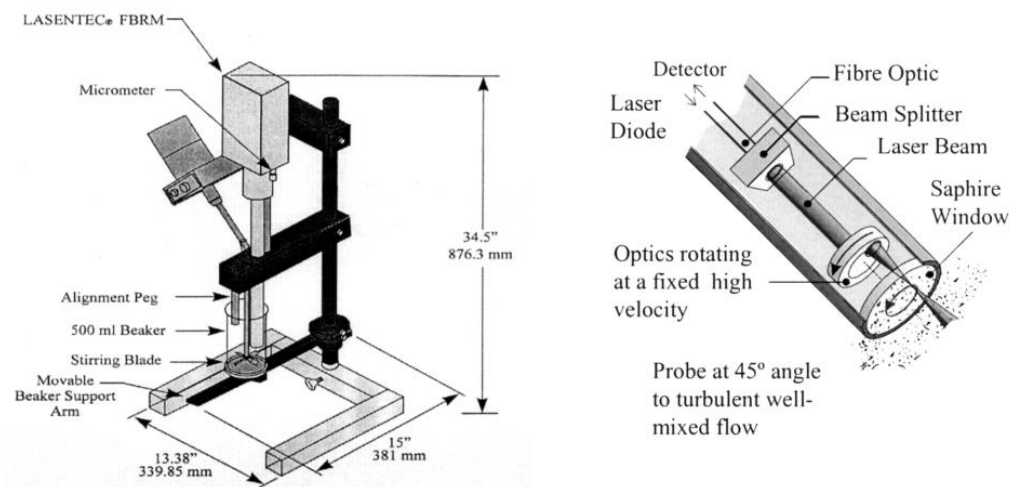


Figure 12. Schematic presentation of the FBRM equipment.

### 7.1 Flocculation matrix

FBRM is a versatile device and therefore some measurement parameters had to be optimized before the application testing could be started. The first step was to decide the flocculation matrix. Kaolin and bentonite were tested, and due to formation of larger flocs, bentonite was selected.

Bentonite is a natural clay consisting of several minerals in varying amounts, but the main component is montmorillonite mineral. The structure of sodium montmorillonite mineral is demonstrated in Figure 13<sup>32</sup>. In aqueous solution the clay particles swell, and as most colloidal particle they possess a negative surface charge.

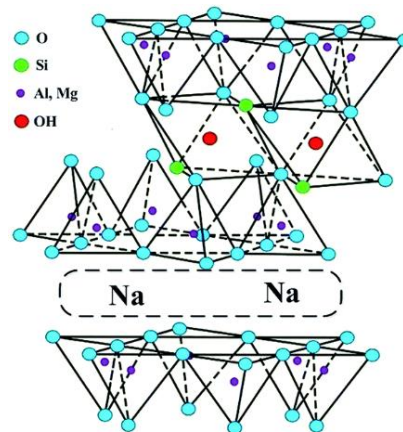


Figure 13. The structure of montmorillonite clay.

The FBRM device measures the number of particles and therefore the solids concentration of the flocculation matrix is one of the key parameters to be optimized. The solids concentration optimization was performed by coagulating the clay with commercial PAC product containing 17 %  $\text{Al}_2\text{O}_3$  and 9 %  $\text{Al}^{3+}$ . The tested bentonite is commercially available Altonit SF. The optimal solids concentration was found to be 0,5 % solids in a sample volume of 500 ml.

## 7.2 pH of the bentonite sample

The surface charge of a particle depends on pH. At higher pH the surface charge is more negative while in acidic environment the charges are screened to some extent by protonation. The next parameter to be tested was the influence of pH on the flocculation performance. When aluminium salt is added to the aqueous sample, it reacts with water molecules forming hydroxides and causes the pH of the samples to decrease. As the amount of water molecules is much higher compared to the number of colloidal particles with the negative surface charge, the drop in pH is always observed. The magnitude of the change depends on alkalinity of the water and the basicity of the aluminium product. Different coagulants have varying optimal pH-ranges.

Based on the application, the tests were initially planned to be conducted in neutral pH. The plan was to buffer the bentonite sample matrix into pH 7,2 by phosphate buffer, but it was noticed that flocculation does not occur in the buffered solution. It appeared that the high concentration of the negative phosphate ions disturbs the performance of the cationic coagulant.



Also, the neutral pH was not optimal for the coagulant in question. Consequently, it was decided to adjust the initial pH of the bentonite samples into 7,2 by phosphoric acid and let the pH decrease upon coagulant addition without buffering. The pH of the bentonite sample rose to a maximum of 7,8 while storing the sample in normal atmosphere between the tests. The sample used in the tests was up to one day old.

### 7.3 Coagulant dosage

Next, the optimal dosage of the PAC coagulant was studied. As the pH of the sample is not buffered higher dosage of the coagulant affects in two ways. Firstly, as the concentration is increased, the number of positive patches on the negative particle surface is increased. Secondly, the pH of the medium decreases more. Consequently, the combination of these two effects was studied. Optimization of the coagulant concentration is important because too low amount hinders the performance and too high concentration causes charge reversal. In case of charge reversal, the particle aggregation is again prohibited by the electrostatic repulsion, but this time it is caused by the positive charge of the coagulant layer.

The optimization was performed by two different polymers being the PAM 1 and CMC C1. It was noticed that the optimal dosage of polyaluminium chloride is very different for the two products. The coagulant concentration for the flocculation with the two synthetic PAMs was decided to be 100 kg/ton PAC product per dry bentonite and 200 kg/ton with all the biobased flocculants.

### 7.4 Result interpretation

The FBRM device is set to measure the number of particles within the size range of 1-1000  $\mu\text{m}$ . The range is divided logarithmically into 90 channels, and the size distribution of the sample is drawn based on the number of particles in these 90 channels. The particle count is followed online as a function of time. There are several different statistical modes that can be used to interpret the data. In this study, it was decided to follow the evolution of six different particle size groups in addition to the mean size of all particles. Flocculation was tested by stirring the sample with overhead stirrer at the speed of 1000 revolutions per minute, rpm.

The test procedure with data grouping is listed in Table 10. The baseline was measured for 10 seconds followed by the coagulant addition. After stirring for additional 20 seconds, the flocculant was added, and evolution of particle size groups was followed for 1 minute and 30 seconds. After total time of 2 minutes, the stirring speed was decreased to 300 rpm to see whether re-flocculation occurs.

Table 10. Test procedure and data grouping.

**Test procedure**

Time	Action
0 sec	Start
10 sec	PAC addition
30 sec	Flocculant addition
2 min	Speed decreased from 1000 rpm to 300 rpm
3 min	Stop

**Data grouping**

Group number	Description
1	1-5,0 $\mu\text{m}$
2	4,6-10 $\mu\text{m}$
3	10-25 $\mu\text{m}$
4	23-54 $\mu\text{m}$
5	46-100 $\mu\text{m}$
6	100-1000 $\mu\text{m}$
7	Mean size, $\mu\text{m}$

There are several different possibilities to interpret the measured data. For an example, the flocculation results of the synthetic polyacrylamide sample PAM 1 are shown below. In this test, the flocculation matrix is 0,5 % bentonite, PAC addition is 100 kg/ton and flocculant addition is 1 kg/ton.

One option to interpret the results is to follow the evolution of particle size distribution as showed in Figure 14. In the figure, the purple line (0 s) shows the particle size distribution at the beginning of the test when mixing at 1000 rpm before adding any chemicals. The turquoise line (20 s) is the situation ten second after the PAC addition. Since the distribution is the same as initially, it can be concluded that the PAC addition does not cause any particle aggregation. The green line (40 s) shows the result ten seconds after the flocculant addition. It is observed that the particle size distribution shifts to right on the x-axis meaning that larger particles are formed while the number of small particles decrease drastically. The flocculating polymer is working efficiently.

When stirring with high speed is continued, the flocs start to break due to mechanical shear force. This behavior is observed in the pink line (110 s) which shows the situation 80 seconds after the flocculant addition. Compared to the green line, the number of small particles has increased as the flocs have broken. The blue line (180 s) is the situation after decreasing the stirring speed from 1000 rpm to 300 rpm right before the flocculation experiment is stopped.

The particle size distribution has moved to the same position as it was after adding the flocculant, meaning that the broken flocs re-flocculate. Re-flocculation is a typical phenomenon when the flocculation occurs by the patch mechanism which most often is the case when coagulants are added prior to the flocculant.

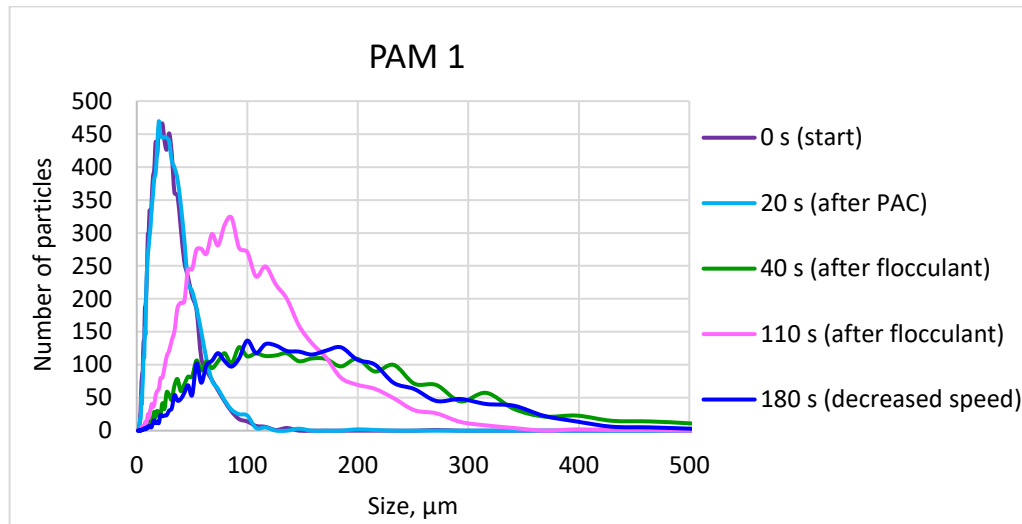


Figure 14. Evolution of particle size distribution.

Figure 15 shows the evolution of the six different particle size groups. In this figure, it can be observed that initially the sample contains mostly particles within the size range from 10 to 54  $\mu\text{m}$ . Upon flocculant addition the number of small particles decrease drastically while the number of large particles increase. The coagulant and flocculant additions at 10 s and 30 s respectively in addition to the decrease in speed at 120 s can also be observed in the figure.

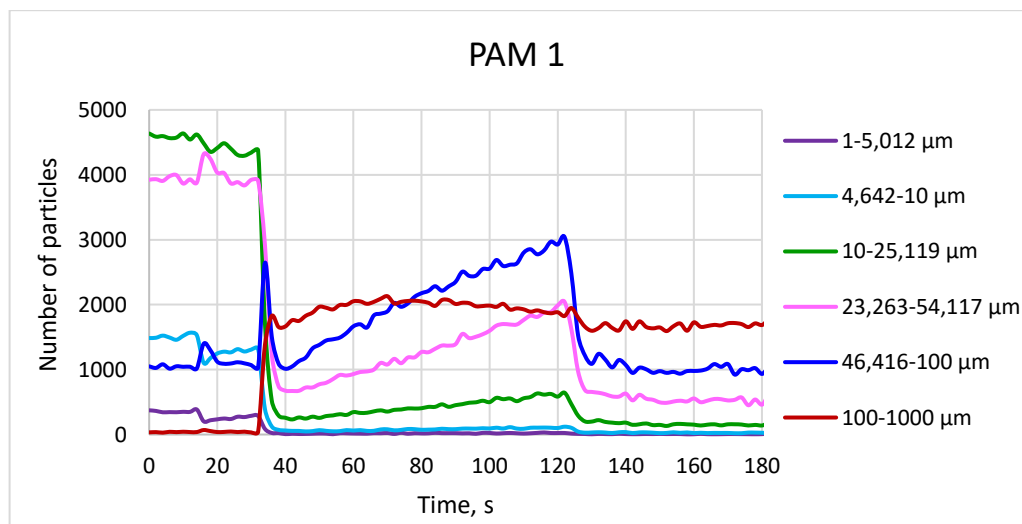


Figure 15. Evolution of particle size groups as a function of time.

In Figure 16 the mean size of all particles is followed as a function of time. Based on the result, the coagulant addition at 10 s is observed, but it does not have a remarkable effect on the size of the particles. The flocculant addition at 30 s raises the mean size significantly, but it also starts to decline immediately due to high shear force. At 120 seconds the decreased speed allows re-flocculation to occur, which is observed as the increased mean size due to particle aggregation. It is interesting to note that the re-formed flocs actually gain the same size as was initially achieved by the flocculant addition. To compare the biobased polymers in the application testing it was decided to follow the evolution of the mean size.

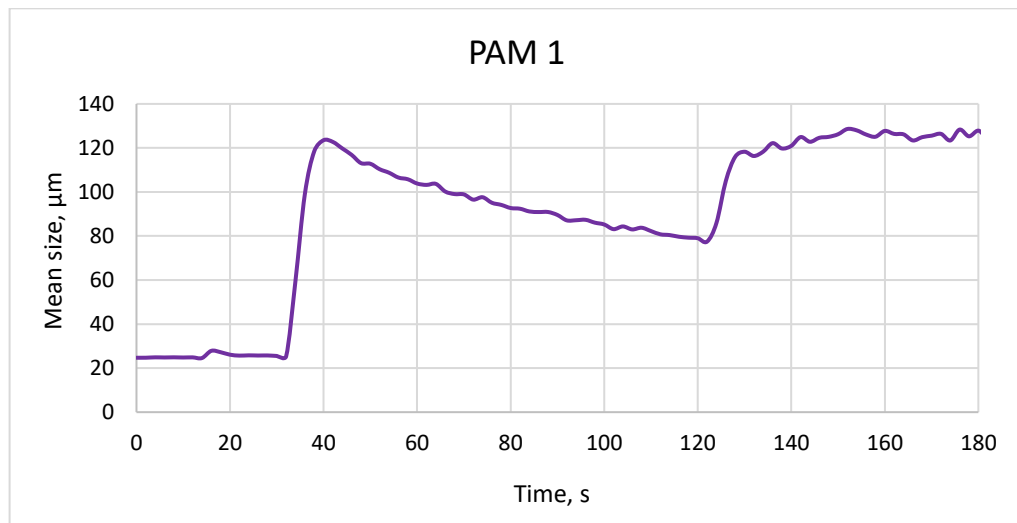


Figure 16. Evolution of the mean size of all particles as a function of time.

## 8 Performance of the biobased products in bentonite flocculation

Performance of the biobased products was tested by coagulation-flocculation of bentonite following the performance online with focused beam reflectance measurement. The test and monitoring parameters are listed previously in Table 10. The performance of the products was studied by testing varying dosages of the flocculating polymer by keeping the bentonite and PAC concentrations constant. The solids concentration of the bentonite was 0,5 %, volume 500 ml and initial pH 7,2-7,8. The final pH of the samples in all the tests with the biobased polymers was 5,1-5,5 and with the synthetic PAMs the final pH was 6,5-6,7. The final pH is mostly affected by the PAC addition which was 200 kg/ton in the biobased product flocculation tests and 100 kg/ton when the synthetic PAMs were studied. Results were interpreted by the evolution of mean size of the particles.

Figure 17 demonstrates how the sample looks like after successful and poor flocculation. The sample on the left-hand side shows a flocculation test with 1 kg/ton synthetic PAM 1. The formed flocs are large, and supernatant is clear indicating that the polymer performance is good at the selected dosage. On the right-hand side sample flocculation was performed with 1 kg/ton CMC C1. With this product, the dosage has been too small since the particles did not flocculate well.



*Figure 17. Demonstration of good and poor flocculation.*

### 8.1 Optimal dosage

To find the optimized flocculant concentration for each product, maximum mean size of the flocs in each test was found out and used to draw a curve. The results for all the 9 biobased products and the two synthetic references are shown in Table 11 and the curves of maximum floc size as a function of concentration are shown in Figures 18-20. The graphs of all flocculation tests are shown in Appendix 2. It is important to emphasize that due to limited schedule of the thesis, the concentration of PAC was optimized only by one biobased and one synthetic polymer. However, to get the best performance in application, the dosage optimization should be performed for each coagulant-flocculant combination individually, and that could affect the maximum floc size values in Table 11 to some extent. However, the differences between the samples are prominent, and therefore it can be assumed that the order of efficiency between the samples would be sustained although the coagulant concentration was slightly changed. In this case the indicative optimization fits for purpose.

Table 11. Maximum mean size result,  $c$  (PAC)=200 kg/ton for biobased products and 100 kg/ton for PAMs.

<b>c, kg/ton</b>	<b>Xanthan gum G1</b>	<b>Xanthan gum S1</b>	<b>CMC C1</b>	<b>CMC S1</b>	<b>Guar gum</b>
1	36 $\mu\text{m}$	35 $\mu\text{m}$	31 $\mu\text{m}$	33 $\mu\text{m}$	32 $\mu\text{m}$
5	83 $\mu\text{m}$	73 $\mu\text{m}$	58 $\mu\text{m}$	45 $\mu\text{m}$	49 $\mu\text{m}$
10	103 $\mu\text{m}$	84 $\mu\text{m}$	75 $\mu\text{m}$	59 $\mu\text{m}$	62 $\mu\text{m}$
15	99 $\mu\text{m}$	101 $\mu\text{m}$	82 $\mu\text{m}$	65 $\mu\text{m}$	71 $\mu\text{m}$
20	113 $\mu\text{m}$	101 $\mu\text{m}$	86 $\mu\text{m}$	71 $\mu\text{m}$	72 $\mu\text{m}$

<b>c, kg/ton</b>	<b>Alginate 1</b>	<b>Carrageenan</b>	<b>Starch W1</b>	<b>Starch H1</b>
1	31 $\mu\text{m}$	30 $\mu\text{m}$	28 $\mu\text{m}$	29 $\mu\text{m}$
5	46 $\mu\text{m}$	44 $\mu\text{m}$	34 $\mu\text{m}$	33 $\mu\text{m}$
10	52 $\mu\text{m}$	44 $\mu\text{m}$	42 $\mu\text{m}$	39 $\mu\text{m}$
15	46 $\mu\text{m}$	42 $\mu\text{m}$	46 $\mu\text{m}$	50 $\mu\text{m}$
20	47 $\mu\text{m}$	41 $\mu\text{m}$	52 $\mu\text{m}$	55 $\mu\text{m}$

<b>c, kg/ton</b>	<b>PAM 1</b>	<b>PAM 2</b>
0,7	114 $\mu\text{m}$	102 $\mu\text{m}$
1	135 $\mu\text{m}$	129 $\mu\text{m}$
1,3	150 $\mu\text{m}$	144 $\mu\text{m}$
1,6	150 $\mu\text{m}$	150 $\mu\text{m}$

Figure 18 demonstrates the results of the CMC and xanthan gum samples, which are the best biobased products for the bentonite flocculation since they form the largest flocs. Based on the results, xanthan gum is the most efficient product and out of the two tested samples, Xanthan gum G1 is better. The highest floc size achieved is approximately 100  $\mu\text{m}$ . The results of flocculation performance correlate well with rheological properties of the biobased polymers. Xanthan gum has the highest viscosity indicating the largest size and therefore it is able reach bentonite particles most efficiently.

In Figure 18 it can be observed that all the curves start to bend after the dosage of 10 kg/ton meaning that it is the optimal dosage. Excessive polymer dosage leads to inefficient flocculation due to charge repulsion. The mean size of bentonite particles before adding any chemicals is 25  $\mu\text{m}$ . The test with 15 kg/ton of Xanthan gum G1 was repeated since the result drops compared to the dosage of 10 kg/ton. The repeated test gave exactly the same result indicating that 15 kg/ton is an overdose causing decrease in the maximum floc size due to the charge repulsion.

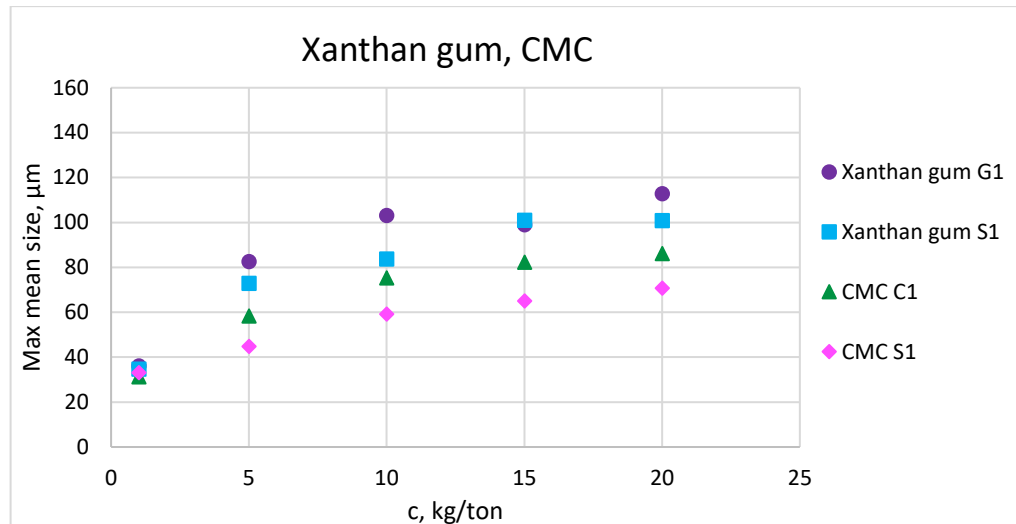


Figure 18. Flocculation results for xanthan gum and CMC samples.

Figure 19 shows the results for guar gum, alginate, carrageenan and the two starch samples. The performance of these samples is much weaker compared to the two xanthan gums and CMC C1 samples. The performance of Guar gum is equivalent to CMC S1, and the maximum mean floc size is approximately 70  $\mu\text{m}$  gained with the dosage of 15 kg/ton. The tested alginate and both starch samples have relatively poor flocculation ability with the maximum performance at 10 kg/ton dosage. Carrageenan has the poorest performance and increasing the concentration above 5 kg/ton does not make a difference.

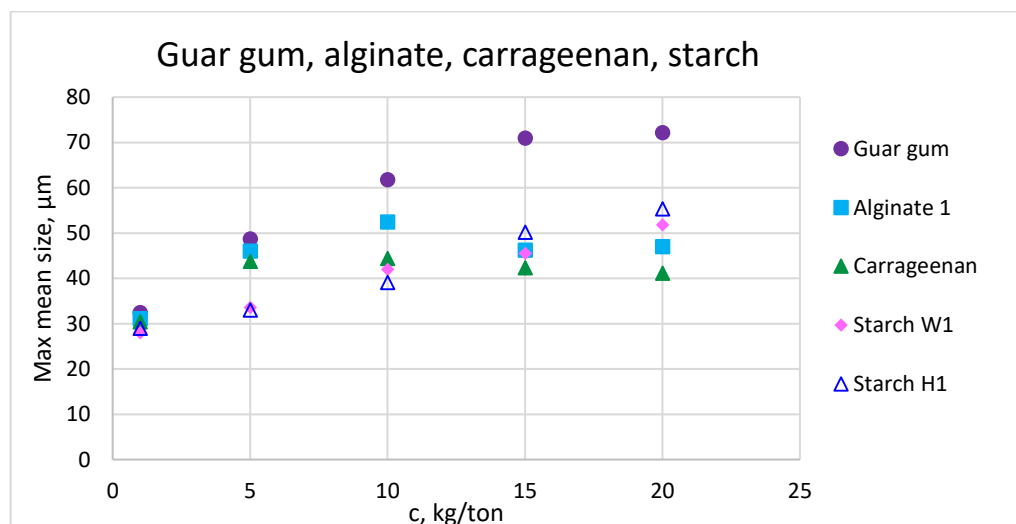


Figure 19. Flocculation results for guar gum, alginate, carrageenan and starch samples.

Figure 20 presents the results of the two synthetic polyacrylamide samples. The optimal dosage for both samples is 1,3 kg/ton to gain the maximum mean floc size being approximately 150  $\mu\text{m}$ . According to the results, PAM 1 has slightly better performance although it has a lower molecular weight based on the viscosity results. The PAC dosage was optimized by PAM 1 explaining the difference. The performance of the synthetic polyacrylamides in bentonite flocculation is better compared to the biobased polysaccharide derivatives since larger flocs are formed with lower dosage.

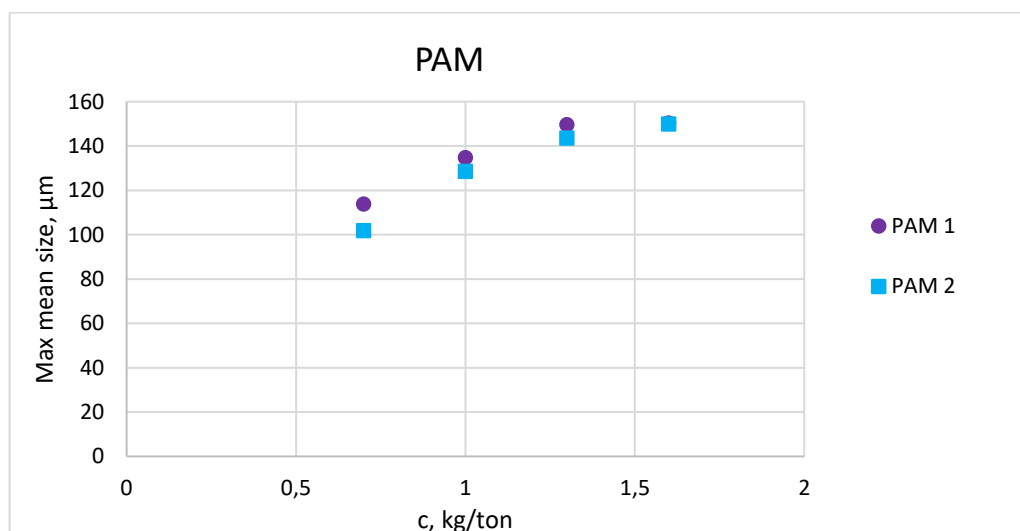


Figure 20. Flocculation result for reference PAM samples.

## 8.2 Floc stability and re-flocculation ability

In addition to the optimal dosage, also the floc stability and re-flocculation ability were followed during the flocculation test. Figure 21 shows the evolution of the mean size as a function of time for all the biobased samples. The dosage for all the samples is 200 kg/ton PAC and 10 kg/ton flocculant. This figure demonstrates well how the most potential biobased polymers for bentonite flocculation are xanthan gum, CMC and guar gum samples. The performance of the alginate, carrageenan and starch samples is relatively poor. Based on how fast the mean size starts decreasing at 1000 rpm speed after adding the flocculant (at 30 s), the floc stability seems to be very similar for all the samples. When the speed was decreased to 300 rpm (at 120 s), all other samples except the two xanthan gums re-flocculate.

Both xanthan gum samples, Xanthan gum S1 and G1 re-flocculate slightly in the tests where the flocculant concentration is 1 or 5 kg/ton, but above that re-flocculation is not observed. Since the structure of the xanthan gum contains large side groups it is suggested that the high mechanical shear breaking the flocs when mixed with 1000 rpm also cause breakage of the polymer chain.



It is suggested that the chain scission hinders the performance and therefore re-flocculation is not observed when the speed is decreased.

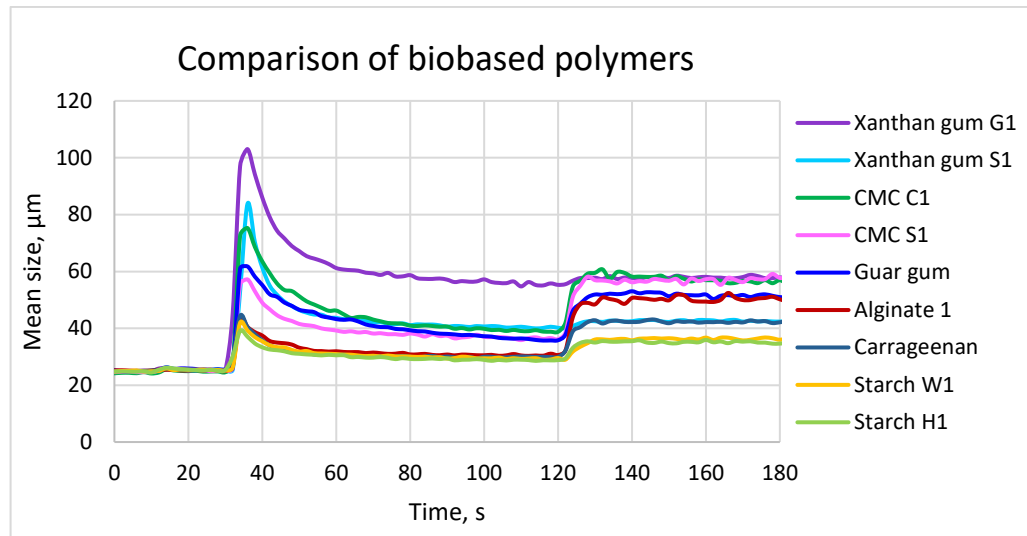


Figure 21. Comparison of biobased products: 200 kg/ton PAC and 10 kg/ton flocculant.

The results of the two synthetic polyacrylamides are shown in Figure 22. Compared to the biobased products, the flocs are more shear resistant when the synthetic PAMs have been used in flocculation. This is observed by more gradual decrease in the floc size. As expected for the flocculation by the patch mechanism, re-flocculation occurs as the speed is decreased.

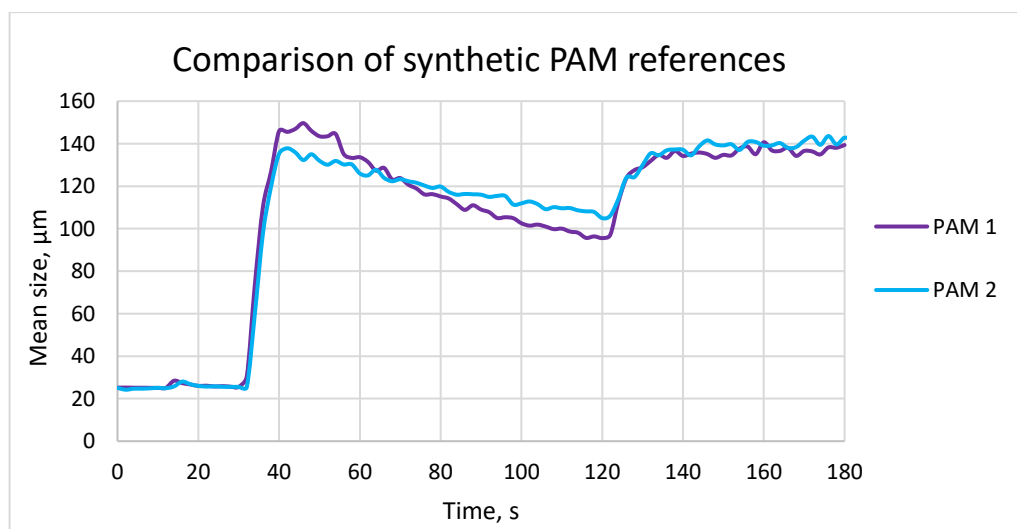


Figure 22. Comparison of synthetic PAM references: 100 kg/ton PAC and 1,3 kg/ton flocculant.

Compared to the tested biobased products, the synthetic PAMs are more efficient as they give higher maximum floc size (150  $\mu\text{m}$  for synthetic PAM 1 and 100  $\mu\text{m}$  for Xanthan gum G1) at smaller optimal dosage (1,3 kg/ton for synthetic PAM 1 and 10 kg/ton for Xanthan gum G1). The combination of higher molecular weight and charge density leads to better performance. However, the flocculation results reveal that the biobased products have a high potential to replace the synthetic polymers in the future. The biopolymer derivatives already work, and by modifying their structure, the performance in flocculation can be further improved. The comparison of the selected products show that the xanthan gum, CMC and guar gum are the most potential biobased products.

## 9 Additional performance testing

Two additional tests were performed for the biobased products regarding oilfield applications. Polyacrylamides are widely used in oil sands treatment to flocculate tailings and in enhanced oil recovery applications to increase oil production. The biobased products were tested in tailings flocculation and also quick thermal stability screening was performed.

### 9.1 Flocculation of oil sands tailings

It is estimated that producing one barrel of oil from surface-mined oil sands produces also 1,8 metric tons of solid tailings suspended in two cubic meters of water. The tailings waste was previously discharged into settling ponds to allow the solids to sink over decades or even longer. Due to tightened regulations, more efficient method is needed to separate the solid tailings from the water.<sup>33</sup>

The oil sands tailings sample tested in flocculation is mature fine tailings. When the tailings are pumped to a settling pond, the heaviest material separates from the top layer of water and sinks to the bottom. The middle layer is called mature fine tailings and its phase separation could take centuries without any flocculating additives. The sample in question contains 24 % solids, which is mostly clay, and 1 % bitumen. For the flocculation test it was diluted in deionized water to get final solids concentration of 0,5 %. Flocculation was performed with carboxymethyl cellulose sample CMC C1 with and without the PAC coagulant, and also with the reference polyacrylamide PAM 1. Both polymers were tested at two different concentrations. In tests performed without the coagulant the flocculant was added at 10 seconds, and in the test with the coagulant PAC was added at 10 seconds and flocculant at 30 seconds. The speed was initially 1000 rpm and it was decreased down to 300 rpm at 120 seconds. List of the tests is shown in Table 12.

Table 12. Oil sands tailings flocculation tests.

Test number	PAC dosage	Flocculant	Dosage
1	-	PAM 1	1 kg/ton
2	-	PAM 1	10 kg/ton
3	-	CMC C1	10 kg/ton
4	-	CMC C1	20 kg/ton
5	200 kg/ton	CMC C1	10 kg/ton

The results of flocculating the mature fine tailings are shown in Figure 23. With both polymers the mean size of particles decreases upon adding the chemical. The effect is higher for the synthetic PAM compared to the biobased CMC. This behavior is opposite to what was expected. Even when cationic coagulant was added before the anionic CMC flocculant, the addition of high molecular weight polymer decreases the mean size of the particles. The decrease in the mean size seems to be of the same magnitude independent of the flocculant concentration in the tested concentration range. When the speed is decreased down to 300 rpm, the mean size of particles in the CMC tests decrease even more, and in the PAM tests the speed does not have a notable effect.

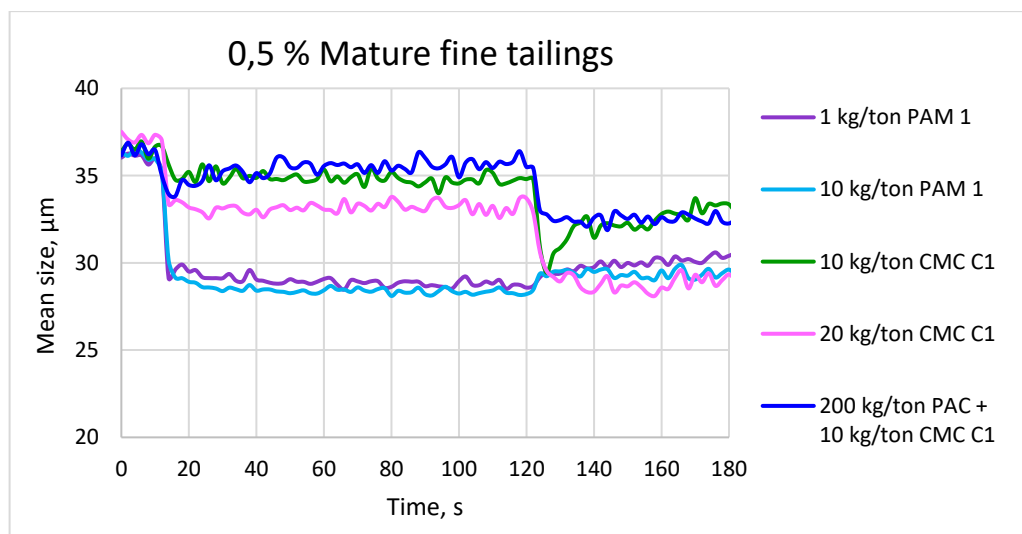


Figure 23. Flocculation of oil sands tailings.

The decreased mean size upon polymer addition indicates that the PAM and CMC act as dispersing agent instead of flocculating agent. It seems that the polymer chains adsorb to a great extent on the surface of the particles and keep them separated due to charge repulsion. To understand the dispersion mechanism better, it is suggested that the surface charge of the particles in the mature fine tailings should be studied in more detail. As the aim of this thesis is to study the flocculation

efficiency of the biobased materials instead of their performance as dispersing agents, flocculation tests of the oil sands tailings were not continued.

## 9.2 Thermal stability

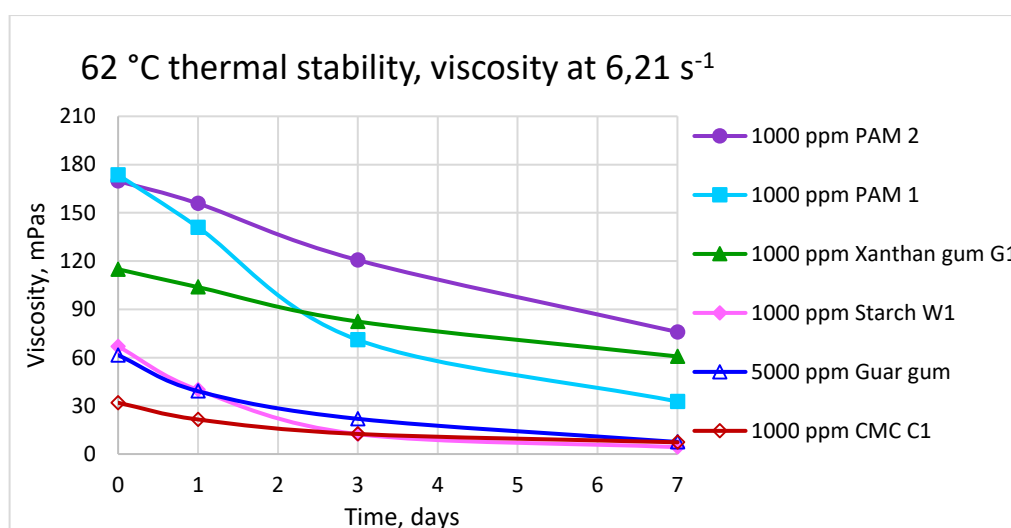
Crude oil is produced from underground sandstone or carbonate rock formations in three different recovery phases. At the first stage, oil is produced to the surface through a drilled wellbore utilizing natural driving forces such as gas or water drive or gravity drainage. As the natural pressure drive becomes insufficient for commercially viable oil production, secondary oil recovery method is applied. In this phase, external fluid, for example water or gas, is injected to the reservoir to maintain the pressure and displace some of the remaining hydrocarbons. After applying the secondary recovery method, there is still about two thirds of the original oil in place left behind in the reservoir, and therefore tertiary recovery methods called enhanced oil recovery, EOR, have been developed. EOR technologies can be divided into chemical, thermal or gas techniques, and polymer flooding is the most commonly used chemical treatment.<sup>8</sup>

As the oil reservoirs are located deep in the ground, the reservoir temperature is typically much higher compared to the surface temperature. Therefore, the polymers used in polymer flooding must be thermally stable in the selected reservoir conditions. Thermal stability of the most potential biobased chemistries was analyzed by incubating the samples in 62 °C heating chamber for a week. Other samples were dissolved as 1000 ppm concentration and Guar gum in 5000 ppm concentration in deionized water. Guar gum was also tested in 1000 ppm concentration, but the viscosity at the selected shear rate was so low to begin with, that the effect of heating could not be observed. The samples were placed in heating chamber in sealed pressure tubes. After 1, 3 and 7 days of incubation, the viscosity profiles of the samples were measured in 25 °C with Anton-Paar MCR 302 rheometer using DG 26.7 bob. The shear rate was increased gradually from 0,1 to 1000 s<sup>-1</sup>. Carboxymethyl cellulose CMC C1, Xanthan gum G1 and Guar gum were selected for the test since they demonstrated good performance in the bentonite flocculation tests. The sample starch W1 was selected to represent the least potential sample, and both synthetic PAMs were tested as a reference.

To compare the products, it was decided to follow the viscosity at the shear rate 6,21 s<sup>-1</sup>, which is an example of a typical shear rate encountered in the porous reservoir. Viscosity results at the selected shear rate are shown in Table 13 and visualized in Figure 24. Viscosity profiles of all thermal stability measurements are shown in Appendix 3.

Table 13. Viscosity results at shear rate  $6,21 \text{ s}^{-1}$ .

Time, days	Viscosity, mPas, at shear rate $6,21 \text{ s}^{-1}$		
	1000 ppm CMC C1	1000 ppm Xanthan gum G1	5000 ppm Guar gum
0	32	115	62
1	22	104	39
3	13	82	22
7	7	61	8
Time, days	Viscosity, mPas, at shear rate $6,21 \text{ s}^{-1}$		
	1000 ppm Starch W1	1000 ppm PAM 1	1000 ppm PAM 2
0	67	174	170
1	40	141	156
3	12	71	121
7	4	33	76

Figure 24. Viscosity as a function of time at shear rate  $6,21 \text{ s}^{-1}$ .

The remaining viscosity was calculated as a percentage of the original viscosity and the results are demonstrated in Figure 25. Based on the results, the most thermally stable biobased product is xanthan gum, which is even slightly more stable compared to the synthetic reference PAM 2. In the polymer characterization and bentonite flocculation tests, the two synthetic polyacrylamides have revealed similar results. However, in the thermal stability test they differ remarkably PAM 2 polymer being notably more thermally stable. When comparing the most potential biobased flocculants, CMC and xanthan gum, it can be concluded that the CMC degrades faster and to higher extent. Out of all tested samples, the starch sample degrades the most. Thermal stability of the biobased polymers can be increased by modifying their chemical structure. For example, grafting

acrylamide functional groups on various biobased products have proved to increase the thermal stability in addition to enhancing the flocculation performance.

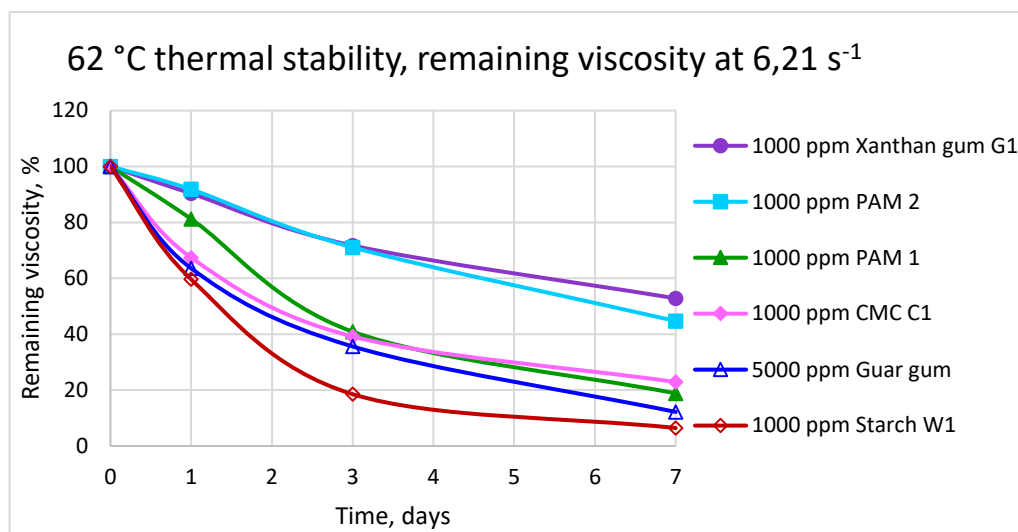


Figure 25. Remaining viscosity as a function of time at shear rate 6,21 s<sup>-1</sup>.

The thermal stability test was performed in deionized water in aerobic conditions to get an indicative comparison between the products in short time. It is important to understand that the polymer degradation is affected by several external factors of which the presence of oxygen is one of the most severe components. When designing the polymer flooding application, the thermal stability tests are typically performed in a sample matrix matching the reservoir conditions as well as can be simulated in a laboratory scale. Since the reservoirs are anaerobic, the samples are often prepared in a glove box and electrolytes are added to simulate the produced water composition.

## SUMMARY

The aim of the thesis was to identify and test anionic biopolymer derivatives having high enough molecular weight and charge density to function in flocculation application. Based on literature, there are several different types of polysaccharides available from the renewable resources. At least agar, agarose, alginate, carrageenan, cellulose, chitosan, dextran, glucan, glycogen, guar gum, lignin, pullulan, starch, tannin and xanthan gum are listed to be potential flocculating agents. However, the natural products often need some chemical modification to improve their performance in the application. Commercially available anionic derivatives of the biobased polysaccharides were requested and totally 28 samples representing 10 different polysaccharides were received from varying suppliers.

The samples were screened by viscosity and charge density. Viscosity indicates the magnitude of molecular weight and only polyelectrolytes with sufficient charge density are able to aggregate the

charged colloidal particles in aqueous solution. Based on the screening results, 12 most potential biobased products in addition to 2 synthetic anionic polyacrylamide references were purified. Purification by dialysis was required to remove impurities formed during the production since the presence of additional electrolytes would affect the rheological behavior of polyelectrolytes.

The selected polymers were characterized by charge density and rheology. The charge density was quantified by titrating with cationic polyDADMAC. The apparent viscosities were measured with rotational Brookfield viscometer in deionized water and in brine. In electrolyte solution, the charged groups along the polymer chain are screened and therefore the polyelectrolyte effect affecting the chain conformation is eliminated. The samples having the best combination of high viscosity and charge density are carboxymethyl cellulose, xanthan gum and guar gum. Xanthan gum was found to reveal very exceptional behavior in salt solution as its viscosity increases upon salt addition opposite to the normal behavior of polyelectrolytes. The viscosity increase is explained by conformational change from coil to helix. Screening the charged groups by electrolyte addition enables the large side chains to form hydrogen bonds to the backbone stiffening the overall structure of the polymer.

CMC, xanthan gum, guar gum and the two reference PAMs were also characterized by intrinsic viscosity describing properties of individual polymer chains. Several concentrations of each polymer were measured by Ubbelohde capillary viscometer in salt solution. The reduced viscosities were calculated and plotted as a function of concentration to solve the intrinsic viscosity by extrapolating the Huggins equation to infinite dilute solution. The intrinsic viscosities were used to estimate the magnitude of molecular weights and critical overlap concentrations of the selected polymers.

The application testing was performed by coagulation-flocculation of bentonite slurry using polyaluminium chloride as the coagulant. The tests were monitored online by focused beam reflectance measurement device. The technique quantifies particle size distribution by measuring backscattering of light from the suspended particles. 9 biobased polymers representing 6 different types of polysaccharides in addition to the reference PAMs were measured to study the optimal dosage, floc stability and re-flocculation ability. As expected, none of the biopolymers reached the performance level of the PAMs. However, carboxymethyl cellulose, xanthan gum and guar gum revealed a great potential as their flocculation results were relatively good. These are the same products that have the best combination of molecular weight and charge based on the characterization results supporting the statement that these two parameters are key factors in adjusting the flocculation performance. The performance of the biobased polymers can be enhanced by modifying their structure, for example by increasing the molecular weight or

incorporating functional groups that boosts the flocculation ability. For example grafting by acrylamide has proved to increase flocking performance of some biobased polymers.

Synthetic polyacrylamides are used in a wide variety of applications. Enhanced oil recovery is an example of application where they are commonly used and where renewable substitutions are searched for. In the oilfields, thermal stability of the polymers pumped underground is one of the key characteristics. To compare thermal stability of the selected biobased polymers and the reference PAMs they were incubated for a week in 62 °C in deionized water in aerobic conditions. Viscosity profiles of the samples were measured with rheometer after 1,3 and 7 days of incubation to follow the degradation of the polymer. CMC, xanthan gum, guar gum, starch and PAM were tested, and out of these samples xanthan gum seems to be the most thermally stable. The result is suggested to ascribe for the structure of the xanthan gum. Compared to the other polymers, it has the largest side chains which shield the backbone. The relative abundance of pyruvate and acetate groups affects the stability of xanthan gum. Based on the exceptional rheological behavior in electrolyte solution, the thermal stability of xanthan gum is expected to be even better in salt solution.

As a conclusion it is justified to claim that in the future the biobased products have a great potential to offer alternative solutions for synthetic polymers originating from fossil resources. Out of the tested polymers xanthan gum and carboxymethyl cellulose have the best performance in flocculation application. The possibilities of using the xanthan gum in brine applications are numerous owing to its extraordinary rheological behavior in electrolyte solution. The results of guar gum are also encouraging although the tested product has relatively low charge density. The performance of polysaccharides in flocculation can be enhanced by modifying their chemical structure. Varying reaction mechanisms to modify polysaccharides can be found in literature. Esterification and etherification by nucleophilic reaction of saccharide oxygen are examples of typical mechanisms of polysaccharide modification.

The recommended path forward is to continue with the most potential polysaccharides being xanthan gum, CMC and guar gum. It is suggested to study how the performance of these polymers could be improved in the selected application. Approaches for chemical modification are for example increasing the size of naturally occurring polymers and attaching functional groups to the backbone. Different synthesis routes for modification should be studied also to find the most efficient mechanisms. In addition to flocculation, the biobased polymer derivatives are important topic in many other applications as well. The research should be broad-minded and co-operative to



find sustainable alternatives together for varying applications. Based on the results presented in this thesis, the future of biobased products from renewable resources looks promising.

## References

1. Visakh, P., Bayraktar, O., & Picó, G. (2014). *Polyelectrolytes: Thermodynamics and rheology*. Switzerland: Springer.
2. Bernards, M. (2015). Environmentally responsive polyelectrolytes and zwitterionic polymers. In Z. Zhang (Ed.), *Switchable and responsive surfaces and materials for biomedical applications* (pp.45-64). UK: Woodhead Publishing.
3. Evans, D.F., & Wennerström, H. (1999). *The colloidal domain: Where physics, chemistry, biology, and technology meet* (2<sup>nd</sup> ed.). USA: Wiley.
4. Brandrup, J., Grulke, E., & Immergut, E. (1999). *Polymer handbook*, Chapter VII (4<sup>th</sup> ed.). USA: Wiley.
5. Goodwin, J. (2009). *Colloids and interfaces with surfactants and polymer: An introduction* (2<sup>nd</sup> ed.). UK: John Wiley & Sons.
6. Grosberg, A., & Khokhlov, A. (2010). *Giant molecules: Here, there, and everywhere* (2<sup>nd</sup> ed.). USA: River Edge.
7. Manning, G., & Ray, J. (1998). Counterion condensation revisited. *Journal of Biomolecular Structure and Dynamics*, 16 (2), 461-476. doi: 10.1080/07391102.1998.10508261
8. Williams, P. (2008). *Handbook of industrial water-soluble polymers* (1<sup>st</sup> ed.). UK: John Wiley & Sons.
9. Brookfield engineering labs. (2012). *More solutions to sticky problems - A guide to getting more from your Brookfield viscometer*.
10. Shaw, M. (2012). *Introduction to polymer rheology* (1<sup>st</sup> ed.). USA: John Wiley & Sons.
11. Pamies, R., Hernández, C., López, M., & García, J. (2008). Determination of intrinsic viscosities of macromolecules and nanoparticles. *Colloid and Polymer Science*, 286 (11), 1223-1231. doi: 10.1007/s00396-008-1902-2
12. Suopajärvi, T. (2015). *Functionalized nanocelluloses in wastewater treatment applications* [Dissertation]. Finland: University of Oulu.
13. BTG MG. (2003). Operation manual PCD 03 particle charge detector.

14. Sharma, B., Dhuldhoya, N., & Merchant, U. (2006). Flocculants - an ecofriendly approach. *Journal of Polymers and the Environment*, 14 (2), 195-202. doi: 10.1007/s10924-006-0011-x
15. Lee, C., Robinson, J., & Chong, M. (2014). A review on application of flocculants in wastewater treatment. *Process Safety and Environmental Protection*, 92 (6), 489-508. doi: 10.1016/j.psep.2014.04.010
16. Salehizadeh, H., Yan, N., & Farnood, R. (2018). Recent advances in polysaccharide bio-based flocculants. *Biotechnology Advances*, 36 (1), 92-119. doi: 10.1016/j.biotechadv.2017.10.002
17. Blanco, A., Fuente, E., Negro, C., & Tijero, J. (2002). Flocculation monitoring: Focused beam reflectance measurement as a measurement tool. *The Canadian Journal of Chemical Engineering*, 80 (4), 734-740. doi 10.1002/cjce.5450800403
18. Mettler-Toledo AutoChem Inc. (2004). Lasentec D600 hardware manual 003-1501.
19. Yalpani, M. (1999). Chemistry of polysaccharide modification and degradation. In P. Finch (Ed.), *Carbohydrates: Structures, syntheses and dynamics* (pp. 294-318). Netherlands: Springer.
20. Hasan, A., & Abdel-Raouf, M. (2018). Applications of guar gum and its derivatives in petroleum industry: A review. *Egyptian Journal of Petroleum*. doi: 10.1016/j.ejpe.2018.03.005
21. Belgacem, M., & Gandini, A. (2011). *Monomers, polymers and composites from renewable resources* (1<sup>st</sup> ed.). UK: Elsevier Science & Technology.
22. Pereira, L. (2016). *Carrageenans: Sources and extraction methods, molecular structure, bioactive properties and health effects*. USA: Nova Science Publishers.
23. Davidson, R.L. (1980). *Handbook of water-soluble gums and resins*. USA: McGraw-Hill Book Company.
24. Hiltunen, M. (2013) *Cellulose based graft copolymers prepared via controlled radical polymerization methods* [Dissertation]. Finland: University of Helsinki.
25. Bejenariu, A., Popa, M., Picton, L., & Le Cerf, D. (2010). Effect of concentration, pH and temperature on xanthan conformation: A preliminary study before crosslinking. *Revue Roumaine de Chimie*, 55 (2), 147-152.
26. Moffat, J., Morris, V., Al-Assaf, S., & Gunning, A. (2016). Visualization of xanthan conformation by atomic force microscopy. *Carbohydrate Polymers*, 148, 380-389. doi: 10.1016/j.carbpol.2016.04.078

27. Ghomrassi-Barr, S., & Aliouche, D. (2015). Characterization and rheological study of xanthan polymer for enhanced oil recovery (EOR) application. *Offshore Mediterranean Conference and Exhibition*.
28. Cumpstey, I. (2013) Chemical modification of polysaccharides. *ISRN Organic Chemistry*. doi: 10.1155/2013/417672
29. Sada, E., Morisue, T., & Yamaji, H. (1975). Salt effects on isobaric vapor-liquid equilibrium of isopropanol-water system. The *Canadian Journal of Chemical Engineering*, 53 (3), 350-353. doi: 10.1002/cjce.5450530319
30. Belalia, F., & Djelali, N. (2014). Rheological properties of sodium alginate solutions. *Revue Roumaine de Chimie*, 59 (2), 135-145.
31. Brunchi, C., Morariu, S., & Bercea, M. (2014). Intrinsic viscosity and conformational parameters of xanthan in aqueous solutions: Salt addition effect. *Colloids and Surfaces B: Biointerfaces*, 122, 512-519. doi: 10.1016/j.colsurfb.2014.07.023
32. Chen, H., Thirumavalavan, M., Lin, F., & Lee, J. (2015). A facile approach for achieving an effective dual sorption ability of Si/SH/S grafted sodium montmorillonite. *RSC Advances*, 5 (71), 57792-57803. doi: 10.1039/c5ra10155g
33. Watson, P., Farinato, R., Fenderson, T., Hurd, M., Macy, P., & Mahmoudkhani, A. (2011). Novel polymeric additives to improve oil sands tailings consolidation. *SPE International Symposium on Oilfield Chemistry*, 2, 703-709.

Appendix 1. Intrinsic viscosity graphs

Figures 1-5 in Appendix 1 (A1) show the reduced and inherent viscosity results measured by automated Ubbelohde capillary viscometer. The linear Huggins and Kraemer equations are solved to find out the intrinsic viscosity, which is the intercept in both equations.

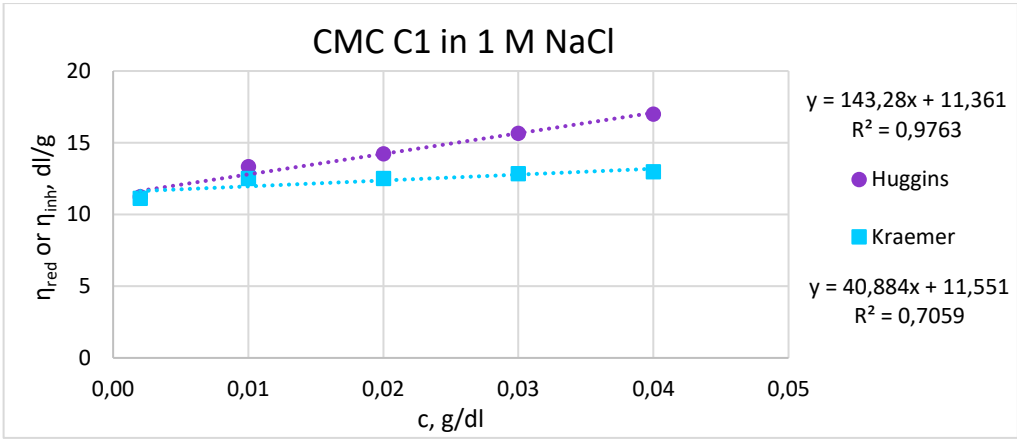


Figure A1-1. Intrinsic viscosity determination of CMC C1 in 1 M NaCl.

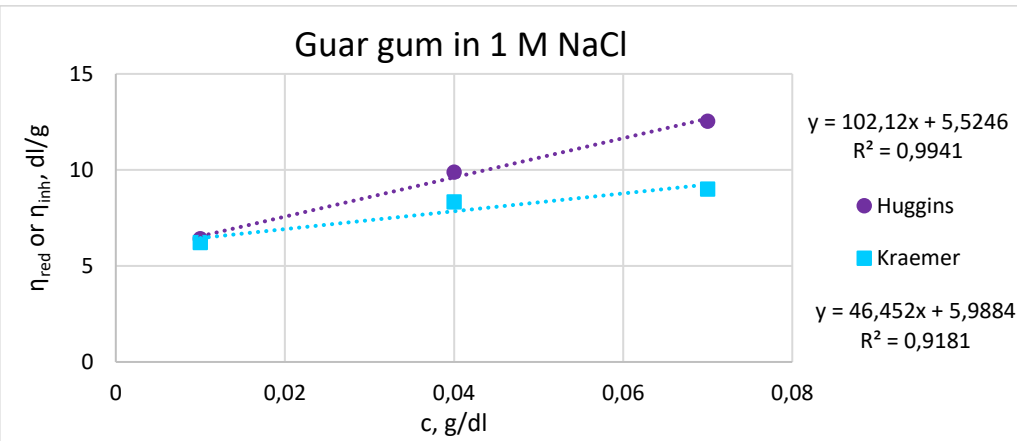


Figure A1-2. Intrinsic viscosity determination of Guar gum in 1 M NaCl.

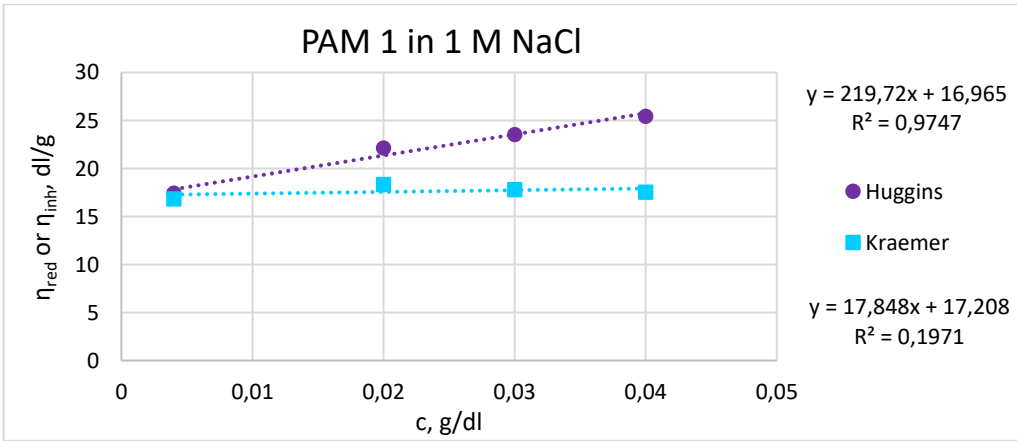


Figure A1-3. Intrinsic viscosity determination of PAM 1 in 1 M NaCl.

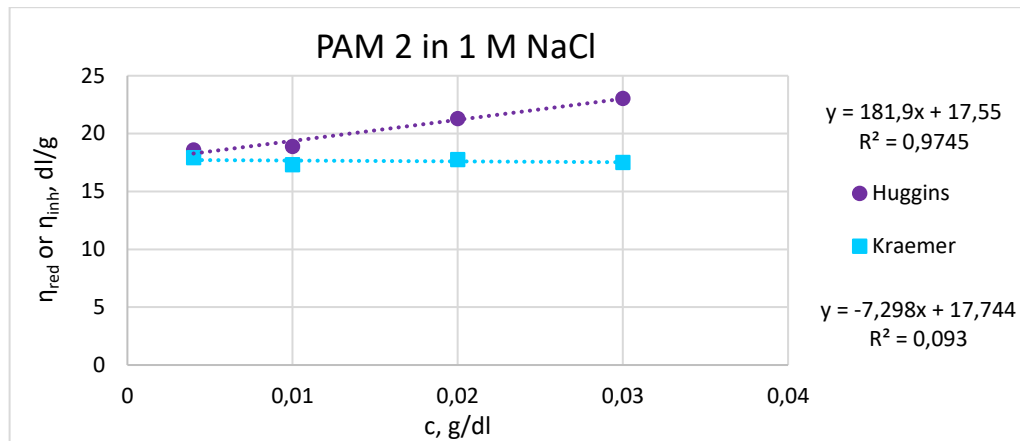


Figure A1-4. Intrinsic viscosity determination of PAM 2 in 1 M NaCl.

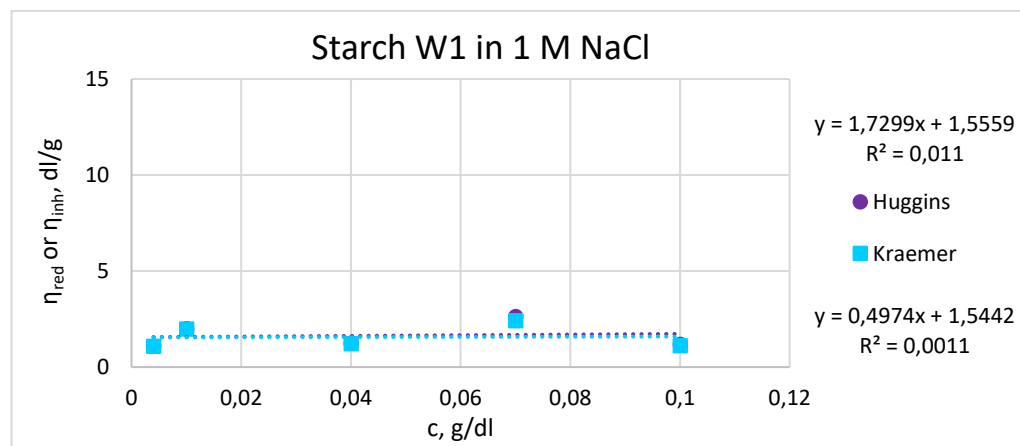


Figure A1-5. Intrinsic viscosity determination of Starch W1 in 1 M NaCl.

## Appendix 2. Bentonite flocculation graphs

Figures 1-11 in Appendix 2 (A2) show the results of the bentonite flocculation tests measured by focused beam reflectance measurement. The bentonite sample is 0,5 % in solids, and each sample contains polyaluminium chloride as a coagulant. The PAC dosage is 200 kg/ton for the biobased products and 100 kg/ton for the polyacrylamide references. Legends in the figures show the flocculant dosages.

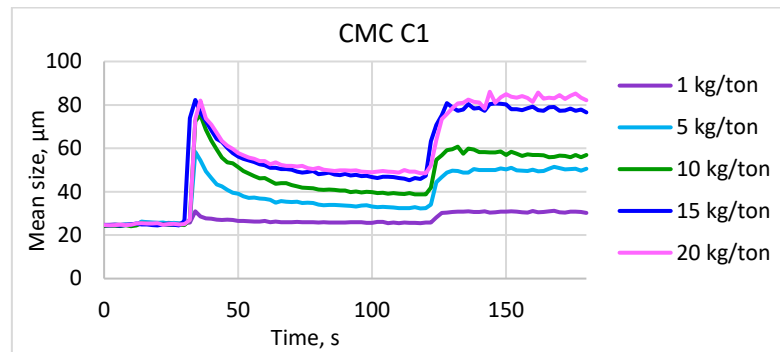


Figure A2-1. Bentonite flocculation graphs for CMC C1.

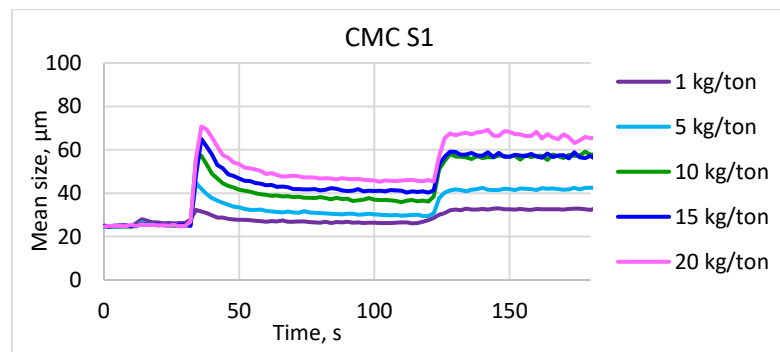


Figure A2-2. Bentonite flocculation graphs for CMC S1.

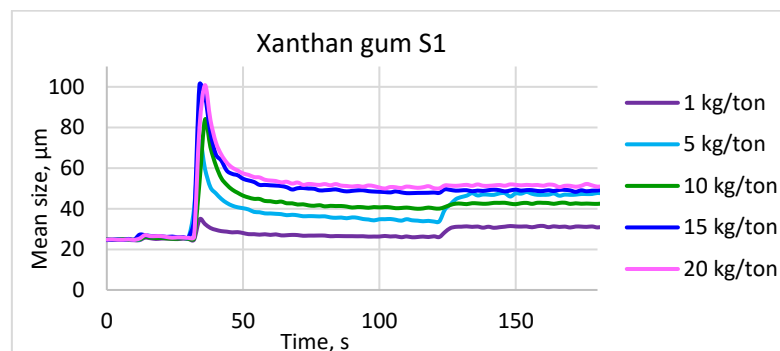


Figure A2-3. Bentonite flocculation graphs for Xanthan gum S1.

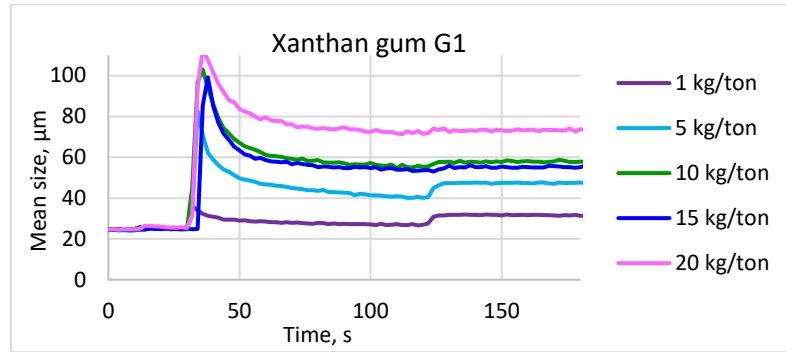


Figure A2-4. Bentonite flocculation graphs for Xanthan gum G1.

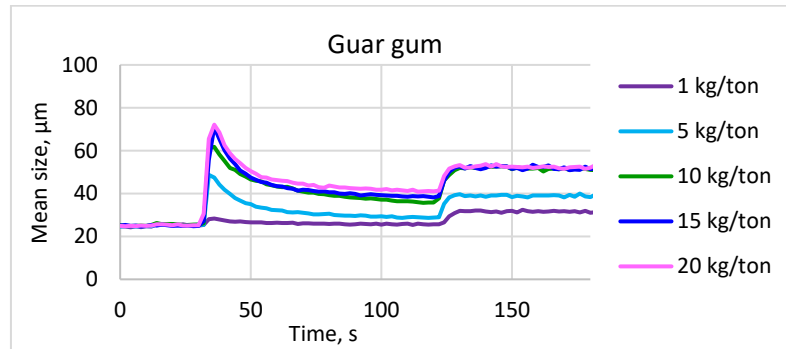


Figure A2-5. Bentonite flocculation graphs for Guar gum.

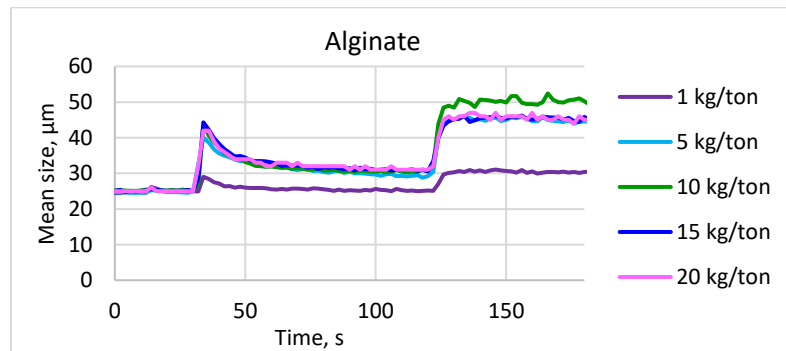


Figure A2-6. Bentonite flocculation graphs for Alginate.

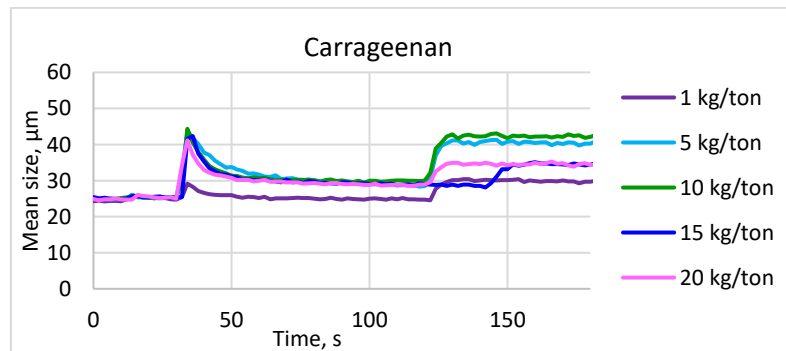


Figure A2-7. Bentonite flocculation graphs for Carrageenan.

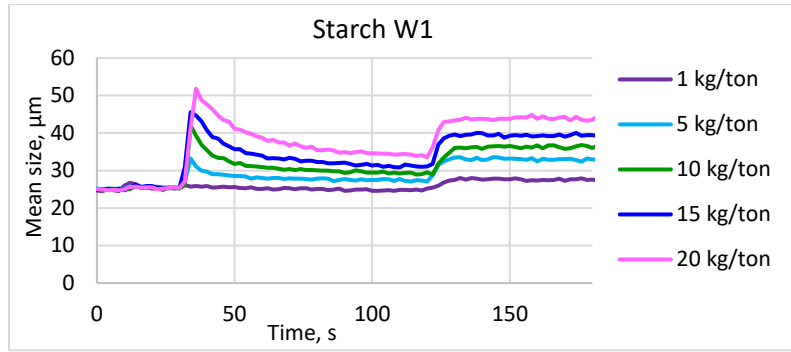


Figure A2-8. Bentonite flocculation graphs for Starch W1.

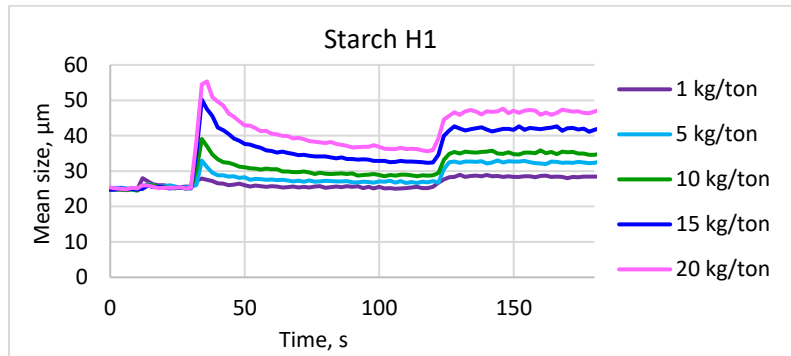


Figure A2-9. Bentonite flocculation graphs for Starch H1.

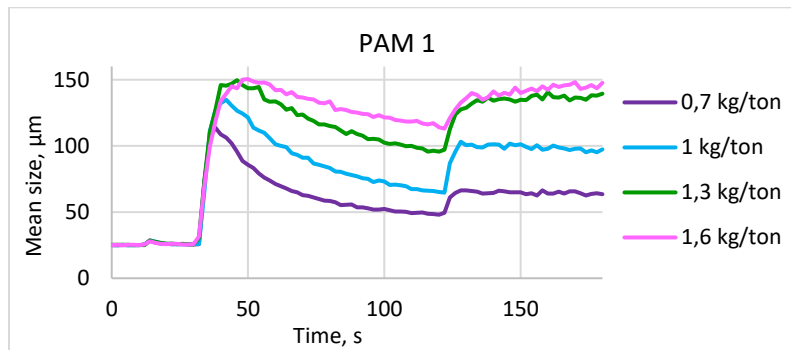


Figure A2-10. Bentonite flocculation graphs for PAM 1.

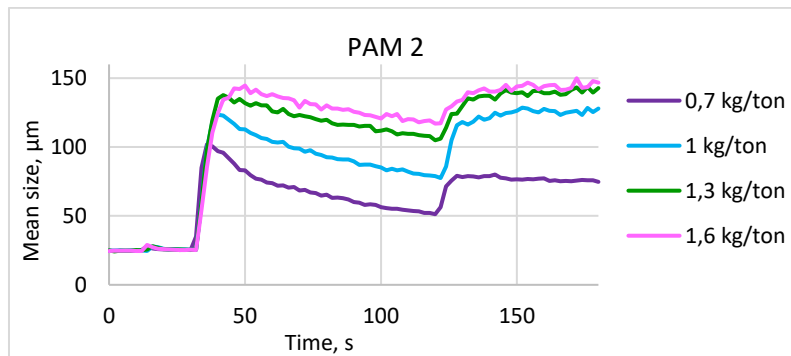


Figure A2-11. Bentonite flocculation graphs for PAM 2.



Appendix 3. Viscosity profiles of thermal stability test

Figures 1-6 in Appendix 3 (A3) show the viscosity profiles of the thermal stability samples measured in 25 °C by rheometer.

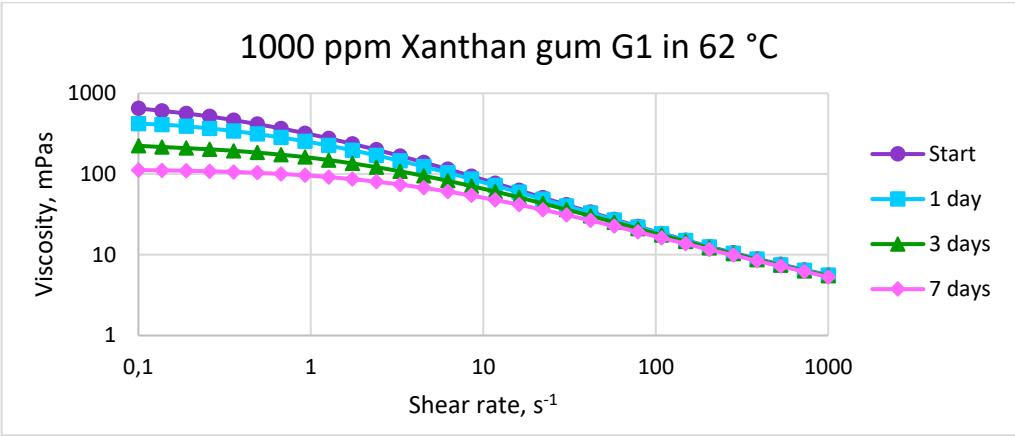


Figure A3-1. Viscosity profiles of 1000 ppm Xanthan gum G1 after incubating in 62 °C.

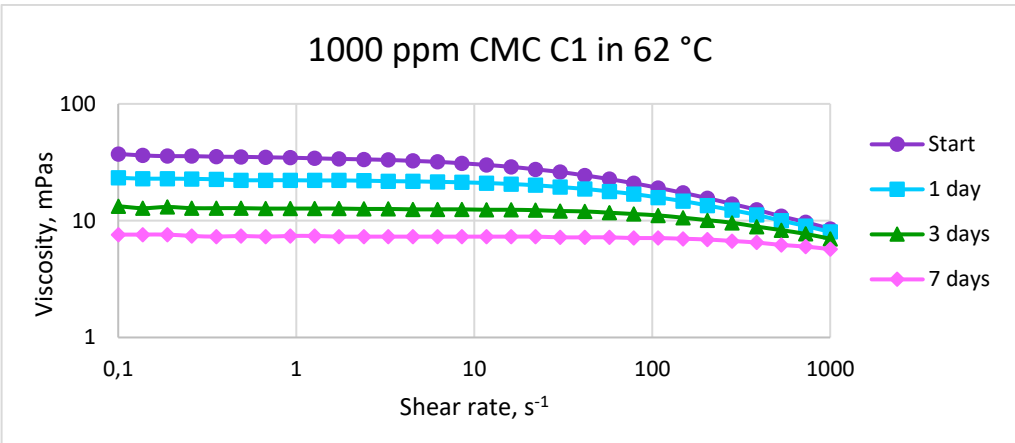


Figure A3-2. Viscosity profiles of 1000 ppm CMC C1 after incubating in 62 °C.

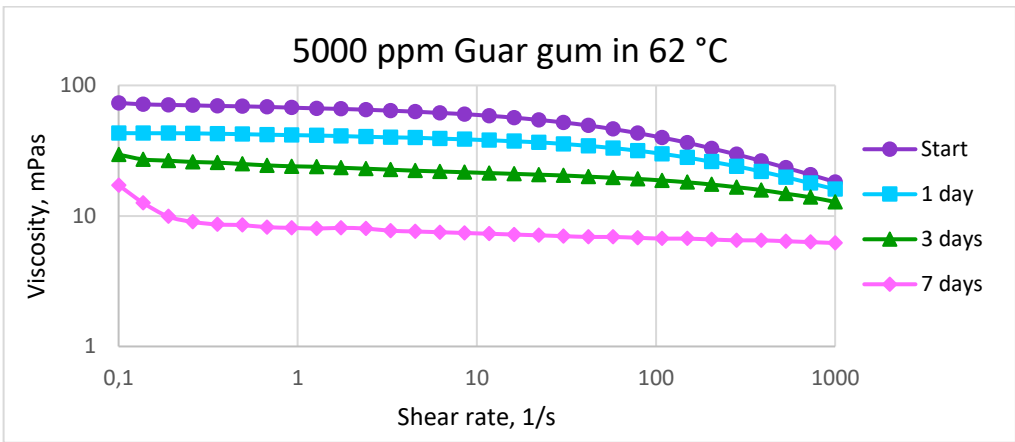


Figure A3-3. Viscosity profiles of 5000 ppm Guar gum after incubating in 62 °C.

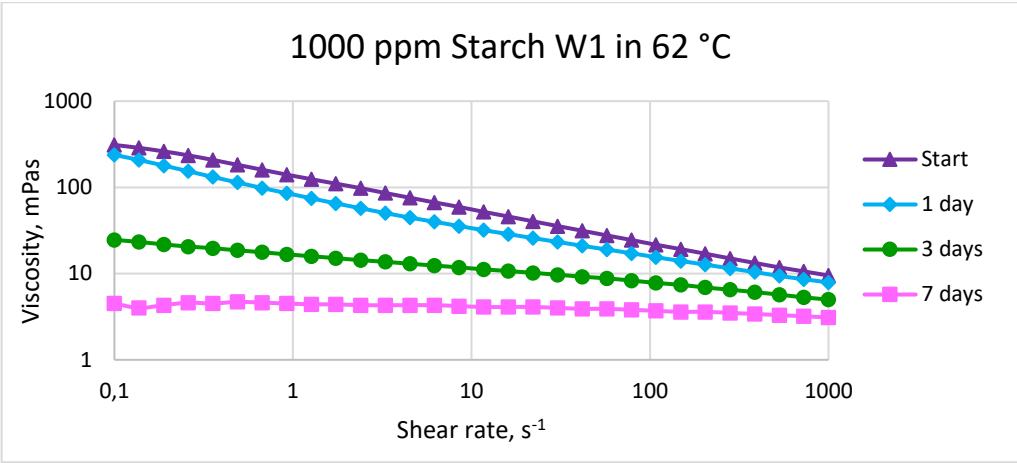


Figure A3-4. Viscosity profiles of 1000 ppm Starch W1 after incubating in 62 °C.

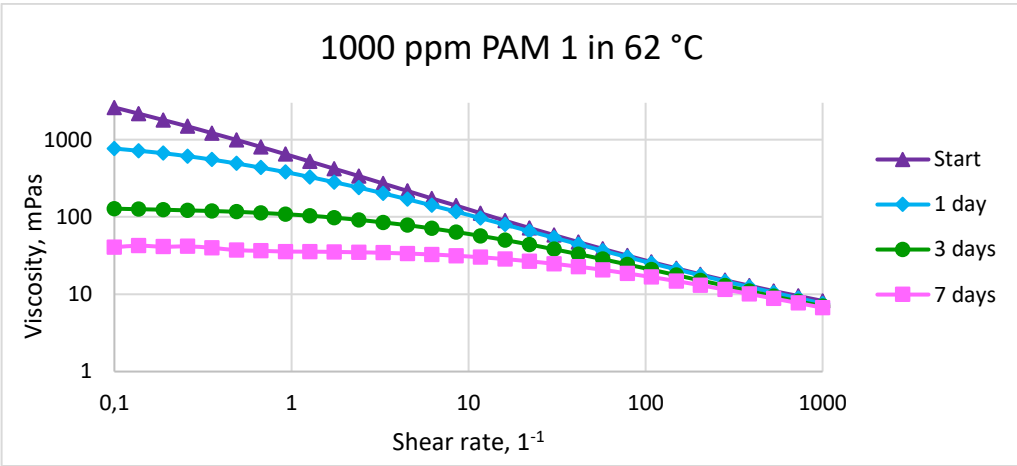


Figure A3-5. Viscosity profiles of 1000 ppm PAM 1 after incubating in 62 °C.

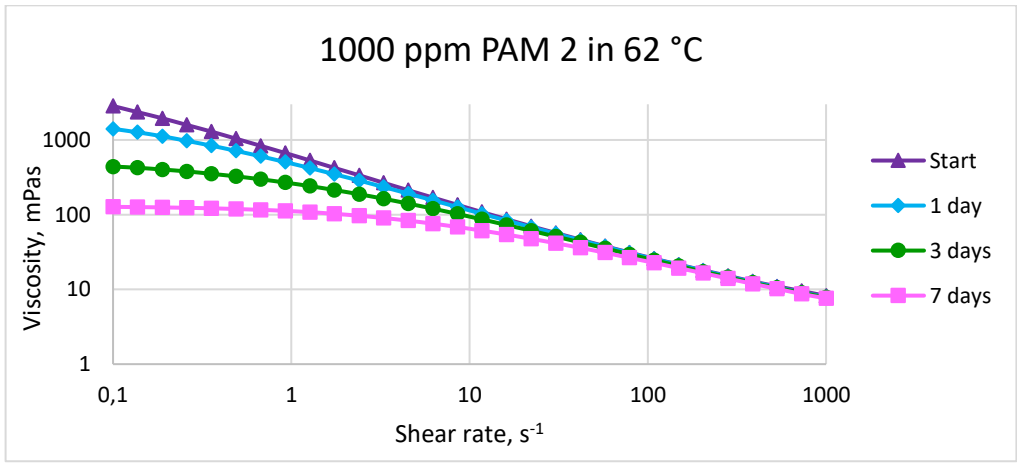


Figure A3-6. Viscosity profiles of 1000 ppm PAM 2 after incubating in 62 °C.